Leveraging Coexistence Theory to Understand the Role of Microbes in Mediating Plant Community Dynamics

by

Jeremy Collings

A dissertation accepted and approved in partial fulfillment of the

requirements for the degree of

Doctor of Philosophy

in Biology

Dissertation Committee:

Lauren Hallett, Chair

Jeff Diez, Advisor

David Levin, Institutional Representative

Stilianos Louca, Core Member

Bitty Roy, Core Member

University of Oregon

Spring 2025

DISSERTATION ABSTRACT

Jeremy Collings

Doctor of Philosophy in Biology

Title: Leveraging Coexistence Theory to Understand the Role of Microbes in Mediating Plant Community Dynamics

Interactions between plants and microbes contribute to the structure and dynamics of plant communities, but exactly how this happens continues to elude plant ecologists. Since the turn of the 21st century, the dominant paradigm for studying the role of microbes in plant community dynamics has been Bever's plant-soil feedback (PSF) theory, which has led to an immense amount of both theoretical and empirical insights. Recently, integration of PSF theory with theoretical insights from Chesson's modern coexistence theory (MCT) have improved the rigor by which we evaluate PSF-mediated coexistence and have identified novel mechanisms by which microbes may affect plant competitive dynamics. In this dissertation, I continue to build upon this recent integration while pursuing two larger questions in plant-microbial ecology. First, I pair a common garden competition experiment with amplicon sequencing of host-associated fungal communites to investigate how differences in fungal community composition alter the competitive dynamics between plant species and ultimately how host-associated microbiomes relate to species coexistence. Second, I investigate how ubiquitous context-dependencies in plant-microbe interactions may alter PSF-mediated competitive dynamics. To do this, I employ both theoretical methods as well as a large-scale greenhouse experiment. In each of my three chapters, I use plant population modeling to move beyond the traditional plant 'performance'

based results of PSF experiments. The result of each of my chapters is a more demographically explicit story about how complex interactions between plants, microbes, and their environment may contribute to plant community dynamics. This dissertation includes previously published, coauthored material.

CURRICULUM VITAE

NAME OF AUTHOR: Jeremy Collings

GRADUATE AND UNDERGRADUATE SCHOOLS ATTENDED:

University of Oregon, Eugene, OR, USA
SUNY Cortland, Cortland, NY, USA

DEGREES AWARDED:

Bachelor of Science, Conservation Biology, 2020, SUNY Cortland

AREAS OF SPECIAL INTEREST:

Quantitative Ecology
Population Ecology
Community Ecology

PROFESSIONAL EXPERIENCE:

Teaching and Research Assistant, University of Oregon, 2021-2025
Statistical Consultant, Michigan Tech, 2023-2025
Statistical Consultant, UC Irvine, 2024
Research Technician, SUNY Cortland, 2018-2021
Nature Educator, Lime Hollow Nature Center, 2015-2020

GRANTS, AWARDS AND HONORS:

Synthesis Skills for Early Career Researchers, NCEAS, 2024/25
SEEDS Alumni Travel Award, ESA, 2022
Barry Goldwater Scholarship, 2019
SPUR Fellowship, ESA, 2019
New York State Flora Association Research Grant, 2018
SUNY Cortland Undergraduate Research Fellowship, 2018

PUBLICATIONS:

Wolfe, J.D., Luther, D.A., Jirinec, V., **Collings, J.**, Johnson, E.I, Bierregaard Jr., R.O., & Stouffer P.C. Climate change aggravates bird mortality in pristine tropical forests. (2025) Science Advances, 11(5), eadq8086

Collings, J.A., Cook, E.J., Delevich, C.A., & Diez, J.M. (2024). Soil mycobiome dissimilarity,independent of fungal guild,is associated with increased probability of plant coexistence. Journal of Ecology, 112(10), 2307-2318

Diez, J., Schlauch, J., DuCharme, E., **Collings, J.**, & Erskine, S. (2024) Germination phenology alters species coexistence outcomes. Journal of Ecology. , 112(10), 2212-2222

Collings, J., Endriss, S. B., & Dávalos, A. (2023). Multiple stressors prevent gains in native plant diversity following invasive species removal. Ecosphere, 14(3), e4458

Collings, J.A., Shoemaker, L.G., & Diez, J. M. Environmental context alters plant-soil feedback effects on plant coexistence. (2025) *Manuscript Accepted at Ecology*

ACKNOWLEDGEMENTS

First, I would first like to acknowledge that none of this work could have been done without the support of my lab. I would like to acknowledge my advisor, Jeff Diez, who has consistently encouraged my personal interests and convictions. Thank you, Jeff, for encouraging me to pursue the ideas born out of my curiosity and for helping me shape whatever came of it into, what I believe, is rigorous and important scientific output. Fellow lab members Sarah Erskine, Emily Cook, and Katelin Kutella have served as fantastic colleagues as well as dear friends. Additionally, those that I have had the pleasure of mentoring during my Ph.D. have each likely taught me more about science and the world than I could hope to have taught them. Austyn Tavernier, Macy Patel, Lindsay Villano, and Sarah Kirby-Ruggiero, thank you for enjoying both the fun and frustration of research with me. I have also been immensely lucky to have worked with many collaborators outside of my lab that have inspired me to think about the world in interesting and fun ways. Thank you to Lauren Shoemaker, Jared Wolfe & the brilliant ornithologists that you have introduced me to, Cascade Sorte & Ryan Beshai, and all of the folks in the NCEAS SSERC program. Finally, I would like to thank my committee as well as other faculty in the department such as Lauren Ponisio, Brendan Bohannan, and Peter Ralph for providing valuable mentorship and sharing intellectually satisfying conversations about ecology and science as a whole. In addition to those who have aided my intellectual work in my Ph.D., I am endlessly grateful to those who encouraged my work as an ecologist prior to my Ph.D. First, I would like to thank Peter Harrity who initiated me into the world of natural history. I did not see the world so deeply before you encouraged me to make friends with the flowers

and birds in my environment. I would also like to thank my undergraduate research advisor, Andrea Dàvalos, for teaching me how to be an ecologist. Beyond teaching me how to conduct research, analyze data, and struggle with complexity, your strength and confidence has continued to inspire me throughout my career.

Outside of academia, I have many others to thank. First, I would like to thank my drum instructor Garin Rosen. Your encouragement has energized me through some of the most challenging periods of my Ph.D., and learning to channel my pent up energy into drumming has helped me to ground myself in my humanity outside of the consuming demands of academia. I would also like to thank Princess Maliena, who's BINGO nights have been there for me when I desperately needed a distraction. In addition to outfitting my apartment with many prizes from my BINGO wins, your renditions of high energy pop tracks and heartfelt ballads have brought me many laughs and many tears. I would like to acknowledge my parents, who instilled in me a deep curiosity about complex things and encouraged me to enjoy retreating into deep thought. Much more importantly, I would like to acknowledge their love and support in all of my pursuits in and out of academia. I would also like to acknowledge my brother Ryan, who has served as dear friend and a role model for me. I would like to thank my close friends in the department, both Rebecca Hayes and Carolyn Delevich. I feel so deeply grateful to have had folks who consistently inspire me to do interesting and good research, and who I can decompress from the pressures of grad school with. Rebecca, I truly could not have done this without you. Further, many friends near and far have supported me in my work here: Brittany, Doug, Janiellee, Jonathan, Jonah, Leanne, Patrick, Ryan. I would like to write each of you an ode, but I'm limited to two pages here.

I dedicate this work to all of the odd forms and assemblages that life takes on. Such peculiarity and deviance, inherent in earth's systems, fuel my curiosity and love.

TABLE OF CONTENTS

Chapter Page

LIST OF FIGURES

LIST OF TABLES

Table Page

CHAPTER I

INTRODUCTION

The colonization of land by the ancestor of green plants was likely enabled by interactions between plants and microrganisms, most notably fungi which helped plants access water and nutrients in exchange for carbon (Selosse & Le Tacon, 1998). The importance of microbes has been recognized by plant ecologists practically since the inception of the field of community ecology (Clements, 1916). Now, for over two decades, community ecologists have been methodically studying the role of plant-microbe interactions in structuring plant communities, and have found substantial evidence that the reciprocal effects of plants on microbial communities and microbes on plant communities may be essential forces for the structure of plant communities (van der Putten, Bradford, Pernilla Brinkman, van de Voorde, & Veen, 2016). It is thought that differences between plant species in the types of interactions that they form with microbes may mediate apparent interactions between plant species, thus structuring plant communities. Thus, interactions between plants and microbes entered the vast cannon of diversity-promoting mechanisms in plant community ecology and been a pillar of plant ecology since at least the dawn of the 21st century.

Although researchers had been studying the role of plant-microbe interactions in shaping plant community dynamics for decades prior, the most influential theoretical framework for studying such microbe-mediated plant community dynamics was introduced in the late 1990's by James Bever and collaborators (Bever, Westover, & Antonovics, 1997). Bever's work had the two key ingredients for impactful ecological theory: 1) a coherent mathematical model for an ecological process along with 2) an accompanying (and tractable) empirical

method for estimating parameters of interest (Bever, 2003). Bever's plant-soil feedback (PSF) theory states that plant species cultivate unique communities of soil microbes which in turn have distinct net effects on different plant species. A substantial amount of work from microbial ecology and plant pathology back up this claim that plant species produce distinct metabolites which select for distinct microbial communities, and plant species differ in their responses to the same microbial taxon, ranging from benefitting from to being pathogenized by a given microbial taxon. Bever used these simple assumption to adapt Lotka-Volterra models of competing plant populations to incorporate the population dynamics of their associated microbial communities, and by making a few additional assumptions, derived parameters which seem to determine the coexistence outcome of two competing plant species. He then proposed and implemented an empirical method for estimating this quantity as to predict the contribution of soil microbes to plant coexistence. In the subsequent decades, plant ecologists have conducted both empirical and theoretical offshoots of this work to continue to explore the role of microbes in shaping plant community dynamics (Van der Putten et al., 2013). However, the inability of this work to explain observed plant community dynamics in field settings has plagued the field and led to a variety of offshoot frameworks for investigating plant-microbe community dynamics which address particular complicating factors (Forero, Grenzer, Heinze, Schittko, & Kulmatiski, 2019; Heinze, Sitte, Schindhelm, Wright, & Joshi, 2016).

One offshoot of PSF research that has recently emerged is actually an integration of PSF theory and a historically separate theoretical framework for studying questions about diversity maintenance: modern coexistence theory (MCT). The basis of MCT is Peter Chesson's monograph Mechanisms of

Maintenance of Species Diversity 2000 which synthesized the many proposed mechanisms for species coexistence into a finite set of about five canonical mechanisms. Equipped with Lotka-Volterra models and the invasibility criterion (perhaps the most widely accepted operationalization of 'stable coexistence'), Chesson partitioned coexistence mechanisms into 'equalizing mechanisms', those which lower the differences between species average fitness, and 'stabilizing mechanisms', those which lower the niche overlap between two species, and further defined specific fluctuation dependent and independent types of stabilizing mechanisms. Although this synthetic framework organizing coexistence mechanisms into a consolidated canonincal set was a highly influential contribution to community ecology, simply acknowledging that fitness differences determine the degree of niche differentiation required for stable coexistence changed how many community ecologists study community dynamics, moving away from methodologies which simply quantified niche overlap without considering the balance of niche differences and fitness inequalities. Although MCT and PSF theory developed in parallel, assessing PSF-mediated coexistence using insights from MCT (notably the acknowledgement of microbe-mediated fitness inequalities) was instigated only recently (Kandlikar, Johnson, Yan, Kraft, & Levine, 2019; Ke & Wan, 2020).

In addition to implementing a more rigorous standard for identifying PSF-mediated coexistence, integrations of PSF theory and MCT have opened the door to new sorts of questions about how microbes influence plant community dynamics. In this dissertation, I build upon such integrative theoretical frameworks to explore two under-explored phenomena in plant-microbe ecology. In Chapter Two, I investigate a key assumption of PSF theory, that differences in species-specific microbial communities determine coexistence outcomes via their effects on niche

differences, by pairing a common garden competition experiment with amplicon sequencing of soil fungal communities. In Chapters Three and Four, I explore the role of context-dependent PSFs in mediating plant coexistence first through theoretical simulations and analysis and then through a large-scale greenhouse PSF experiment. In each of these chapters, I leverage methods from population ecology to more mechanistically understand the role of plant-microbe interactions in shaping entire plant communities.

Chapter Two: Although a key step in Bever's Bever et al. (1997) PSF framework is the cultivation of a particular microbial community by a given plant species, this cultivation has largely been studied implicitly in plant-soil feedback experiments (Pernilla Brinkman, Van der Putten, Bakker, & Verhoeven, 2010; Rinella & Reinhart, 2018). Sequencing soil microbial communities in PSF research has become more common over the past decade, but few studies have used these sequencing approaches outside of confirmation of microbial community differences amongst experimental treatments or field samples. Meanwhile, research in both agriculture and microbial ecology have attempted to explicitly characterize differences between plant species in the microbial communities that they cultivate (Burns, Anacker, Strauss, & Burke, 2015; Dagher, de la Providencia, Pitre, St-Arnaud, & Hijri, 2019; Fox, Lüscher, & Widmer, 2020). We still lack an understanding of how differences between plant species' associated microbial communities might influence interactions between competing plant species. Meanwhile, researchers in coexistence theory have been attempting to identify which plant traits are correlated with niche or fitness differences and how these traits affect coexistence. To study the relationship between plant species associated microbial communities and plant competition, I have conducted a common garden

experiment and paired this experiment with fungal sequences of monospecifically cultivated soils. Treating the host associated mycobiome as a species-specific trait, I apply methods from MCT to quantify the relationship between mycobiome dissimilarity, niche & fitness differences, and coexistence. This work is contained within Chapter Two of this dissertation and has been co-authored with Emily Cook, Carolyn Delevich, and Jeff Diez.

Chapter Three: Plant-microbe interactions are known to depend on the underlying environmental context, yet most efforts to understand how plant-soil feedbacks mediate species coexistence have not considered these context-dependencies. Environmental gradients may impose selective pressures which alter the composition of plant-associated microbial communities (Francioli, Schulz, Buscot, & Reitz, 2018; Pérez-Jaramillo et al., 2019), or pairwise interactions between plant species and microbial taxa may shift quantitatively or qualitatively along environmental gradients (N. C. Johnson, Graham, & Smith, 1997; Rogalski, Stewart Merrill, Gowler, Cáceres, & Duffy, 2021). Nevertheless, understanding how such context-dependent interactions may impact microbe-mediated niche and fitness differences in plants is currently unexplored. Building on a set of Lotka-Volterra models developed in Ke and Wan 2020, I incorporate the scaling of species interactions by some environmental gradient and implement both analytical and simulation-based methods to identify if and how such context-dependent plant-microbe interactions may shift coexistence outcomes among competing plant species. This work is contained in Chapter Three of this dissertation and has been co-authored with Lauren Shoemaker and Jeff Diez.

Chapter Four: Complementing the theoretical work of Chapter Three, I have conducted a greenhouse PSF experiment with a few modifications which

have enabled me to ask more nuanced and mechanistic questions about drought-dependent PSFs and species coexistence in Willamette Valley prairies. First, I modified the original PSF experimental design, including a density gradient to better estimate plant-plant species interactions. I also collected data to estimate multiple demographic processes, enabling me to fit models of annual plant population dynamics. Using theoretical advancements from MCT, I calculated niche and fitness differences which incorporate the role of indirect species interactions for 3+ species communities (Saavedra et al., 2017), and I used simulation-based methods with my parameterized plant population models to explore the consequences of drought-dependent plant-microbe interactions on plant diversity. In doing so, I was able to identify unique processes related to context-dependent PSFs that have not been described due to the lack of demographic data collected in traditional PSF studies (Dostálek, Knappová, & Münzbergová, 2022). This work is contained in Chapter Four of this dissertation and has been co-authored with Katelin Kutella, Bryn Callie, Macy Patel, Austyn Tavernier, Lindsay Villano, and Jeff Diez.

CHAPTER II

SOIL MYCOBIOME DISSIMILARITY, INDEPENDENT OF FUNGAL GUILD, IS ASSOCIATED WITH INCREASED PROBABILITY OF PLANT COEXISTENCE

2.1 Contributions

With the help of the PI, Jeff Diez, I designed this study, and along with Emily Cook, conducted all field work. I performed all molecular work on the soil samples, and Carolyn Delevich did all the bioinformatics. I performed all statistical analyses and wrote the first draft of the manuscript which was then revised with the help of all coauthors.

From Collings, J.C., Cook, E.J., Delevich, C.A., & Diez, J.M. Soil mycobiome dissimilarity, independent of fungal guild, is associated with increased probability of plant coexistence. Journal of Ecology, 112, 2307–2318.

2.2 Introduction

Interactions between plants and microbes have been central to many key hypotheses in plant community ecology (Bever et al., 1997; Keane & Crawley, 2002; Terborgh, 2020). Although definitive tests of whether microbes structure plant communities remain challenging (Harris, 2009), there is growing evidence that feedbacks link the structure of plant communities to that of soil microbial communities (Bauer, Blumenthal, Miller, Ferguson, & Reynolds, 2017; Fahey, Koyama, Antunes, Dunfield, & Flory, 2020). Theory has shown how plant-microbe interactions may mediate plant community dynamics (Ke & Wan, 2020; Schroeder, Dobson, Mangan, Petticord, & Herre, 2020), and emerging sequencing technologies have expanded our understanding of interactions between plants and their microbial communities (Y. Liu, Yu, Xie, & Staehelin, 2012; Rallo et al., 2023;

Wilschut et al., 2019). Still, the discrepancy between the pace of theoretical and empirical research leaves many unexplored opportunities for the integration of theory and molecular characterization of microbial communities.

Theories explaining how plant-microbe interactions scale up to influence plant community dynamics commonly assume that different plant species cultivate unique microbial communities. While there is growing empirical support that plant species are important indicators for soil microbial communities (Burns et al., 2015; Dagher et al., 2019; Fox et al., 2020), it remains unclear why plant species microbiomes differ. For example, the relationship between plant phylogeny and plant-microbe interaction similarity has received mixed support (Mehrabi & Tuck, 2015; Sweet & Burns, 2017), suggesting that phylogenetic relatedness per se may not be able to explain the role of species-specific microbial communities in mediating plant community dynamics. Thus, understanding exactly how dissimilarity of plant-associated microbial communities mediates plant-plant interactions remains necessary for describing how microbes may structure plant communities.

The ability of species to coexist in communities is generally related to trait differences among the species, as formalized by advances in quantitative ecology now referred to as modern coexistence theory (Chesson, 2000). Modern coexistence theory explores the mechanisms which maintain species coexistence by partitioning species differences into niche differences and fitness inequalities. While fitness inequalities describe intrinsic differences between species in their performance in a given context, niche differences are species differences that stabilize competitive dynamics by causing species to limit themselves moreso than they limit their competitors (Adler, HilleRisLambers, & Levine, 2007). Whether two species are

able to coexist depends on whether their niche differences are sufficiently large as to overcome their fitness inequalities (Blackford, Germain, & Gilbert, 2020; Godoy & Levine, 2014; Kraft, Godoy, & Levine, 2015). Importantly, any trait difference that influences species interactions, by definition, alters both niche and fitness differences (C. Song, Rohr, & Saavedra, 2017), so quantifying the degree to which a given trait influences niche and fitness difference respectively is an important yet still understudied goal for community ecologists. Here, we contribute to this objective by treating dissimilarity between species' microbiomes as a trait difference (corresponding to ideas about microbiomes as extended phenotypes (de la Fuente Cantó et al., 2020)). Thus, the degree of dissimilarity in species' microbiomes may either stabilize coexistence (by increasing niche differences) or destabilize coexistence by increasing fitness advantages of one species over another. In fact, the importance of microbe-mediated fitness differences in plant-soil feedbacks have gained recent support (Yan, Levine, & Kandlikar, 2022).

The mechanisms by which plant microbiome dissimilarity may impact plant competition are related to the diverse array of functionally distinct microbial taxa. The hypotheses proposed for how particular functional groups of microbes may impact plant communities often depend on the degree of species-specificity of the microbial taxa (Bever et al., 2010; Semchenko et al., 2022). For example, species-specific plant-pathogens are hypothesized to induce negative intra-specific density-dependent feedbacks that contribute to niche differences and promote coexistence, but shared generalist pathogens may also affect inter-specific interactions and affect both niche and fitness differences (Mordecai, 2013). Conversely, plant mutualists may induce positive feedbacks, increasing fitness differences between species, if their benefit to the host plant differs across plant species (Zhang et al., 2010).

However, species-specific mutualists and saprotrophs may also stabilize competitive interactions if they mediate resource partitioning among competitors (Barry et al., 2019). The role of these different functional groups in mediating plant interactions requires further empirical study.

To elucidate the role of microbiome divergence in plant community dynamics, we paired a common garden competition experiment with molecular characterization of plant species' mycobiomes (fungal component of the microbiome). We hypothesized that mycobiome dissimilarity would be associated with both increased niche and fitness differences. However, because recent research has identified a larger role of plant-associated microbes in mediating fitness inequalities (Kandlikar, Yan, Levine, & Kraft, 2021), we hypothesized that mycobiome divergence would promote exclusion by increasing fitness inequalities moreso than niche differences. Finally, we hypothesized that the relationship between mycobiome dissimilarity and competitive dynamics would differ across the functional groups of plant-associated fungi.

2.3 Methods

2.3.1 Competition Experiment. In November of 2021, in partnership with the Friends of Buford Park Native Plant Nursery, in Lane County Oregon, we set up a common garden competition experiment with the goal of measuring intraspecific and interspecific competitive effects across all pairwise combinations of eight species: *Acmispon americanus* (Nutt.) Rydb., *Calandrinia ciliata* (Ruiz & Pav.) DC., *Clarkia amoena* (Lehm.) A. Nelson & J.F. Macbr., *Clarkia purpurea* (W. Curtis) A. Nelson & J.F. Macbr., *Collomia grandiflora* Douglas ex Lindl., *Navarretia intertexta* (Benth.) Hook., *Plagiobothrys nothofulvus* (A. Gray) A. Gray, and *Plectritis congesta* (Lindl.) DC.. All species are native

annual plants that occur in upland prairies throughout the Willamette Valley, Oregon. This ecosystem has a cool, wet winter and warm, dry summer, so species are adapted to germinate in the fall and winter after the first significant rains, and persist through the following summer. Additionally, all species were actively being grown for seed production in nearby monoculture plots at the nursery.

For each species, we established a background competitor plot in which a single background species was sown. Each plot was subdivided into three 0.8x1.0m subplots that varied in the density of the background competitor. Background plots were separated by about 0.5m of weed cloth. We sowed different numbers of seeds of each species (measured out by weight) in order to achieve the desired density gradient. All analyses of density are based on counted numbers of adult plants in each competitive neighborhood, not the density of seeds sown. In addition to the background species, seeds of each of the eight species were sown into each subplot and later thinned such that each subplot contained two focal individuals of every species. Thus, for each species, two focal individuals experienced competition at low, medium, and high density from each of the other seven species as well as from its own species. Additionally, two "alone plots" were established, in which two individuals of each of the eight species grew in the absence of a background competitor, to help estimate the performance of each species in the absence of competition (λ, below).

In April of 2022, the number of competitors growing within a circle with a 19cm radius around each focal individual was recorded. In the summer of 2022, we harvested focal individuals at the end of the season, after the last spring rains, defined as the apparent cessation of growth and new reproduction. To estimate fitness (seed output) for each focal individual, we counted the number of flowers

or inflorescences on each focal plant and combined this with estimates of seeds per flower or inflorescence, similar to Wainwright, HilleRisLambers, Lai, Loy, and Mayfield (2019) and Bimler, Stouffer, Lai, and Mayfield (2018). For those species that produce inflorescences, we counted the number of flowers per inflorescence for a random sample of at least 500 inflorescences and used those averages to estimate the number of flowers for the rest of the individuals. For species that produce multiple seeds per fruit, we similarly counted the number of seeds per fruit for a random sample of at least 80 fruits and used those averages to estimate the number of seeds for the remaining individuals of that species.

2.3.2 Soil Sequencing. In July 2022, we collected five 1 x 10 cm soil cores from monoculture plots where each species had been growing alone for two or three years. These monoculture plots were established by the nursery and offer a unique field-based analog to the "culturing" phase of many plant-soil feedback experiments, for quantifying each species' microbial signature. In addition, we collected soil cores from the competition experiment directly after harvesting the focal species. Cores were collected directly under focal plants from the experimental con-specific competition plots (2 plants x 3 con-specific competition plots = 6 soil cores) and the competition-free control plots (n = 4), for a total of 15 soil cores per species. Soils were transported to the University of Oregon and stored at -20 ^{o}C for no more than nine months.

Individual soil cores were homogenized, and genomic DNA was extracted from 0.25 g of soil using DNEasy PowerSoil kits (Qiagen). The fungal ITS1 region was targeted using primers ITS1F (Gardes & Bruns, 1993) and ITS2 (White, Bruns, Lee, Taylor, et al., 1990). Primers, barcodes, and Illumina adapters were annealed through a two-step PCR. The first PCR was a 20 uL reaction with

Promega GoTaq Green (10 uL), nuclease-free H_2O (7.9 uL), 0.5 uL of each primer with TruSeq stubs incorporated, bovine serum albumin (BSA; 0.1 uL), and 1 uL of genomic DNA template. The thermocycler was run for one cycle at 94^{o}C for 3 min, 30 cycles of 94^{o}C for 45 s, 54^{o}C for 1 min, 72^{o}C for 1.5 min, and one cycle at 72^{o}C for 10 min. The second PCR annealed Illumina-specific adaptors and multiplexed samples using the iTag protocol developed by the California Institute for Quantitative Biosciences at UC Berkeley. Samples were run in the thermocycler for one cycle of 94^{o}C for 3 min, 12 cycles of 94^{o}C for 45 s, 52^{o}C for 1 min, and 72^{o}C for 1.5 min, followed by one cycle at 72^{o}C for 10 mins. Following each PCR, the PCR products were visualized on a 1% agarose gel. Samples were pooled in equimolar concentrations ($\sim$1.5 ng DNA per sample). Pools were then purified using Omega Mag-Bind TotalPure NGS Beads at 0.8x uL concentration of beads per pool. Sequencing was performed on a shared Illumina MiSeq lane using the v3 mode, which synthesizes paired-end reads up to 300 bp in length. This run configuration produces up to 25 million reads per lane, making the target sequencing depth 30k reads per sample for these samples.

Resulting sequencing depth averaged 27,947 +/- 18,782 reads per sample. 3.15 million forward and reverse reads were demultiplexed, and primers were removed using cutadapt v. 4.4 (Martin, 2011). Raw reads were quality filtered using the DADA2 bioinformatics pipeline, adapted to account for interspecific variation in ITS1 region lengths in fungi (Callahan et al., 2016). Primers were trimmed with cutadapt v. 4.4 (Martin, 2011). Reads less than 50 bp were filtered out, and those with maximum expected errors greater than two for both forward and reverse reads were removed. Amplicon sequence variants (ASVs) were inferred using DADA2's core denoising algorithm, after which forward and reverse reads

were merged. Chimeras were detected de novo using DADA2's isBimeraDenovo, which is more sensitive to nearby chimeras compared to other chimera detection algorithms, making it better suited for ASVs. Taxonomy was assigned to 5,124 ASVs using the naïve Bayesian classifier method (Q. Wang, Garrity, Tiedje, & Cole, 2007) with the UNITE fungal reference database (Nilsson et al., 2019). Samples were rarefied to 1953 reads. Low abundance ASVs ($<$ 5 reads/sample and occurancce in $<$ 5% samples) were removed per sample, leaving a total of 658 ASVs and a mean of 177.91 ASVs per sample. Ecological functions of ASVs were assigned using FUNGuilds (Nguyen et al., 2016), keeping only assignments labeled as probable or highly probable. Classifications were broadly defined as pathotroph, saprotroph, and symbiotroph (including mutualists like mycorrhizal fungi as well as presumably commensalist endophytes). Because FUNGuild may classify taxa as any combination of these three guilds, we included any taxa that could be a given guild when subsetting the dataset by guild (e.g. a pathotroph/saprotroph taxon would be included in both the pathotroph and saprotroph datasets).

2.3.3 Statistical Methods.

2.3.3.1 Calculating Coexistence. To estimate key demographic parameters involved in predicting competitive outcomes for each of the 28 species pairs, we fit population models for each of the eight species. We fit three different population models that varied in how competition affects fecundity (Beverton-Holt, Lotka-Volterra, & Ricker), and ultimately used parameter estimates from the Beverton-Holt model (Hart, Freckleton, & Levine, 2018) as it fit our data the best (description of model selection in Appendix A.1). Competition coefficients were constrained to be competitive during parameter estimation ($>$ 0) because downstream analyses assume competitive interactions and because there was no

apparent facilitation except for one interaction coefficient (Appendix A.1). Thus, we fit population models with the following structure:

$$N_{i,t+1} = N_{i,t}\frac{\lambda_i}{1 + \alpha_{ii}N_i + \alpha_{ij}N_j} \tag{2.1}$$

which models next year's population size of species i ($N_{i,t+1}$) as the product of the current population size of species i and the per capita fecundity. Fecundity is defined as species i's growth rate in the absence of competition (λ_i) divided by the number of competitors and their associated per capita competition coefficients (α_{ij}).

From this model, we estimated λ for each species as well as all αs for all pairwise combinations of species to calculate niche and fitness differences. Following Godoy et al. 2014, we used these parameters to calculate niche overlap between each pair of species as:

$$\rho = \sqrt{\frac{\alpha_{ij}\alpha_{ji}}{\alpha_{ii}\alpha_{jj}}} \tag{2.2}$$

and niche differences were calculated as $1 - \rho$. We then calculated the fitness inequalities:

$$\frac{\kappa_j}{\kappa_i} = \frac{\lambda_j}{\lambda_i}\sqrt{\frac{\alpha_{ij}\alpha_{ii}}{\alpha_{ji}\alpha_{jj}}} \tag{2.3}$$

where species j is the competitively superior species within the species pair. Note that unlike Godoy et al. 2014, we do not include germination or seed survival parameters Dostál (2023). Thus, the fitness inequalities are equivalent assuming that germination and seed survival rates are 1 (though our results are rather insensitive to the assumed value; Appendix A.1:Figure S1). We estimated these

parameters using Bayesian hierarchical modeling in RSTAN (Stan Development Team, 2023a) and used noninformative priors for all parameters. To propagate uncertainty in parameter estimates to inference about competition and coexistence, we retained 5000 samples from the distributions of both niche differences and fitness inequalities to use in subsequent analyses.

2.3.3.2 Characterizing Fungal Communities.

Using the fungal community data, we first assessed whether plant species influenced microbial community structure using PERMANOVAs with Bray-Curtis dissimilarity which included plant species, sample type (monoculture or experimental) and an interaction between species and sample type. We paired these statistical tests with NMDS ordinations to visualize fungal community compositional differences. We repeated this procedure with pathotroph, saprotroph, and symbiotroph subsets of the dataset.

To estimate the mean dissimilarity between plant species' associated fungal communities, we first computed a distance matrix between all samples using Bray-Curtis dissimilarities. We then estimated the mean dissimilarity within samples for each species as well as between species. We repeated this procedure for pathotroph, saproptroph, and symbiotroph communities. Posterior distributions of these average dissimilarities were retained to use in subsequent analyses. We also assessed the degree to which mean fungal dissimilarity (total and guild specific) was predicted by plant phylogenetic dissimilarity by fitting linear models with phylogenetic distances retrieved from V.PhyloMaker (Jin & Qian, 2019). Residuals from this model were used to ensure subsequent analyses weren't biased by any phylogenetic signature. Methods and results for these phylogenetic analyses can be found in Appendix A.2.

2.3.3.3 Assessing Dissimilarity/Competition Relationship.

To assess whether fungal community dissimilarity is associated with competition strength (α_{ij}), we fit linear models using random pulls from the posterior distribution of the α_{ij} parameter as a response variable and mean dissimilarity estimates as a predictor. To propagate the uncertainty in both population parameters and our estimated average fungal community dissimilarity, we repeated this process 5000 times, generating distributions that quantify the uncertainty in association between competition coefficients and microbial dissimilarity. Although excluded from subsequent models, these competition models include the mean dissimilarity within species (D_{ii}), representing the degree of variability within a species' associated soil microbiome. We repeated this process with all competition coefficients as well as either inter- or intraspecific competition coefficients.

To assess how niche and fitness inequalities are related to fungal dissimilarity, it's necessary to take into account that, according to theory, niche differences must range from negative infinity to one, and fitness inequalities range from one to infinity. Therefore, instead of fitting linear models (which would make predictions outside of these ranges) we fit exponential models for niche and fitness differences that conformed to their natural asymptotes but were also free to vary in the direction and magnitude of their growth/decay rate (see Appendix A.3 for further rationale and interpretation of results). Thus, the function for niche differences was:

$$1 - \rho = 1 + a_{ND} \cdot e^{D_{ij} k_{ND}} \tag{2.4}$$

where k_{ND} is the growth/decay rate at which niche differences changed with increasing dissimilarity, D_{ij}. We bound the intercept parameter a_{ND} to be negative,

which constrains this function to remain below the asymptote of one. Given this constraint, negative values of k_{ND} represent a positive relationship between dissimilarity and niche differences.

Similarly, we fit an exponential model for fitness inequalities with the structure:

$$\frac{\kappa_j}{\kappa_i} - 1 = a_{FI} \cdot e^{D_{ij} k_{FI}} \tag{2.5}$$

where we bound a_{FI} to be positive, constraining the predicted fitness inequalities to be greater than the asymptote zero. Thus, positive values of k_{FI} represent a positive relationship between dissimilarity and fitness inequalities. We fit similar models for the competitive ratio ($\sqrt{\frac{\alpha_{jj}\alpha_{ji}}{\alpha_{ii}\alpha_{ij}}}$) and the demographic ratio ($\frac{\lambda_i}{\lambda_j}$) to identify whether an association with increased competitive ability or demographic performance drove the potential trend in fitness inequalities. For each of these models, we again fit models using 5000 random pulls from the posterior distributions of niche and fitness differences and competitive and demographic ratios and mean fungal community dissimilarities to generate distributions of a and k. To assess whether niche differences or fitness inequalities changed more or less steeply with fungal community dissimilarity, we constructed a contrast distribution by subtracting the absolute values of k_{ND} and k_{FI}. Finally, to evaluate the effect of fungal dissimilarity on the probability of coexistence, we first calculated coexistence probability as the proportion of posterior samples from the demographic models that predicted coexistence given the following criterion for coexistence reported in Chesson & Kuang 2008:

$$\rho < \frac{\kappa_j}{\kappa_i} < \frac{1}{\rho} \tag{2.6}$$

We fit a quasi-binomial regression using random pulls from the posterior distribution of mean fungal community dissimilarities and the calculated coexistence probabilities (a fractional response variable including values of zero and one). For each draw from the posteriors, we fit a glm using the glm() function in R with a logit link function, yielding a distribution of the relationship between coexistence probability and microbiome dissimilarity that takes into account underlying uncertainties in the estimates of each variable. The coexistence criterion (Eq. 6) was also used for determining the required niche differences for coexistence based on our predicted fitness inequalities (from the fitted asymptotic model of fitness inequalities as a function of mycobiome dissimilarity).

2.3.3.4 Assessing Transferability of Models. It is not uncommon to find very little predicted coexistence for species pairs in competition experiments despite their known co-occurrence in the field (Kraft et al., 2015). This discrepancy may influence our confidence that any coexistence mechanisms identified within experiments translate well to field systems. Thus, we have conducted additional analyses to try to explain any discrepancies between the predictions from our population models and known co-occurance patterns of our species pairs. Many mechanisms of coexistence in the field are, by design, absent from isolated experiments. However, we were able to investigate two other potential sources of this discrepancy: 1) poor model fit (Armitage, 2022) and 2) the omission of stabilizing indirect species interactions (Saavedra et al., 2017). Our model selection procedure outlined above and in Appendix A.1 serves as an attempt to limit the potential for poor model fit to influence our results, and we provide additional

information regarding the posterior predictions of our population models within Appendix A.1 to further contextualize our results.

To quantify the degree to which indirect interactions may lead to more or less coexistence than predicted by our pairwise approach, we have additionally implemented the structural approach for multispecies coexistence (Saavedra et al., 2017). Using this approach, we can assess which species might feasibly coexist as well as the degree to which indirect interactions underlie multispecies coexistence. To do this, we calculated the percent of species combinations across all possible n-species combinations that were predicted to feasibly coexist. We also calculated the community-pair differential, a metric which describes the degree to which n-species coexistence is more or less feasible than the coexistence of the component species pairs (Saavedra et al., 2017). For both the percent of feasible combinations and the community-pair differential, we repeated these calculations across all samples from our posterior distributions.

2.4 Results

2.4.1 Species Effect on Fungal Community Composition. The composition of fungal communities in soil samples varied among both plant species and sample type (monoculture v.s. experimental) (Figure 1). We found stronger evidence for an association between composition and sample type ($p < 0.001$; $F = 7.4655$; $R^2 = 0.0582$) than that of composition and species ($p = 0.002$; $F = 1.6102$; $R^2 = 0.0879$). Importantly, results from a PERMANOVA for the entire fungal community suggest an interaction effect between species and sample type ($p < 0.001$; $F = 1.7874$ $R^2 = 0.0976$). Because the effect of species depends on differences between the experimental and monoculture plots, we report analyses using both sample types aggregated into one dataset in the main text and include

analyses using each sample type separately in Appendix A.4. Further, a model with the z-scores of mean fungal dissimilarity and phylogenetic distance between species pairs showed a positive relationship between phylogenetic distance and fungal dissimilarity (Median Estimate = 0.57; 95% CI[0.21, 0.92]; $R^2 = 0.31$; Appendix A.2:Figure S10). These results were similar when segregating the community into trophic mode, but the average distances between plant species's fungal communities varied across the trophic modes (Appendix A.5:Figure S16).

2.4.2 Plant Population Models and Coexistence Outcomes. Out of the four model structures we assessed, the Beverton-Holt model provided the best fit to the data (Appendix A.1), so we used parameter estimates from this model for all downstream analyses. Median estimates of niche differences between the 28 species pairs were variable (Median = 0.41; Standard Deviation = 0.47). Although most species pairs had positive niche differences, four species pairs had negative niche differences, suggesting destabilized interactions. Median estimates of fitness inequalities also varied across species pairs (Median = 5.66; Standard Deviation = 33.60). Species pairs varied in their expected outcome of competition, and thus, varied in their probability of coexistence (Figure 2). Predictions made from the medians of parameters' posterior distributions suggest that competition between three species pairs result in coexistence, 25 species pairs result in exclusion, and no species pairs result in priority effects.

2.4.3 Fungal Dissimilarity and Competitive Dynamics. Overall, there was no relationship between fungal community dissimilarity and competition strength (Median = -0.61; 95% CI[-4.88,3.43]). Similarly, when divided into intra- and interspecific competition, fungal community dissimilarity was not associated with interspecific competition (Median = -0.38; 95% CI[-5.31,4.59])

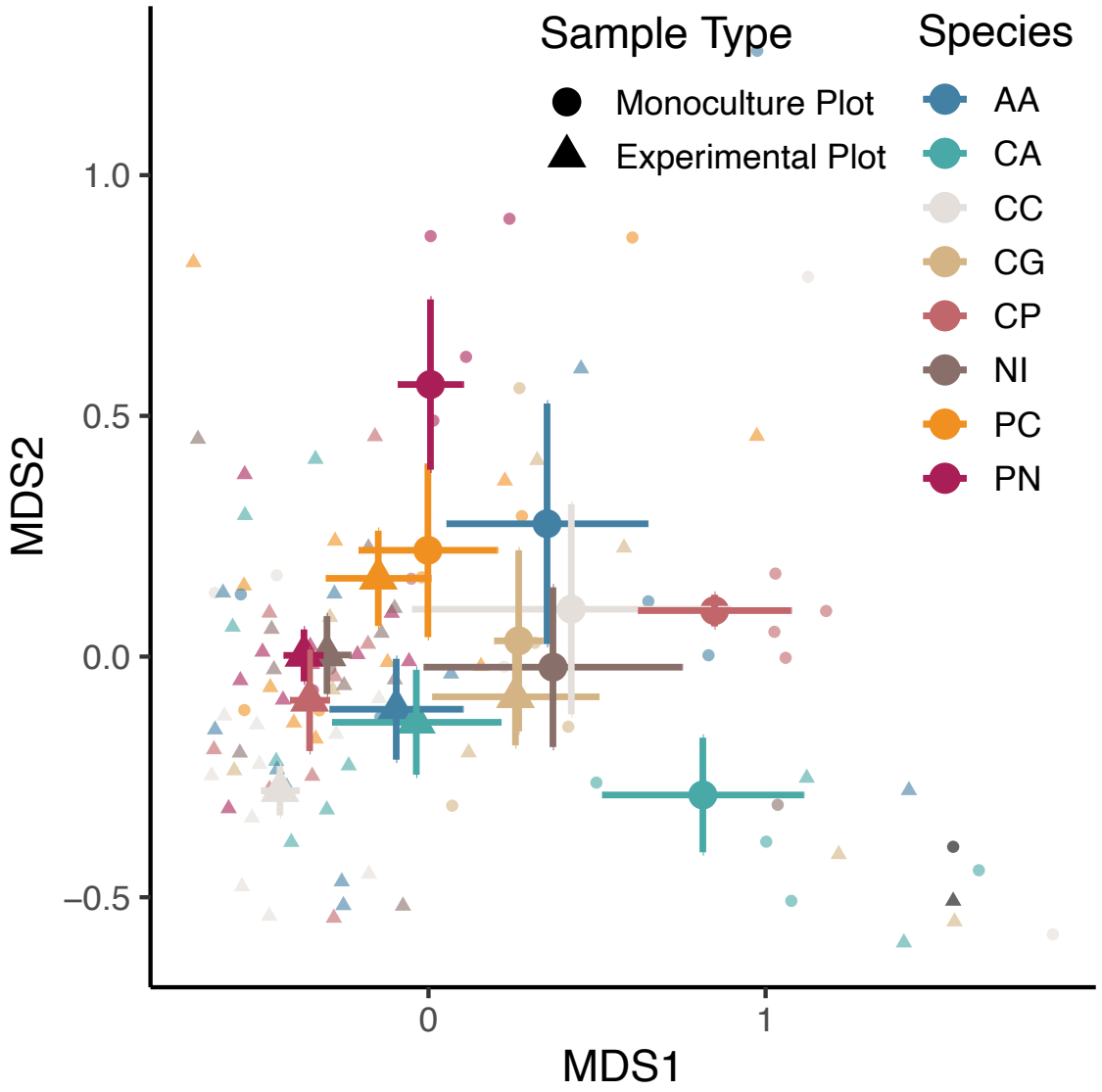

Figure 1. Non-metric multidimensional scaling using Bray-Curtis dissimilarities of total fungal community composition across all samples. Small transparent points represent sample scores; larger solid points represent the average scores with errorbars equal to one standard error. Shape of points represents which plots samples came from, and color represents which species samples are associated with.

or intraspecific competition (Median = 5.17; 95% CI[-6.57,17.70]). There was a positive association between fungal community dissimilarity and both niche differences and fitness inequalities (Figure 3A). From our distribution of 4287 niche difference k parameters, 86.49% of samples predict a positive association between dissimilarity and niche differences (Median = -6.16; 95% CI[-16.63,4.50]). From the distribution of 1063 fitness inequality k parameters, 90.03% of the ks predict a positive association between dissimilarity and fitness inequalities (Median = 6.95; 95% CI[-3.38,13.84]). There was no relationship between the competitive ratio and fungal community dissimilarity (Median = 0.58; 95% CI[-13.99, 11.78]). However, there was a positive relationship between fungal community dissimilarity and the log demographic ratio, with 88.40% of the 4959 samples predicting a positive association (Median = 3.39; 95% CI[-2.24, 10.16]). Finally, there was no difference between k_{ND} and k_{FI} (Median = -0.64; 95% CI[-12.68, 9.82]).

Interpreting these functions together, to evaluate how dissimilarity affects coexistence, the asymptotic niche difference function was consistently outside the area of coexistence calculated from the asymptotic fitness inequality function throughout the range of the observed fungal community dissimilarities. This suggests that these fungal dissimilarities, per se, cannot explain any observed coexistence (Figure 3A). However, the gap between the predicted niche differences and the minimum required niche differences for coexistence (a function of the predicted fitness inequalities) becomes more narrow as fungal community dissimilarity increases, suggesting an increased chance of coexistence. This is congruent with the results from the quasi-binomial regression which suggested that, although coexistence probabilities are consistently low within the range of fungal dissimilarity, there is a positive association between fungal dissimilarity and

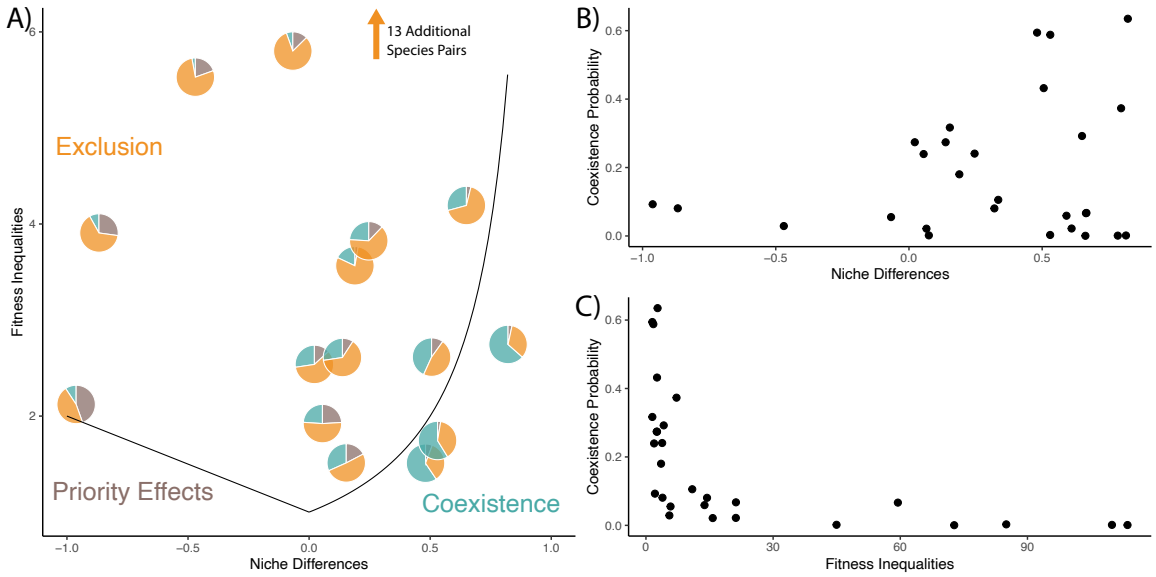

Figure 2. A) Scatterpie plot of niche differences and fitness inequalities. Each point is a pie chart representing the probability of each competitive outcome (Coexistence, Exclusion, or Priority Effects) for a given species pair. Probabilities were calculated as the proportion of posterior samples corresponding to each outcome. Position of the pie charts corresponds to the median of the distributions of niche difference and fitness inequality. Black lines represent the inequalities between niche and fitness differences that partition the outcomes (from Eq. 6). Thirteen species pairs were excluded from this graph but had large fitness inequalities and high probabilities of exclusion. B) Niche differences and C) fitness inequalities plotted against the coexistence probability for all 28 species pairs.

the probability of coexistence (Figure 3B; 96.36% $>$ 0, Median = 2.77, 95% CI[-0.25,5.89]). These trends were similar across all guilds: pathotrophs, saprotrophs, and symbiotrophs (Appendix A.5: Table A.7).

2.4.4 Model Transferability. Because the population models parameterized with the experiment overwhelmingly predicted exclusion, we explored possible reasons why the predictions of our population models do not correspond with known co-occurance patterns. Although it is possible that such discrepencies could be related to poor model fit, we used model selection of three common annual plant population models (Appendix A.1) and used parameter

estimates from the best performing model. From a posterior predictive check from this model, 95.77% of our fitness data fell within the 95% credible intervals of our posterior predictive distributions.

Additionally, indirect interactions that are not captured within our pairwise approach may cause such discrepencies between coexistence predictions and the co-occurrence patterns in the field. However, the multispecies analysis found minimal evidence for diversity-promoting intransitive competitive dynamics, with most credible intervals overlapping with 0 (Appendix A.6). All median estimates of community-pair differentials for our species combinations were between -0.1 and 0.1 (Appendix A.6: Figure S22), whereas for reference, other studies have calculated empirical community-pair differentials that spread across nearly the entire range of possible values from -1 to 1 (Granjel, Allan, & Godoy, 2023). Moreover, the percent of feasibly coexisting species combinations decreased with species richness and was highest for the two-species combinations (Appendix A.6: Figure S23).

2.5 Discussion

Most of our understanding of how microbes influence plant community dynamics have come from theory (Bever et al., 1997; Kandlikar et al., 2019; Ke & Wan, 2020) and experimental tests of net microbial effects (Kulmatiski, Beard, Stevens, & Cobbold, 2008; Pernilla Brinkman et al., 2010), yet we still lack a robust (predictive) understanding of how differences in plant species-associated microbial communities contribute to observed plant community dynamics (Forero et al., 2019). To tackle this gap in our understanding of plant-soil feedbacks, we linked molecular characterization of plant-associated fungal communities with a competition study and theoretical models of species coexistence. We found that the fungal community dissimilarity of all trophic groups of fungi (saptrophs,

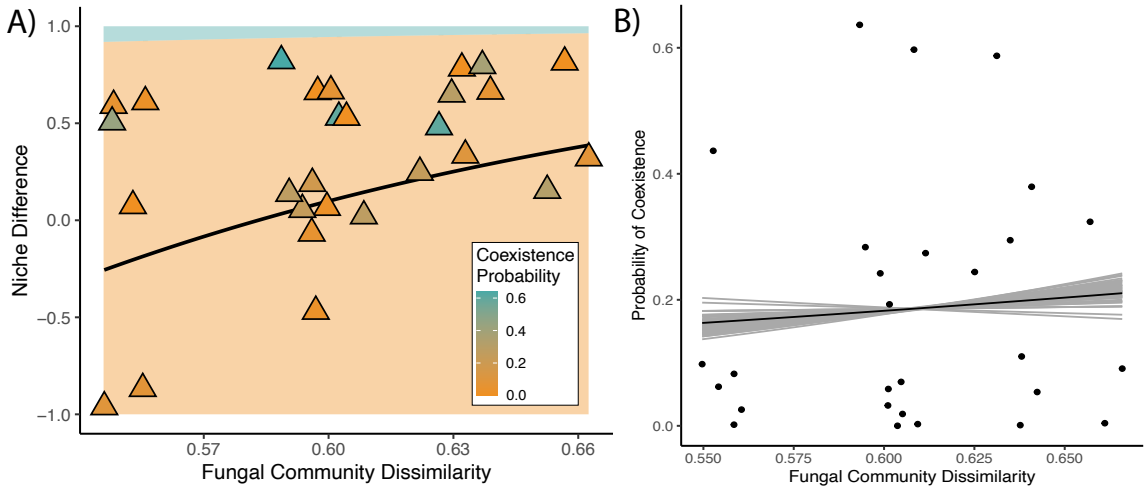

Figure 3. A) Niche differences as a function of fungal community dissimilarity. All points represent the median of the distribution for their respective quantities, and their color indicates that species pair's probability of coexistence. The black curve is the fit asymptotic equation relating niche differences to fungal community dissimilarity. The blue shaded area represents the coexistence domain when including the fit asymptotic function of fitness inequalities into the inequality statements derived from the criterion for coexistence (Eq. 6). Similarly, the orange shaded area represents the area at which species pairs would not be expected to coexist based off of the estimated fitness inequalities as a function of fungal community dissimilarity. B) Probability of coexistence as a function of fungal dissimilarity. Dissimilarity values correspond to the median posterior distributions for species pair dissimilarities. Probability of coexistence was calculated as the proportion of samples from the posterior distribution that were predicted to coexist. The black curve is the fractional logistic regression using the median slope and intercept parameters. Grey curves are 50 random draws from the distributions of slope and intercept parameters.

pathogens, mutualists/endophytes) was positively associated with both niche and fitness differences; however, fungal community dissimilarity alone was insufficient to promote coexistence. Nonetheless, a positive relationship between fungal community dissimilarity and coexistence probability suggests that the net effect of mycobiome differences contributes to competitive stabilization and thus increases in the probability of plant coexistence. These results help elucidate how shared microbes may impact the competitive dynamics of host species, suggesting that dissimilarities between species' mycobiomes cause differences in competitive dynamics that may ultimately contribute to coexistence between competing species.

Theory suggests that contributions of fungal interactions to plant competition should depend on the trophic mode of the fungus as well as species-specificity of the plant-fungal interactions (Bever et al., 2010). Overall, we found little evidence suggesting that fungal community dissimilarity affects coexistence outcomes differently between fungal trophic modes. Notably, however, we found that interspecific competition was stronger among species with more similar symbiotroph communities, counter to all other trophic modes. Symbiotroph dissimilarity also had the weakest association, although still positive, with coexistence probability. These results offer and interesting counterpoint to the long-standing hypothesis that species-specific mutualists should destabilize coexistence (C. A. Johnson, 2021). The larger lack of evidence for trophic mode-specific effects on competitive dynamics may result from our incomplete understanding of fungal ecology at the species level. Although datasets such as FunGuild offer the best understanding of the ecological characteristics of different taxa, we lack resolute functional characterization of most fungal species. Even within genera, fungi vary greatly in their ecology (Zanne et al., 2020), and particular species can exhibit a

great degree of plasticity, interacting differently with host organisms depending on their abiotic or biotic context (Donald et al., 2021; Lee, Eo, Ka, & Eom, 2013). These are general challenges to functional characterization of microbes across host-microbe systyems (S. Liu et al., 2022). Thus, continued research into the natural history and functional ecology of host-microbial interactions will allow deeper understanding of the role of particular functional groups of microbes in mediating host community dynamics.

The result that differences in mycobiome composition among plant species help stabilize coexistence is consistent with hypotheses implicating host species-specific microbial interactions (e.g. pathogenic interactions) in diversity maintenance (Bever et al., 2010). Congruent with other studies of plant-microbe mediated coexistence, there was a relationship between mycobiome dissimilarity and fitness inequalities between species pairs (Kandlikar et al., 2019; Yan et al., 2022). Unlike previous studies, however, we further dissected this relationship into the demographic and interaction components of the fitness inequalities. Interestingly, this increase in fitness inequalities was driven by a positive association between fungal community dissimilarity and differences in the demographic performance of species (measured as the demographic ratio). Thus, as opposed to exacerbating competitive asymmetries between species, distinct fungal associations may increase fitness inequalities by shifting species intrinsic growth rates, independent from competitive interactions.

Notably, our models predicted very little pairwise coexistence and that fungal community dissimilarity, *alone*, was insufficient to promote coexistence. Results from our model fit assessment suggest that poor model fit is an unlikely explanation for the discrepancy between our model predictions and known field

dynamics. Additionally, the multispecies analyses suggest that indirect interactions amongst our species pairs are not likely to increase species coexistence. It is possible that interspecific variation in germination and survival rates (unmeasured in this study) might alter fitness differences, but we have no a priori reason to believe that this variation should consistently decrease fitness inequalities (increasing predicted coexistence). Thus, it is likely that this study (and similar competition experiments) underestimates the niche differences of the community (and the stabilization offered by fungal community divergence) because both the experimental design and downstream calculations of niche and fitness differences are designed to quantify fluctuation independent mechanisms of coexistence. Although these mechanisms may be crucial for species coexistence (Armitage & Jones, 2019; Zepeda & Martorell, 2019), environmental variation leads to a myriad of fluctuation-dependent mechanisms of coexistence (Chesson, 2000). It is likely that microbial communities could also affect fluctuation-dependent stabilization, whereby the effects of fungi on plant competition interact with environmental fluctuations, because many plant-microbe interactions are highly dependent on the environmental context (Hoeksema et al., 2010; N. C. Johnson & Pfleger, 1992). Specifically, Willamette Valley prairies host considerable heterogeneity in edaphic variables (Reed & Hallett, 2023), which was absent from our experiment, and may further mediate the stabilizing potential of plant mycobiomes.

The functional traits relevant to plant-microbe interactions are likely related to the evolutionary history of plant species, suggesting an interdependence of phylogeny, traits, and species interactions (Williams et al., 2022). We found support for a plant phylogenetic signature in the soil mycobiome data, but mycobiome dissimilarity explained competitive dynamics even after accounting

for phylogenetic relatedness (Appendix A.2). Although the effects of phylogenetic distance (Godoy, Kraft, & Levine, 2014) and plant trait dissimilarities (Kraft et al., 2015) on coexistence have been explored, this is the first attempt to quantify how dissimilarity in species interactions per se (here, associated mycobiomes) may mediate coexistence. This approach may help elucidate whether plant-microbe interactions are a key mechanism underlying the complex relationships between phylogenetic distance and plant competitive dynamics (Cadotte, Davies, & Peres-Neto, 2017; Godoy et al., 2014). Future studies that also analyze plant genomes and soil metabolomics may further help identify which traits mediate the relationships between phylogeny and plant-soil feedbacks (Kardol, Veen, Teste, & Perring, 2015; Leff et al., 2018).

We collected soil samples from the competition experiment as well as monoculture beds maintained by the plant nursery for multiple years. Although the effects of dissimilarity on niche and fitness differences were generally similar when analyzing the whole dataset or samples from our experimental/monoculture plots (Appendix A.4:Figure S17), the effects on competition strength and coexistence probability differed between the datasets. These differences are related to the interaction effect between plant species and sample type in mediating fungal community composition. Species mycobiomes might vary between the two sample types for two reasons. First, monoculuture beds were spatially separated from experimental plots and had a different management history than experimental plots (i.e. recent tilling in experimental plots). Although there were no observable differences between soils during collection, we did not measure soil abiotic or chemical properties which could also vary across space. Plant-microbe interactions are highly idiosyncratic, and both spatial autocorrelation as well as management

legacy effects may mediate plant-soil feedbacks (Crawford et al., 2019; Eppinga, Van der Putten, & Bever, 2022; Wubs & Bezemer, 2016). Another reason for this soil sample discrepancy is the difference in cultivation time between these plots. In a system dominated by linear dynamics, we might expect that the effect of species in our monoculture samples resembles that in our experimental sample, but each species average composition diverges due to the additional two years of cultivation of the mycobiome. However, nonlinear dynamics that may be common in microbial communities may explain why the relative difference between species' associated fungal communities could shift as cultivation time increases (Faust, Lahti, Gonze, De Vos, & Raes, 2015). If cultivation time does lead to nonlinear trends in community composition across time, this limits the insight we can possibly gain from the sorts of ecological snapshots that are commonplace in the plant-microbe literature (Ke, Zee, & Fukami, 2021), but promising research in time-series analysis may help overcome this challenge (Chang et al., 2021; Munch, Rogers, & Sugihara, 2023).

Our results, along with others showing that microbes can affect the fitness of plant species (Kandlikar et al., 2019; Yan et al., 2022), may also have implications for the eco-evolutionary dynamics of plant-microbe systems. In addition to the mycobiome composition varying among plant species, we found considerable sample-level variation in fungal community composition even within plant species, in accordance with other studies finding significant intra-specific variation in plant-associated microbial communities (Foster et al., 2022; Lankau, 2011; Lumibao et al., 2020). If this variation is heritable, and multiple mechanisms of hertitability have been proposed for microbiomes (Opstal & Bordenstein, 2015; Wagner, 2021), the association between microbial communities and host fitness suggest

that microbiome composition may be subject to selection. Although evidence for intraspecific variation is ample and hypotheses for 'holobiont' evolution have received increased attention in the past decade (Guerrero, Margulis, Berlanga, et al., 2013; Roughgarden, 2023; Roughgarden, Gilbert, Rosenberg, Zilber-Rosenberg, & Lloyd, 2018), few models incorporate interspecific variation in shared microbial taxa between host species. Scaling up these models to a host community context may provide essential insight for understanding the mechanisms of microbiome evolution. A more refined understanding of how variation in microbial communities influences host species interactions is a key step in unravelling the eco-evolutionary dynamics of host-associated microbial communities.

2.6 Conclusion

Using a novel approach to studying the role of microbial communities in mediating plant community dynamics, we have identified a strong association between fungal community dissimilarity and both niche and fitness differences. Although the data predicts low overall probabilities of coexistence in this system, fungal dissimilarity was positively related to the probability of coexistence. Further, fungal dissimilarity was related to the demographic ratio as opposed to the competitive ratio, suggesting the predicted rise in fitness inequalities is likely due to shifts in plant species' intrinsic demographic performance in response to distinct fungal associations. Overall, these results add support for the importance of microbes in mediating plant competition. Further, these results suggest that studying the cultivation of particular microbial communities may provide insights that traditional exploration of bulk microbial effects on plants (e.g. greenhouse plant-soil feedback experiments) may miss.

2.7 Bridge

In this chapter, I have contributed to a longstanding question in community ecology: what sorts of differences between species lead to coexistence? By treating the host-associated mycobiome as a species-specific trait, I also tested a key assumption in PSF theory that differences between plant-associated microbial communities creates coexistence-altering feedbacks. The results of this chapter certainly suggest that differences in mycobiome composition may be associated with key axes of plant competitive dynamics, but these results also suggest that there are likely additional mechanisms at play that contribute to coexistence among these species. This study, like most studies in plant-microbe ecology, neglects the ubiquitous context-dependency of plant-microbe interactions. Such shifts in the composition or function of the plant-associated microbial community may alter PSF dynamics such that these snapshot studies with static models of plant-microbe interactions are unable to identify more complex processes. Both Chapters 3 and 4 investigate the potential for context-dependent plant-microbe interactions to alter plant coexistence outcomes.

CHAPTER III

ENVIRONMENTAL CONTEXT ALTERS PLANT-SOIL FEEDBACK EFFECTS ON PLANT COEXISTENCE

3.1 Contributions

I conceptualized this study and with the help of Lauren Shoemaker and Jeff Diez, carried out all analyses. I wrote the first draft of this manuscript which was further revised with the help of Lauren and Jeff.

From Collings, J.A., Shoemaker, L.G., & Diez, J. M. Environmental context alters plant-soil feedback effects on plant coexistence. (2025) *Manuscript Accepted at Ecology.*

3.2 Introduction

A central goal in community ecology is to understand the mechanisms that maintain species coexistence and promote ecological diversity, for example leading to different spatial patterns of species' contemporary distributions (Usinowicz & Levine, 2018) or temporal variability in dominance (Hallett, Shoemaker, White, & Suding, 2019). Understanding how coexistence is mediated by environmental conditions—and their inherent variability—is crucial for predicting how global change might alter these patterns of distributions and range limits, species interactions, and coexistence (Valladares, Bastias, Godoy, Granda, & Escudero, 2015). Modern coexistence theory (MCT, Chesson 2000) has become a powerful conceptual framework for investigating the underlying mechanisms maintaining species diversity, and has highlighted how differences among species may either promote coexistence or lead to competitive exclusion. This framework has recently been integrated with plant-soil feedback (PSF) theory (as originally formulated

by Bever et al., 1997) to predict how plant-microbe interactions may influence the outcomes of plant competition (Kandlikar, 2024; Ke & Wan, 2020).

Efforts to study plant-soil feedbacks using MCT have, however, neglected an important finding from plant-microbe research: that the strength and even direction of plant-microbe interactions can change depending on environmental conditions (Hahn et al., 2018; Nuske et al., 2021; Van Nuland, Ke, Wan, & Peay, 2023). Plant-soil feedbacks may exhibit environmental context-dependency either due to changes in the microbial community across environmental gradients (Francioli et al., 2018; Pérez-Jaramillo et al., 2019), or shifts in the function of particular plant-microbe interactions. The physiology of plant and/or microbial symbionts are known to depend on environmental conditions, shifting pairwise interaction along a mutualism-parasitism gradient (N. C. Johnson et al., 1997; Rogalski et al., 2021). Accounting for these context-dependencies is among the foremost challenges in applied PSF research (Smith-Ramesh & Reynolds, 2017; van der Putten et al., 2016), and although many empirical studies have highlighted its importance for PSFs (Dudenhöffer, Luecke, & Crawford, 2022; Manning, Morrison, Bonkowski, & Bardgett, 2008; Smith & Reynolds, 2015), context-dependent PSFs have not been incorporated into theory, making it unclear how much specific empirical results may generalize.

Modern coexistence theory is especially well-suited to address context-dependent plant-soil feedbacks as it provides a framework for disentangling the effects of the environment and competitive interactions on species' fitness and niche differences (Van Dyke, Levine, & Kraft, 2022; Wainwright et al., 2019; **?**). The general approach for using MCT to predict the outcome of competition involves parameterizing population models to calculate the effects of density independent

growth, intraspecific, and interspecific competition on species realized fitness (Hallett et al., 2019; Kraft et al., 2015). These competition coefficients can then be used to calculate the niche differences and fitness ratios between species, and predict whether coexistence, competitive exclusion, or priority effects will occur (Chesson, 2000; Grainger, Letten, Gilbert, & Fukami, 2019). MCT provides the conceptual and mathematical framework to then determine whether any process (such as PSF) that affects these niche differences (stabilization) and/or fitness ratios (equalization) will shift competitive interactions enough to alter coexistence outcomes.

Recent studies have demonstrated the value of modeling PSFs using the MCT framework. For example, Kandlikar et al. (2019) use a MCT framework to explore traditional models of PSFs and found that explicitly including PSF effects on fitness ratios, in addition to niche differences, can alter predictions of PSF-mediated competition compared to traditional models. An empirical application of this work found that, in fact, microbial effects on fitness ratios rather than niche differences drove the outcomes of plant-soil feedbacks (Kandlikar et al., 2021). Ke and Wan (2020) similarly developed demographic models of PSF-mediated plant population and microbial community growth to predict coexistence outcomes between competing plant populations, finding that soil microbes and plant-competitive interactions jointly determine coexistence outcomes. Although these studies have not incorporated context-dependence of PSFs, MCT is well suited to do so because of its ability to assess the role of environmental effects in mediating species interactions (Hart & Marshall, 2013; Van Dyke et al., 2022; Wainwright et al., 2019). For example, MCT can be used to compare coexistence

outcomes between sites along spatial gradients or between current and projected environmental conditions.

Another benefit of using MCT to study context-dependent PSFs is that this framework can include detailed mechanisms of how species interact while remaining analytically tractable. As a consequence, the relative importance of different interactions for driving coexistence can be assessed. For example, understanding how an abiotic variable affects PSFs and plant coexistence depends on quantifying the effect of the abiotic variable on specific species interactions and the effect of these species interactions on niche differences and fitness ratios. Although empirically quantifying all of the species interactions within a complex PSF network may be difficult (Shang et al., 2017), sensitivity analyses may be used to assess which interactions are most important for niche differences and fitness ratios (Cariboni, Gatelli, Liska, & Saltelli, 2007). The sensitivities of niche differences and fitness ratios can help identify which species interactions, and which abiotic gradients, should be the focus of empirical field and greenhouse studies.

In this study, we develop a set of models to predict species coexistence outcomes that allow for environmental context-dependency of plant-microbe interactions. We first use these models to predict how context-dependency of PSFs may impact species coexistence in a general theoretical model, highlighting the flexibility of this approach to accommodate different levels of microbial community complexity and different microbial guilds, including pathogens, mutualists, and decomposers. We then conduct a set of sensitivity analyses on the microbe-dependent plant niche difference and fitness ratio equations to compare how different environmental dependencies of particular species interactions vary in their influence on niche versus fitness differences. Finally, we adapt our models to a case

study of the invasion dynamics of garlic mustard (*Alliaria petiolata*), showing how plant-microbe interactions can mediate potential range expansion and coexistence patterns.

3.3 Method Overview

3.3.1 General Theoretical Model. Our models extend the approach formulated by Ke and Wan (2020), with two important adaptations. First, we developed a taxon-specific model of plant-soil feedbacks instead of treating the microbial community as a single generic entity (Figure 1A). Second we allowed parameters of the models to vary depending on environmental conditions. These two extensions allowed us to incorporate more biological realism and discern the specific contributions of pathogenic or mutualist taxa, as well as role of environmental variation for shaping coexistence outcomes. We use this model structure with phenomenological interaction coefficients because this approach is similar to other approaches that treat species interactions as dependent on environmental conditions (Hallett et al., 2019; Van Dyke et al., 2022; Wainwright et al., 2019). However, when species interactions are dependent on the abundance of consumable resources, system dynamics may be determined by more complicated feedbacks between plants, microbes, and resources which may be captured better with more mechanistic resource-consumption models.

In this formulation, competing plant population growth was modeled for each plant species A and B:

$$\frac{dN_A}{dt} = r_A N_A(1 + c_{AA}N_A + c_{AB}N_B + \sigma_{AX}S_X) \tag{3.1}$$

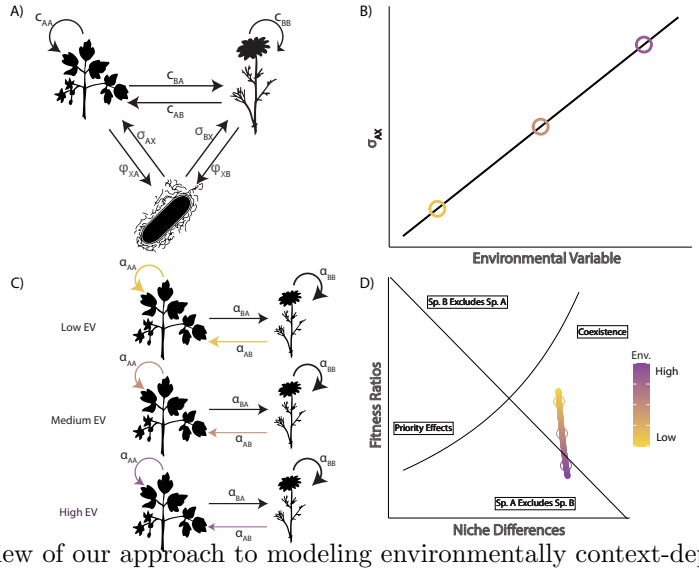

Figure 4. Overview of our approach to modeling environmentally context-dependent PSF-mediated coexistence. We first constructed a taxon-explicit model of a plant-soil feedback A) in which any number of microbial taxa may have taxon-specific interactions with the two competing plant species. Plants compete with one another directly through the microbe-independent competition coefficients (c) and indirectly through the cultivation of soil microbes (ϕ) and the consequential effect of these microbes on each plant species (σ). We define a function B) that scales a parameter of interest (σ_{AX} in this example, though other parameter scaling combinations are explore elsewhere in the text) across an environmental gradient. Colored circles indicate discrete environmental contexts to be examined in C) and D). The downstream effect of scaling this particular parameter is shown in C) where overall competition coefficients (α) vary depending on where the species interaction is taking place along the environmental gradient. Finally, these shifts in competition coefficients lead to shifts in niche differences and fitness ratios, D) that might alter predicted coexistence outcomes. Here, the environmental context-dependency of these plant-microbe interactions acts as an equalizing mechanism, reducing fitness ratios at low values of the environmental variable (EV) enough to maintain stable coexistence. Organism silhouettes retrieved from PhyloPic (phylopic.org). Modified silhouettes for species A, B, and X were originally created by T. Michael Keesey, David García-Callejas, and Matt Crook respectively. The license for the species A and B silhouettes are both `https://creativecommons.org/publicdomain/mark/1.0/` and the license for species X is `https://creativecommons.org/licenses/by-sa/3.0/`.

$$\frac{dN_B}{dt} = r_B N_B(1 + c_{BB}N_B + c_{BA}N_B + \sigma_{BX}S_X) \tag{3.2}$$

where N_i is the population sizes of plant species A when $i = A$ and species B when $i = B$, respectively. Parameter r_i is the intrinsic growth rate, c_{ii} denotes the intraspecific competitive effect, c_{ij} denotes the competitive effect of plant species j on species i, and σ_{iX} is the effect of a microbial taxon X on plant population i. S_X is the population size of microbial taxon X, and its growth was modeled using the logistic equation:

$$\frac{dS_X}{dt} = g_X S_X(1 - \frac{S_X}{k_X}) \tag{3.3}$$

where g_X is the intrinsic growth rate of the microbe X. To reflect the expectation that microbe abundance is strongly affected by the plants, the carrying capacity of the microbe, k_X, was defined as:

$$k_X = \phi_{XA}N_A + \phi_{XB}N_B \tag{3.4}$$

where ϕ_{Xi} is the rate by which each plant i cultivates the microbe X. This adaptation of the original models proposed by Ke and Wan (2020) allowed flexibility to include any number of microbial taxa as well as the ability for each taxon to have either generalist or species-specific σ_{iX} and ϕ_{Xi} terms.

To incorporate environmental context-dependence of PSF, each model parameter above (i.e. c_{ij}, σ_{iX}, or ϕ_{Xi} terms) could vary with environmental conditions according to a scaling function (Figure 1B). Here, we focused on the direct effect of microbial taxa on plant population size (σ_{iX}) because of its central importance in PSF research (Bever, 2003; Bever et al., 1997; Caruso & Rillig,

2022), and conducted a sensitivity analysis (described below) to determine the importance of each parameter on overall outcomes. We also assumed a linear effect of environmental conditions on these parameters, but explored the implications of nonlinear relationships (Appendix B.1). Thus, a generic structure for these linear scaling functions of, for example parameter σ_{iX}, where v is an environmental variable, is:

$$\sigma_{iX} = \hat{\sigma}_{0,iX} + v * \hat{\sigma}_{1,iX} \tag{3.5}$$

where the observed value of the microbial effect on a plant species, σ_{iX}, is a function of the intercept of the linear scaling function, $\hat{\sigma}_{0,iX}$, the value of the environmental variable, v, and the sensitivity of σ_{iX} to the v, $\hat{\sigma}_{1,iX}$. The hat denotes intermediate parameters that alter the net microbial-plant interactive effect.

3.3.2 Calculating Coexistence. Similar to Ke and Wan (2020) and consistent with the two-species Lotka-Volterra formalization (Chesson, 2013), we calculated the two axes of coexistence - fitness ratios and niche differences - as a function of the interspecific and intraspecific competition coefficients (α_{ij}). Using the Lotka-Volterra model structure defined by Ke and Wan (2020), we calculate α_{ij} values as:

$$\alpha_{ij} = c_{ij} + \sum_{X=1}^{n} \sigma_{iX}\phi_{Xj} \tag{3.6}$$

where i and j can each be either plant A or B and X are the microbial taxa.

Using these α_{ij} values, we calculated fitness ratios as:

$$\frac{f_B}{f_A} = \sqrt{\frac{\alpha_{AA}\alpha_{AB}}{\alpha_{BB}\alpha_{BA}}} \tag{3.7}$$

We calculated niche overlap (ρ) as:

$$\rho = \sqrt{\frac{\alpha_{AB}\alpha_{BA}}{\alpha_{AA}\alpha_{BB}}} \tag{3.8}$$

and niche differences were then defined as $1 - \rho$. As we have calculated them, the fitness ratios measure the relative difference between the overall competition experienced by the two species, and the niche differences measure the extent to which the interaction is stabilized by negative frequency dependency. Together, fitness ratios and niche differences can be used to evaluate the outcome of competition according to the predictions made by MCT. Given that the environment alters σ_{iX}, it also modifies competition coefficients α_{ij} and both niche differences and fitness ratios between plant species (Figure 1C,D). These metrics depend on the exact structure of the bipartite plant-microbe network, which can vary in microbial taxonomic richness and specificity of plant-microbe interactions. We explore multiple plant-microbe interaction structures in this paper, and an overview of the model structures referenced in the main text can be found in Appendix B.2.

3.4 Results & Case Studies

3.4.1 Theory Simulations.

3.4.1.1 Methods. We first conducted a set of theoretical simulations, with varying effects of microbes and complexity of microbial communities to test how interactions between microbes and the environment influence plant coexistence. In each of the simulations, we began with microbe-independent

competition coefficients that allowed the competing species to stably coexist: $c_{AA} = -0.06$, $c_{BA} = -0.05$, $c_{BB} = -0.075$, and $c_{AB} = -0.06$. For each set of simulations, we calculated niche differences and fitness ratios to predict coexistence, competitive exclusion, and priority effects outcomes. Because we are particularly interested in the scaling of species interaction terms, we assumed that plant species have the same intrinsic growth rates. Because of this assumption, the exact value of the plant intrinsic growth rate does not influence the results of our analyses but would alter the exact equilibrium abundances of species. Therefore, we do not specify values for intrinsic growth rates.

To first simply ask how the presence of microbes may influence plant coexistence, we simulated the competitive dynamics between these two plant species under a constant set of environmental conditions (no scaling function) and three distinct microbial parameterizations that represent three alternative systems: sterile ($\alpha_{ij} = c_{ij}$; ThSi I), a single mutualist associating with species A ($\sigma_{AX} = 0.002$, $\phi_{XA} = 10$; ThSi II), and an additional mutualist taxon associating with species B ($\sigma_{BZ} = 0.0025$, $\phi_{ZB} = 10$; ThSi III).

To explore how an environmental gradient can affect plant coexistence in the absence of microbially-mediated context-dependence, we then used the same baseline parameterization in sterile conditions to simulate competitive dynamics along an environmental gradient by scaling the microbe-independent competition coefficients. We defined the scaling parameters such that species A experienced less competitive effects with higher values of the environmental variable (as in the case of a species limited by a particular resource). Thus, we defined the scaling parameters for the slope of competition across environmental gradient v as $\hat{c}_{1,AA} = 0.0025$, $\hat{c}_{1,BA} = 0.001$, $\hat{c}_{1,BB} = 0.001$, and $\hat{c}_{1,AB} = 0.0015$; intercepts are defined

according to the sterile conditions above ($\hat{c}_{0,AA} = -0.06$, $\hat{c}_{0,BA} = -0.05$, $\hat{c}_{0,BB} = -0.075$, and $\hat{c}_{0,AB} = -0.06$).

Finally, we parameterized our models to explore how microbial symbionts may indirectly mediate plant coexistence along an environmental gradient. Thus, we defined linear functions to scale both mutualists' effects on their respective plant symbionts (σ_{iX}) in the ThSi III model by an environmental variable such that both mutualists became less beneficial, and even became pathogenic, as the value of the environmental variable increased (but at different rates, with $\hat{\sigma}_{1,AX} = -0.00015$ and $\hat{\sigma}_{1,BZ} = -0.0003$). Intercepts are defined as above, with $\hat{\sigma}_{0,AX} = 0.002$ and $\hat{\sigma}_{0,BZ} = 0.0025$.

3.4.1.2 Results. Introducing a mutualist associated with species A resulted in a loss of coexistence due to reduced intraspecific competitive effects for Species A (Figure 2A, grey circle). While one species possessing a mutualist allows this species to outcompete the other, when both species have species-specific mutualists (Figure 2A, black circle) decreased niche differences destabilize coexistence, thus resulting in priority effects, where competitive exclusion is based on species arrival order. These simulations demonstrate the possible destabilizing effects of species-specific mutualists.

We also assessed the role of environmental variation, independent of microbial effects, in influencing plant species coexistence through fluctuation-independent mechanisms of coexistence (Figure 2B). Scaling competition coefficients linearly by the environmental variable yielded different coexistence outcomes along an environmental gradient. Specifically, because competitive effects on species A were more environmentally sensitive than those on species B, fitness ratios increased along the gradient and caused competitive exclusion. This

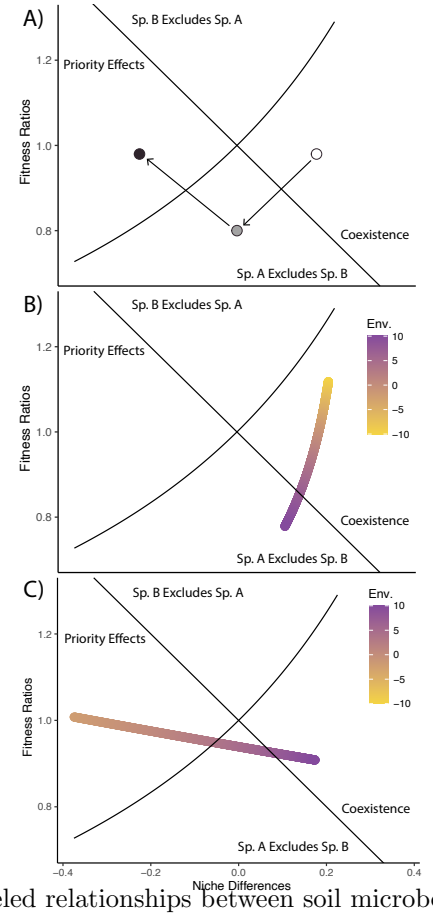

Figure 5. Synthesis of modeled relationships between soil microbes, environmental variables, and plant competition outcomes. A) Simulated competition outcomes under sterile conditions (open circle) and two live conditions independent of environmental variability. Live conditions include the sequential addition of a species-specific mutualist for sp. A (grey circle) and for sp. B (black circle). Arrows represent how the addition of microbes might alter niche differences and/or fitness ratios between competing species, thereby altering the predicted outcome of competition. B) Simulated competition outcomes in sterile conditions along an environmental gradient independent of microbes. The circle around the first colored point indicates the point in coexistence space in live conditions when the value along the environmental gradient is 0. C) Simulated competition outcomes live conditions (colored points) along an environmental gradient. The circle around the first colored point indicates the point in coexistence space in live conditions when the value along the environmental gradient is 0. The environmental variable affects plant competition indirectly through linear scaling of σ terms.

illustrates a microbe-independent avenue for altered competitive outcomes along an environmental gradient.

The final set of theoretical simulations incorporated PSF with environmental context dependency (Figure 2C). As the environmental condition increases, the benefit received from the mutualist decreases, but unequally for these species. Ultimately, this results in priority effects when the environmental variable is low (with both symbionts behaving like mutualists), coexistence when the environmental variable is high (with both symbionts behaving like pathogens) and exclusion by species A at intermediate values for the environmental variable.

3.4.2 Sensitivity Analysis.

3.4.2.1 Methods. To identify which types of species interactions may influence plant coexistence dynamics the most, we performed a local sensitivity analysis on a PSF model containing two competing plant species and one shared microbial taxon (SeAn model). The output of this analysis identifies whether the environmental-dependence of particular species interactions might be more or less consequential for niche and fitness differences and plant coexistence. To do this, we sequentially varied each parameter, holding all other parameters constant, and computed the niche differences and fitness ratios across the parameter range. The baseline parameterization for this analysis was $c_{ii} = -0.06$, $c_{ij} = -0.055$, $c_{jj} = -0.075$, $c_{ji} = -0.05$, $\sigma_{iX} = -0.002$, $\sigma_{jX} = -0.00225$, $\phi_{Xi} = 10.5$, $\phi_{Xj} = 10$. The minimum and maximum parameter values used to constrain the sensitivity analysis were as follows: competition coefficients, $c_{ij} = [-0.1, 0]$; cultivation rates, $\phi_{Xi} = [0, 20]$; and microbial effects on plants, $\sigma_{iX} = [-0.01, 0.01]$. These distributions represent reasonable parameter values, but their magnitudes likely depend on the life history strategy of the microbial taxon. Specifically,

our parameterization represents microbial taxa that are cultivated rapidly but that have small per-capita (per-cell) effects on plants. Alternatively, there may be rare but impactful microbial taxa, or one could parameterize this model in terms of hundreds or thousands of cells, in which case reasonable ϕ values would be relatively small and σ values would be much larger. Because the relative importance of ϕ and σ is dependent on these parameterization decisions (for which there is little empirical research to guide), we also present the sensitivity of niche and fitness differences to the product of ϕ_{ix} and σ_{xj} which represents the indirect effect of a plant on it's competitor via the cultivation of the microbial taxon (ie the plant-microbe feedback). We notate this plant-microbe feedback term as m_{ij} and set the minimum and maximum values for this parameter as -0.2 and 0.2 respectively (ie the minimum and maximum possible values based on the ranges of ϕ and σ defined above). Appendix B.3 contains information about these sensitivities, including a sensitivity analysis of the fitness inequalities, which are the maximum value of the fitness ratios for the two species, a comparison of these results to those of a partial derivative-based local sensitivity analysis and a simulation-based global sensitivity analysis, and a comparison of the sensitivity results across a gradient of microbial taxonomic richness.

3.4.2.2 Results. The component species interactions in our theoretical PSF model vary in their relative contribution to niche differences and fitness ratios (Figure 3). The niche differences monotonically increased (in the case of all plant-microbial interaction terms and the intra-specific competition coefficients) or decreased (in the case of inter-specific competition coefficients). The general steepness of each of these curves (sensitivity) depended on the focal parameter identity and value (Figure 3A, 3C & 3E). Shifts in plant-plant interactions resulted

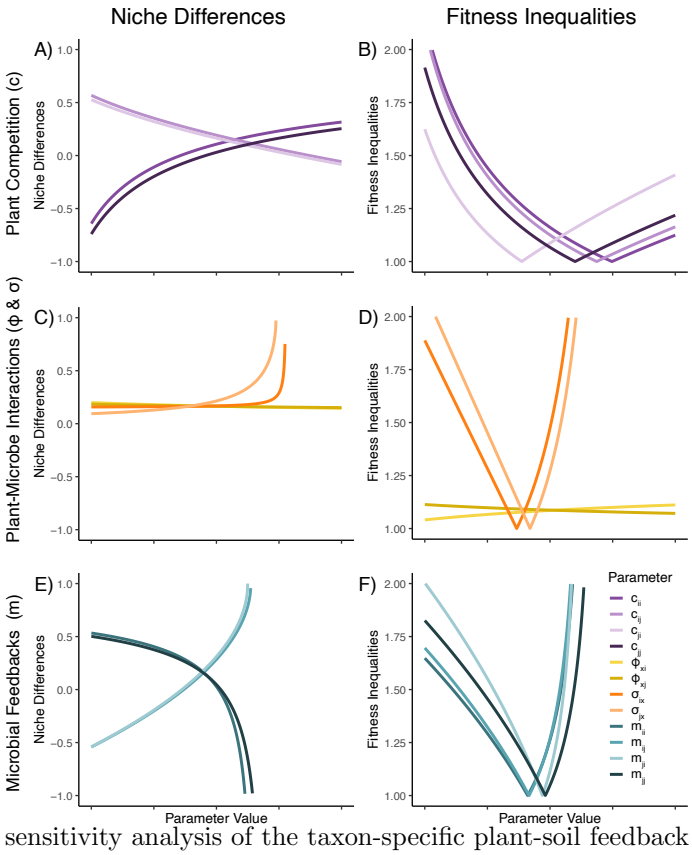

Figure 6. Visual sensitivity analysis of the taxon-specific plant-soil feedback Lotka-Volterra model. Lines represent the changes in niche differences (A, C, & E) and fitness ratios (B, D, & F) as the focal parameter varies from it's minimum to maximum value while all other parameters are held constant at their baseline values. Dashed lines represent interspecific plant interactions. Panels A & B show sensitivity to microbe-independent competition, panels C & D show sensitivity to plant-microbe interactions, and panels E & D show sensitivity to microbial feedbacks (ie the products of the plant-microbe interactions). Horizontal black lines show the value for the niche differences or the fitness ratio at the baseline parameterization, so the point at which each curve overlaps with the horizontal line is the position of the baseline parameter on the standardized axis. Some curves appear truncated as the value of the parameter gets closer to pushing the overall interaction terms (α) into facilitation, for which our definitions of niche differences and fitness ratios are undefined.

in steep shifts in niche differences, whereas plant-microbe interactions had a smaller influence on niche difference (aside from a boundary behavior as the σ values push overall interaction coefficients closer to zero). Finally, increasing the value of the pathogenic microbial feedbacks (m) (thus decreasing the strength of the overall feedback as they become less negative and approach zero) impacted the niche differences more so than direct plant-microbe interactions (σ & ϕ) but less so than microbe-independent competition (c). Interspecific pathogenic feedbacks increased niche differences as they weakened in strength whereas intraspecific pathogenic feedbacks decreased niche differences as they weakened in strength.

Distinct from the niche differences, fitness ratios monotonically increased with those species interactions that decreased the fitness of the competitively inferior species and decreased with those that decreased the fitness of the competitively superior species (Figure 3B, 3D, & 3F). Further, the fitness ratios were much more sensitive to microbial effects on plants (σ) and least sensitive to plant cultivation rates (ϕ) throughout much of the range of the focal parameter. The fitness ratios had intermediate sensitivity to the plant-plant interaction coefficients and the microbial feedback terms. Relationships between parameter values and the fitness inequalities are explored in Appendix B.3 (Figure S3). While most of these results were consistent across different types of sensitivity analyses, the importance of direct plant competition and the importance of microbial feedbacks, as measured by the partial derivative based local sensitivity analysis, did not differ (Appendix B.3: Figure S5).

3.4.3 Application to a Species Invasion.

3.4.3.1 Methods. To explore how these theoretical findings that environmental conditions can mediate the effects of PSFs on plant coexistence, may

help inform empirical examples, we altered simulations based on recent work on an invasive plant, *Alliaria petiolata*, as there is a general hypothesis that context dependencies in PSFs may help facilitate plant invasions and range-expanding native species (van der Putten et al., 2016). *Alliaria petiolata* was introduced to North America from Europe, causing decreased local native plant diversity and altered community structure in northeastern hardwood forests (Rodgers, Stinson, & Finzi, 2008). This invasion is a useful case study because of the well documented shifts in microbial community composition in response to *A. petiolata* invasions (Anthony, Stinson, Trautwig, Coates-Connor, & Frey, 2019; Duchesneau, Golemiec, Colautti, & Antunes, 2021). Additionally, extensive research has been conducted on the potential for allelopathic chemicals produced by *A. petiolata* to inhibit mutualisms between competing plants and soil microbes (Cipollini, 2016; Wolfe, Rodgers, Stinson, & Pringle, 2008). Recent work has called for increased attention to the context-dependencies of species interactions involved in *A. petiolata* invasions (Rodgers et al., 2022). For example, Blossey et al. (2021) found that *A. petiolata* growth rates decrease over time after initial invasion and hypothesized that this decrease might be due to a negative plant-soil feedback. Further, the rate of decrease for *A. petiolata* growth rates varied by geographic location, suggesting that environmental context might alter the dynamics of the plant-soil feedback.

We applied our modeling approach to explore how these geographically distinct plant-soil feedbacks following invasion by *Alliaria petiolata* may arise (Blossey et al., 2021). We started with a baseline scenario in which, under sterile conditions, one species is competitively dominant over the other, and then introduced the effects of environment-dependent PSFs. Microbes were introduced with increasing functional complexity (different microbial guilds) including: 1) a

species-specific pathogen affecting the competitively dominant species, *A. petiolata* (InSi I), 2) the same species-specific pathogen and an additional species-specific mutualist impacting the native, competitively inferior species (InSi II), and 3) both the species-specific pathogen and mutualist as well as a generalist decomposer (InSi III). Finally, in each of these simulations, we calculated coexistence outcomes along a precipitation gradient, with the environmentally-dependent cultivation parameter (ϕ_{XI}). Because we used linear scaling functions, we set all negative values of ϕ to zero. We provide an overview of scenarios here; full details and parameterizations can be found in the Appendix B.4. Note that because the cultivation rate cannot fall below zero, we use a piece wise function that scales linearly when the output of the scaling function is ≥ 0 and remains at 0 otherwise.

We first considered a simplified set of "key players" in the system, where *A. petiolata* (A) competed with a native competitor (B) and cultivated a species-specific pathogen (X). Thus, *A. petiolata* population growth rate was calculated as:

$$\frac{dN_A}{dt} = r_A N_A(1 + c_{AA}N_A + c_{AB}N_B + \sigma_{AX}S_X) \tag{3.9}$$

and the growth rate of the native competitor was calculated as:

$$\frac{dN_B}{dt} = r_B N_B(1 + c_{BB}N_B + c_{BA}N_A) \tag{3.10}$$

such that the pathogen affected the growth rate of *A. petiolata* but not that of the native competitor.

As a baseline, we parameterized the models such that at some environmental average, and in sterile conditions, *A. petiolata* outcompetes its native competitor.

Thus, the c_{ij} terms were set such that $|c_{AA}| < |c_{BA}|$ and $|c_{BB}| > |c_{AB}|$ (absolute values because we define competitive interactions as negative c values). The parameters for σ_{AX} and ϕ_{XA} were selected such that at average environmental conditions, the pathogenic effect on *A. petiolata* enabled species coexistence. Finally, we used a linear scaling function to define how the cultivation of the pathogen by *A. petiolata* increases with increased soil moisture.

We next added two additional taxa, increasing model complexity and realism. First, we added a species-specific mutualist for the native competitor (InSi II). Based on the response of mycorrhizal fungi to drought found by Lozano, Aguilar-Trigueros, Roy, and Rillig (2021), we defined a scaling function such that the cultivation of the mutualist by the native competitor decreases as soil moisture increases. Lastly, we added a generalist decomposer that benefited both species (via, e.g. nutrient mineralization; InSi III) and its cultivation by both species increased as soil moisture increases.

For all simulations, we calculated α_{ij} terms, fitness ratios, and niche differences in sterile and live conditions and under a range of soil moisture values. From these values, we examined how the context-dependency of plant-microbe interactions were predicted to alter competitive outcomes between *A. petiolata* and the native competitor.

3.4.3.2 Results. In the InSi I model, we found that the ability of pathogens to shift competitive outcomes between the native species and competitively superior invader from exclusion to coexistence depended on soil moisture (Figure 4B). At low soil moisture levels, the pathogen was not cultivated quickly enough to confer a stabilizing effect on the invasive species. However, as soil moisture increased, the cultivation of the pathogen occurred more rapidly

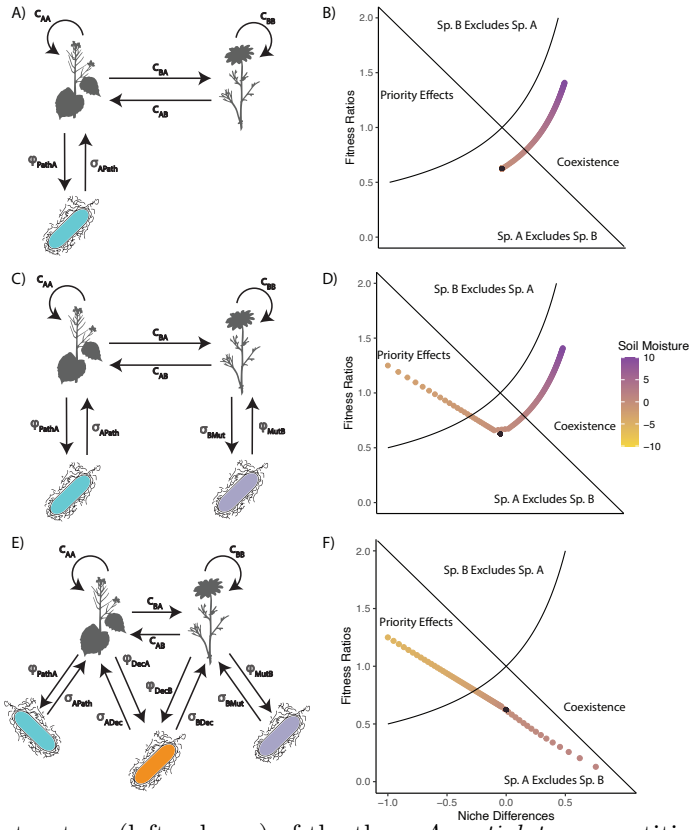

Figure 7. Model structure (left column) of the three *A. petiolata* competition models alongside their simulated competition outcomes across a soil moisture gradient (right column). A) A species-specific pathogen is both cultivated by (ϕ_{XA}) and negatively impacts (σ_{AX}) *A. petiolata*, stabilizing competition between *A. petiolata* and the native competitor. B) Cultivation of the pathogen causes the two species to coexist at high soil moisture, whereas at low soil moisture *A. petiolata* outcompetes the native. C) Adding to the previous model, a species-specific mutualist both cultivates (ϕ_{YB}) and positively affects (σ_{BY}) the native competitor. D) Depending on soil moisture levels, priority effects (low soil moisture), competitive exclusion, or coexistence (high soil moisture) is predicted. E) The last model builds upon previous models by including a generalist decomposer that benefits both *A. petiolata* (σ_{AZ}) and the native competitor (σ_{BZ}) and is cultivated by both *A. petiolata* (ϕ_{ZA}) and the native competitor (ϕ_{ZB}). F) Cultivation of the decomposer by both *A. petiolata* and the native competitor yields priority effects or competitive exclusion of the native, depending on soil moisture. Black dots on the right column panels represent the niche differences and fitness ratios in the absence of microbes. This dot deviates from the curve when the intercept of the scaling functions of multiple microbial terms are unequal (such that simulated microbial systems never become equivalent to sterile conditions). Organism silhouettes retrieved from PhyloPic (phylopic.org). Modified silhouettes for species A, B, and the microbes were originally created by Michelle Jackson, David García-Callejas, and Matt Crook respectively. The license for the species A and the microbe silhouettes are both `https://creativecommons.org/licenses/by-sa/3.0/` and the license for species B is `https://creativecommons.org/publicdomain/mark/1.0/`.

resulting in higher overall intraspecific competitive effects for the invasive species. At high soil moisture levels, stabilization by the pathogen was sufficient to result in coexistence.

When adding a species-specific mutualist that interacts with the native species in the InSi II model, increasing soil moisture not only increased the cultivation of the species-specific pathogen, and thus the intraspecific competitive effect on the invasive species, but it also decreased the cultivation of the mutualists, increasing the intraspecific competitive effect on the native species (Figure 4D). Note that the cultivation rates are constrained to be greater than or equal to zero, creating the piece wise structure to Figure 4D when one or both cultivation rates reach and remain at zero. Thus, at high soil moisture levels, the dynamic still results in coexistence, as in the simulations with no mutualist, but the decreased cultivation of the mutualist equalizes the interaction by keeping fitness ratios closer to zero. Another new outcome from these simulations is that at low soil moisture levels, the decreased cultivation of the pathogen and the increased cultivation of the mutualist result in priority effects. Therefore, the combined alleviation of the invasive species' negative soil feedback and the increase in the native species' positive soil feedback can actually destabilize coexistence, where competitive exclusion now depends on species arrival order.

Finally, we examined how the addition of a generalist microbial decomposer in the InSi III model, cultivated by and providing nutrient access to both plant species, may impact coexistence (Figure 4E). Positively scaling the cultivation of the decomposer by both species with soil moisture resulted in no stable coexistence predicted along the soil moisture gradient (Figure 4F). At low soil moisture levels, the decreased cultivation of the decomposer resulted in similar priority effects from

the previous set of simulations. Increasing the soil moisture increased the niche differences and decreased fitness ratios, eventually resulting in exclusion of the native species by the invasive species.

3.5 Discussion

The strength and effect of species interactions, including plant-soil feedbacks, can depend strongly on underlying environmental conditions, with the magnitude and even direction (e.g. competitive vs. facilitative) of interactions being dependent on the environment (Hahn et al., 2018; Nuske et al., 2021). In order to incorporate the widely-observed environmental context-dependencies into models of plant-soil feedbacks and determine the effects on species coexistence, we have explicitly modeled distinct microbial taxa instead of whole-communities and allowed key PSF parameters to vary with the environment. Simulations support the mounting empirical evidence that context-dependent, inter-guild species interactions may influence the outcome of competition (Karakoç, Clark, & Chatzinotas, 2020; Thurman, Barner, Garcia, & Chestnut, 2019). Our sensitivity analysis suggests that while niche differences are generally more sensitive to shifts in direct plant competition than shifts in plant-microbe interactions, the fitness ratios are generally more sensitive to shifts in plant-microbe interactions. Further, the invasive species simulations suggest that even simple context-dependent interactions can flip coexistence outcomes along an environmental gradient, especially when including multiple microbial guilds, as commonly occur in nature. These findings indicate that ignoring these context-dependent species interactions, as many empirical studies do for logistical reasons, likely leads to erroneous conclusions about competitive dynamics and suggest caution in extending results from one environmental context to other scenarios. Overall, these results suggest

several lines of future research needed to adequately incorporate microbial effects into plant coexistence studies, and highlight the importance of ecological context-dependencies beyond single trophic levels.

The *A. petiolata*-inspired simulations highlight key issues in the biogeography of invasive species. First, these simulations suggest that site-specific environmental conditions (e.g. soil moisture) coupled with PSF could be responsible for the region-specific rates of decline in *A. petiolata* growth rates reported by Blossey et al. (2021). Identification of the key microbial taxa causing the negative PSF and research on their responses to spatial heterogeneity is likely to provide further insight into the invasion dynamics of *A. petiolata* across North America. Second, these results implicate context-dependent species interactions as one reason for inconsistencies across studies of invasive species. Although most hypotheses for invasion success explicitly acknowledge spatial differences (either biotic or abiotic) between invaders' home range and invaded range (Enders et al., 2020), most of these hypotheses have received deeply conflicting support (Gallien & Carboni, 2017). Further, few hypotheses explicitly acknowledge spatial differences within the invaded range. This may, in part, be due to spatial heterogeneity at multiple scales influencing invasion success through context-dependent biological interactions. For example, our findings are consistent with research that has shown how the enemy release of invasive species can be driven by context-dependent interactions with soil microbes (McGinn et al., 2018; Nuske et al., 2021). Recognition of context-dependent interactions between invasive species and soil microbes is likely to help resolve apparent contradictions within traditional invasion biology hypotheses.

The sensitivity analyses indicated that shifts in the component species interactions of plant-soil feedbacks do not equally affect competitive dynamics between plant species. Most notably, we found that while niche differences were generally more sensitive to direct plant competition than plant-microbe interactions, microbial effects on plants affected fitness ratios more so than direct plant competition, demonstrating the importance of microbe-induced fitness ratios (Kandlikar et al., 2021; Yan et al., 2022). Conversely, the local sensitivity of niche differences and fitness ratios, while certainly dependent on baseline parameter values, were the same with respect to microbe-independent competition and microbial feedbacks, highlighting the dependency of sensitivity results to the exact parameterization of the PSF model. Nevertheless, the direct plant-microbe sensitivity results are consistent with recent assessments of multitrophic communities that identified trophic-level-specific relative importances of niche versus fitness differences (C. Song & Spaak, 2024; C. W. Song & Spaak, 2023). The mathematic mechanism for our results involves the additive function within the numerator of the partial derivative of the niche differences with respect to σ (Appendix B.3: Eq B9 & B10), which is absent from that of the fitness ratio (Appendix B.3: Eq 17 & Eq 18). Ecologically, these microbial terms largely determine how species might differ in the degree to which they can capitalize on or are negatively affected by the microbial community that both species are experiencing. Thus, shifts in these microbial-plant species interactions are more so related to the difference in the baseline fitness of species rather than potential differentiation of niche space, as might occur under specialized plant-microbe interactions.

Importantly, network characteristics of the coupled plant-microbe community may determine how context-dependent PSFs mediate plant coexistence. Microbial taxonomic richness, species specificity of plant-microbe interactions, and the exact sign and strength of species interactions are all likely to impact specific mechanisms of plant coexistence, and while it is beyond the scope of this paper to test each of these, we do show how variation in some of these network characteristics influences coexistence in the simulations. Further, we tested whether microbial taxonomic richness impacts the inference we have made about distinctive roles of plant-plant interactions and plant-microbe interactions in determining niche differences and fitness ratios. We found little evidence that taxonomic richness per se influences these key findings. However, other unexplored aspects of network structure may still complicate these findings. Notably, the importance of σ as opposed to ϕ is a result of the baseline parameterization which reflects our assumption that microbes have high equilibrium densities and low per capita impacts on plants (i.e. any one microbe has relatively weak impacts on plants). While the particular plant-microbe interaction (ϕ or σ) which impacts the fitness ratio depends on this assumption, the general finding that one of these terms influences fitness differences more so than direct plant-plant interactions do remains constant across a variety of parameterizations. It is also worth noting that all sensitivity analyses require a priori assumptions about parameters, many of which are untested in plant-microbe communities. Research on general patterns of coupled plant-microbe networks may guide similar analyses in the future.

In addition to spatial context dependencies, plant competition and invasion dynamics are likely to exhibit temporal context-dependencies, given annual climatic variation and now rapid climate change. Directional shifts in annual

climate variables such as temperature, drought, and atmospheric CO_2 levels, are predicted to alter the dynamics of soil microbial communities (Pugnaire et al., 2019). Greenhouse studies have found support for drought-induced legacy effects on PSF's but have found no support for temperature-dependent PSFs J Gundale and Kardol (2021); Kaisermann, de Vries, Griffiths, and Bardgett (2017). However, van Grunsven et al. (2010) suggest that future research on the effect of climate change on PSFs should acknowledge many interacting abiotic and biotic factors. Although these models highlight how directional changes in mean environmental conditions (e.g. via climate change) may impact coexistence outcomes, interannual variation may also be important (Rudgers et al., 2020). Thus, future modeling efforts should extend our approach to modeling context-dependent PSFs by incorporating the potential for fluctuation-dependent stabilization.

Predicted shifts in temporal autocorrelation of environmental variables (e.g. temperature) are likely to influence species interactions (Di Cecco & Gouhier, 2018; Gudmundson, Eklöf, & Wennergren, 2015). These fluctuation-dependent mechanisms of species coexistence have been a cornerstone of modern coexistence theory (Chesson, 2000). However, our work shows that even if plant-plant interactions are constant across an environmental gradient, context-dependent PSFs may also impact coexistence outcomes. Further, both are likely simultaneously operating in many communities. Because the derivation of niche and fitness ratios we have used is restricted to fluctuation-independent mechanisms of coexistence (Chesson, 2013), other approaches such as Ellner et al.'s (2019) decomposition of invader growth rates might be appropriate for extending this framework to incorporate variability in drivers and fluctuation-dependent mechanisms of coexistence. This method has been used to show how other inter-guild interactions

mediate species coexistence and may offer novel insight into interactions between environmental variability and PSFs (Shoemaker, Barner, Bittleston, & Teufel, 2020).

While many biological processes may respond in nonlinear ways to environmental variation, we found that linear approximations may be sufficient for understanding how environmentally-mediated interactions impact competitive interactions, depending on the scale at which systems vary along the gradient (Appendix B.1). However, the linear effects of the environment on interaction strengths in our models resulted in striking nonlinear consequences for fitness ratios and niche differences (Figure 2; Figure 4), emphasizing the complex interdependence between these two axes of coexistence (C. Song, Barabás, & Saavedra, 2019). Other work investigating coexistence have found similar nonlinear trends in these axes of coexistence for both single-trophic (Bowler, Weiss-Lehman, Towers, Mayfield, & Shoemaker, 2022) and multi-trophic systems (Terry, Chen, & Lewis, 2021). This may suggest that predictions based on two discrete experimental conditions (e.g. ambient vs. warmed, low vs. high precipitation etc.) provide inadequate information to extrapolate outside of these conditions or even to intermediate conditions that fall between discrete measurements. Further integration of this theoretical framework and empirical studies could help decompose the direct and indirect PSF effects on both niche differences and fitness ratios.

Though widely recognized as a nearly universal phenomenon, to-date context-dependency has not been studied with a coherent and generailzable methodology capable of quantifying the role of particular environmental dependencies on plant-soil feedback mediated community dynamics. Ke and

Wan (2022) previously proposed a method of parameterizing their models that may be extended to include these context-dependent models of PSF across environmental conditions. Briefly, they suggested a greenhouse study in which microbe-independent competition coefficients (c_{ij}) can be disaggregated from microbial contributions (σ_{iX} and ϕ_{Xi}) to the overall competition coefficients (α_{ij}) by growing plants alone and along a competition gradient in either sterile or competitor-conditioned soil. To assess the role of a given environmental context-dependency, this experiment could be repeated along an environmental gradient, where these parameters could be modeled as a function of the environmental variable. One obstacle to empirically estimating the role of context-dependent species interactions using this approach is identifiability constraint of σ and ϕ. Molecular techniques to estimate the cultivation rate ϕ may be implemented to either quantify that absolute abundance (qPCR), microbial load (hamPCR), or shifts in community composition (amplicon sequencing) along plant density gradients. The link between the presented models and potential experimental approaches is one benefit of the use of phenomenological interaction coefficients. However, to tackle the more mechanistic questions related to context-dependent PSF-mediated coexistence, molecular methods such as transcriptomics might be used to disentangle whether compositional shifts in microbial communities or functional shifts in microbial taxa are responsible for these context-dependent effects (Schenk, Carvalhais, & Kazan, 2012; Xia et al., 2021; Yergeau et al., 2014). More generally, however, we suggest that PSF studies would benefit from incorporating modeling approaches and experimental designs that allow for context-dependent species interactions.

3.6 Conclusion

Recent work has shown how coexistence theory and plant-soil feedback concepts can be productively integrated to better understand species coexistence (Kandlikar, 2024; Kandlikar et al., 2019, 2021; Ke & Wan, 2020; Yan et al., 2022). The dual role of niche differences and fitness ratios in mediating the outcome of species interactions offers a more nuanced and mechanistic understanding of both positive and negative plant-soil feedbacks that should inform empirical studies. PSFs and their context dependencies may be responsible for spatio-temporal trends that previous researchers have noted in niche differences and fitness ratios (Hallett et al., 2019; Sears & Chesson, 2007), and may be a key mechanism mediating coexistence across communities. Our results paired with the ample empirical evidence of abiotic context-dependent plant-microbe interactions (Bennett & Klironomos, 2019; J Gundale & Kardol, 2021) highlight the potential explanatory power of these particular mechanisms, which have the potential to explain cases in which theoretical models of coexistence fail to predict empirical results (Kraft et al., 2015; Wainwright et al., 2019).

3.7 Bridge

In this chapter, I have through a series of simulations that context-dependent plant-microbe interactions may modify PSF-mediated coexistence outcomes. Further, the complexity of the PSF system seems to create more complicated relationships between an environmental gradient and plant competitive dynamics. The results from my sensitivity analyses of modified niche and fitness difference equations suggest, further, that plant-microbe interactions may be especially relevant for determining plant-plant fitness differences, suggesting a possible mechanism for context-dependent PSF dynamics. However, the

question still stands as to whether such context-dependent PSFs *do* modify plant coexistence. Further, how do these context-dependent species interactions function in more diverse communities, beyond just pairwise interactions? In Chapter 4, I present an empirical test of drought-dependent PSFs, using metrics for niche and fitness differences which account for indirect species interactions in multispecies communities. Additionally, I characterize drought-dependent microbial effects on multiple vital rates, provided among the more comprehensive demographic tests of PSF dynamics.

CHAPTER IV

MICROBES BUFFER DIVERSITY FROM INCREASING DROUGHT FREQUENCY THROUGH FLUCTUATION DEPENDENT MECHANISMS MORESO THAN INDIRECT SPECIES INTERACTIONS

4.1 Contributions

With the help of the PI, Jeff Diez, I designed this study. Katelin Kutella, Bryn Callie, Macy Patel, Austyn Tavernier, and Lindsay Villano aided me in constructing the experiment and collecting all data. I performed all statistical analyses and wrote the first draft of the manuscript which was then revised with the help of all coauthors.

4.2 Introduction

Interactions with soil microbes have long been implicated in structuring plant communities (Bever, 1994; Janos, 1980; Van der Putten et al., 2013). Through feedbacks between plant populations and their associated soil microbial communities (plant-soil feedbacks; PSFs), soil microbes may modify competitive dynamics between plant species and may alter the outcomes of coexistence (Bever et al., 1997; Revilla, Veen, Eppinga, & Weissing, 2013). Sensitivities of plant-microbe interactions to their environmental context further complicate these feedbacks (N. C. Johnson et al., 1997), potentially causing a mismatch between PSF experimental results and observed field dynamics of plant communities (Forero et al., 2019; Heinze et al., 2016). Observations of context-dependent PSFs have lead to extensive research programs aimed at identifying the role of climate change in modifying PSFs (Rudgers et al., 2020).

One such global change driver that will likely modify the dynamics and outcomes of PSFs is the increasing intensity and frequency of droughts in some

parts of the world (de Vries, Lau, Hawkes, & Semchenko, 2023; Veresoglou, Li, Chen, & Johnson, 2022). At the population level, drought and microbes interact to impact germination (Hubbard, Germida, & Vujanovic, 2012), mortality (Griffin-Nolan et al., 2021), and overall fitness of plants (Fitzpatrick, Mustafa, & Viliunas, 2019). At the community level, the interplay between drought and PSFs have received a great deal of attention, but many studies report contrasting effects of drought on PSFs as some find that droughts induce positive feedbacks (Martorell, MartÍnez-Blancas, & García-Meza, 2021), induce negative feedbacks (Hassan, Carrillo, & Nielsen, 2022), or neutralize feedbacks (Fry et al., 2018). Thus, identifying exactly how drought might modify the role of PSFs in structuring plant communities remains a priority for understanding how plant communities will respond to global change. Further, holistic explorations of the impacts of drought and microbes on demography, species interactions, and community dynamics remain uncommon, but may be key to more mechanistically describing drought-dependent PSFs (Dostálek et al., 2022; Ke & Wan, 2023).

How, exactly, we should model these context-dependent PSFs is a much debated question, but the recent integration of Modern Coexistence Theory and PSF theory may provide useful tools for leveraging greenhouse PSF studies to make inference about the role of microbes in plant community dynamics (Kandlikar, 2024). Traditional analyses of PSF experiments typically use plant performance data (often biomass) to estimate the (de-)stabilization of competitive interactions between plant species by PSFs (i.e. the effect of PSFs on the niche differences of the species pair) which is then used to make inference about coexistence (Bever et al., 1997). Recently proposed methods, informed by coexistence theory, involve estimating the effect of microbes on vital rates and plant competition and using

analytical or simulation based methods to quantify the downstream effect of PSFs on both niche differences as well as innate fitness differences between plant species (both of which are required to make robust inference about the role of PSFs in species coexistence) (Ke & Wan, 2023). Such methods have already demonstrated the importance of not just coexistence-promoting microbe-mediated niche differences, but even more so, the role of exclusion-promoting microbe-mediated fitness differences (Yan et al., 2022). Thus, quantifying the relative roles of microbes in partitioning plant species' niches (increasing niche differences) and in exacerbating baseline competitive asymmetries between species (increasing fitness differences) has emerged as an important goal for PSF research (Kandlikar et al., 2019; Ke & Wan, 2020). However, comprehensive demographic tests of PSFs are still rare and existing integrations between PSF theory and coexistence theory have thus far ignored the potentially important role of indirect interactions in multispecies community dynamics.

Although the indirect plant-plant interactions have been studied in both the PSF and coexistence theory literature, these explorations have occured somewhat independently (though see Granjel et al. 2023 for multispecies coexistence mediated by foliar pathogens). These indirect interactions seem to be sparsely accounted for in traditional PSF frameworks (Eppinga et al., 2018; Miller, Lechón-Alonso, & Allesina, 2022), but may be important for explaining community dynamics when correctly incorporated into PSF models (Pajares-Murgó et al., 2024). As it stands, however, we still do not know 1) how important indirect PSF interactions are for community dynamics nor 2) how sensitive such indirect PSF interactions are to environmental variables like drought. Conveniently, methodological advancements in coexistence theory have enabled researchers to quantify niche and fitness

differences of multispecies assemblages as well as to quantify the importance of indirect interactions in mediating coexistence (Saavedra et al., 2017). It is possible that by leveraging these methods, we might better understand the underlying dynamics of multispecies PSFs which could, in addition to abiotic context-dependencies, explain mismatches between greenhouse experiments and dynamics of plant communities in the field.

In this study, we have characterized the effects of soil microbes and drought on plant demography and both direct and indirect species interactions, and we investigated the potential for drought and microbes to mediate multispecies coexistence and community dynamics. We conducted a traditional two-phase PSF experiment in the greenhouse, replicated across mesic and drought conditions, and used these data to fit population models of five annual plant species, thus estimating the responses of both demographic terms and species interactions to drought and inoculation of microbial communities. We used the structural approach developed by Saavedra et al. 2017 to quantify niche and fitness differences for all species combinations, and we quantified the role of indirect interactions in mediating coexistence to explore the unique role of drought and microbes in multispecies plant communities. Finally, we ran multispecies community simulations, which uncovered the fluctuation-dependent mechanisms of coexistence. These analyses uncovered general effects of microbes and droughts on plant demography, variable impacts on species interactions and competition among species combinations, and have identified novel microbially-mediated fluctuation dependent coexistence.

4.3 Materials and methods

4.3.1 Cultivation Phase. For this experiment, we selected five annual forbs native to Willamette Valley upland prairies: *Clarkia amoena*, *Clarkia purpurea*, *Collinsia grandiflora*, *Gilia capitata*, and *Plectritis congesta*. In the cultivation phase of the experiment, we grew each plant species in monoculture (three to six plants per pot) and in either control conditions or drought conditions. We manipulated soil moisture conditions by watering the control pots daily and the drought pots every other day. The drought treatment was initiated approximately one month after plants had germinated such that plants had a chance to germinate and establish before undergoing stress, which is representative of the life history of these species which germinate during the wet falls and endure spring and summer droughts.

To offer plants a diverse community of soil microbes from which they could selectively cultivate their own distinct microbial communities, plants were grown in sterilized potting soil (Lane Forest Products; super natural potting mix) that was inoculated with field soil from Heritage Seeds (Salem, OR; 44.892273, -122.914971) in restored prairies with a 9:1 ratio of sterilized soil to inoculum. These plants were grown for five months (four months in the drought treatment) before the initiation of the experimental phase. Each species-watering combination had ten replicate plots, which was more than enough soil to serve as inoculum in the experimental phase.

4.3.2 Experimental Phase. In the experimental phase, we designed a competition experiment in which each plant species was grown alone and in the presence of each other competitor at low and high density. We replicated this design in control and drought conditions as well as in two soil conditions:

uninoculated, sterilized soil and sterilized soil that has been inoculated. We prepared the inoculum by blending the entire contents of each pot from the cultivation phase, keeping each phase I pot's inoculum separate. We chose to keep the inoculum from different phase I pots seperate to avoid the biases introduced by mixing inoculums (Rinella & Reinhart, 2018). For the competition gradient experiment, only soil from the high density cultivation pots was used, and the inoculum type was determined by whichever species was the competitor in a given pot (ie in inoculated pots, focal plants always experienced their competitor's soil). We additionally grew each species alone in uninoculated soil and in soil inoculated by their own species' inoculum.

Approximately one month after seed sowing, counts of germinated focal individuals were recorded. Because we consistently sowed three seeds for every desired focal individual, we used these counts to estimate germination rates for each of our species in various soil conditions. In the subsequent month, we also transplanted in seedlings from flats of extra seedlings grown in sterilized, uninoculated soil in the case of pots with insufficient competitor densities or focal plants that did not germinate. Approximately two months after seeds had germinated, we begun the drought treatment. Pots in the control treatment were watered daily while pots in the drought treatment, as in the cultivation phase, were watered every other day, similar to Germain et al. 2018.

As each individual plant flowered and senesced, we recorded data on their reproductive output. For each species, we used data from either this experiment or concurrent greenhouse experiments to calculate average seeds per fruit and average flowers per inflorescence (for species that formed inflorescences). At the first sign of senescence for each individual, we counted the number of flowers or inflorescences,

and assuming that each flower produced one fruit, we estimated a total seed output (fecundity) for each individual plant. If an individual plant did not produce flowers, it was assumed to have died before reproductive maturity and was used to estimate mortality rates for each species across soil and drought conditions.

4.3.3 Statistical Analyses. To estimate germination rates, we fit simple binomial models for each species in each of the two inoculation treatments. Similarly, we estimated mortality rates with binomial regression for each species in each inoculation treatment and each drought treatment. To estimate intrinsic growth rates and interaction coefficients for all species in each of the four treatment levels, we fit a set of candidate models which represent some common functional forms of species interactions. Included in this set of candidate models were a null model with no species interactions, a Lotka-Volterra form, a Ricker form, and a Beverton-Holt form. For both the Lotka-Volterra and Ricker models, we included models with and without constraints on species interactions to be competitive. The traditional parameterization of the Beverton-Holt is not suited for facilitation, so we only included the constrained version of the Beverton-Holt model. We then used the expected log-predictive density (ELPD) to compare the predictive performance of the candidate models. The Beverton-Holt functional form had the highest ELPD, so we used intrinsic growth rate and interaction coefficient estimates from this model for all downstream analysis (Vehtari, Gelman, & Gabry, 2017). We also fit a Beverton-Holt model with just the individual plants that went to see to identify effects of microbes and drought on fecundity independent of those on mortality. These parameters were only used to make inference about such direct demographic effects and were not used to calculate any downstream quantities nor were they used in our simulations. All models were fit using rStan v2.32.3

((Stan Development Team, 2023b)) and model comparison was conducted using the loo package v2.6.0 in R (Vehtari et al., 2023). Further details about the model selection, as well as the final parameter estimates, can be found in Appendix C.1.

To not only assess the dynamics of pairwise competition, but to also include the potential for indirect species interactions to mediate competition, we adopted a structural approach to coexistence theory (Saavedra et al., 2017). Underlying this approach is the idea that species interactions determine a domain of feasible coexistence. If the vector of species growth rates falls within this domain, the combination of species could feasibly coexist. Thus, we can determine whether any given combination of our five species could feasibly coexist, and we can also calculate structural analogues to traditional niche and fitness differences. The structural niche differences (SND) represent the normalized solid angle of the feasbility domain, and the structural fitness differences (SFD) represent the deviation of the estimated growth rate vector from the centroid of the feasability domain. Finally, this framework provides two measures used to describe the role of indirect interactions in determining competitive outcomes. The community-pair differential (CPD) quantifies the degree to which coexistence of a multispecies combination is more or less likely than coexistence of the component species pairs. The community-pair overlap (CPO) quantifies the degree to which coexistence of the multispecies combination can be explained by coexistence of the component species pairs. To propogate uncertainty in our parameter estimates to our calculations of these downstream quantities, we repeated these calculations for all 4000 samples of our posterior distribution. Thus, for all 2-5 species combinations in each of our four treatment levels, we calculated distributions of feasibility, SNDs, and SFDs, and for all 3-5 species combinations, we calculated distributions of

CPDs and CPOs. To do this, we adapted code from Granjel et al. (2023). To quantify treatment effects, we calculated contrast distributions by subtracting the distributions for these parameters and downstream quantities for the control treatment from those of the experimental treatment. We report descriptions of these contrast distributions in the maintext, and provide additional descriptions and figures of the raw quantities in Appendix C.2.

To further explore the potential for drought-dependent microbial effects on plant community dynamics, we performed a series of whole-community simulations. For these simulations, we compiled our parameter estimates into the following general population model:

$$N_{i,t+1} = N_{i,t} g_i \frac{\lambda_i}{\sum_j N_{j,t} \alpha_{ij}} \tag{4.1}$$

We first ran these simulations in a completely deterministic system using the median parameter estimates for each of our four treatment levels. We then ran a series of simulations designed to simulate demographic stochasticity by sampling the posterior distribution of our parameters (thus retaining covariance of parameter estimates) at each time point in the simulation for each of our four treatments. Finally, to explore the role of environmental stochasticity, we ran a series of simulations in which we began by generating a binary drought time series from a binomial distribution. We used this time series to determine whether to pull parameters from the mesic or drought posterior distributions each year. We ran these simulations across a gradient of drought frequencies (ie the success probability in the binomial distribution) for each of our two inoculation treatments. For each simulation, we started each population off with a population size of one, and we calculated the species richness, Shannon diversity, and Pielou evenness of the

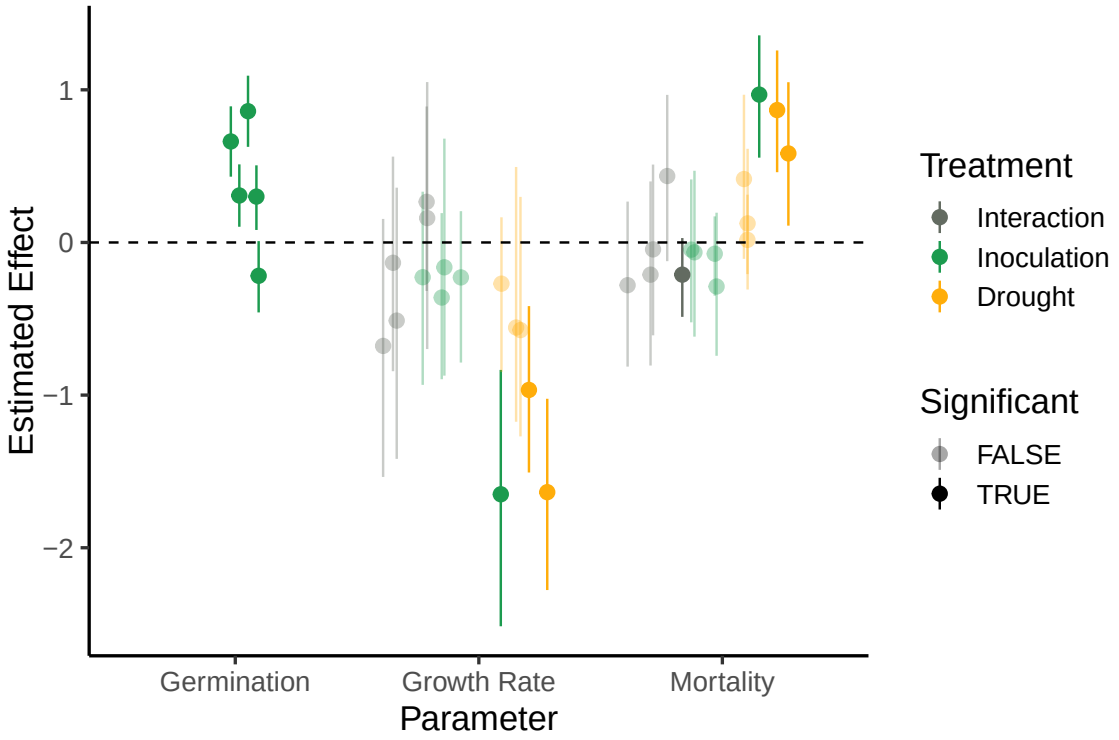

Figure 8. Scaled singular and interactive effects of drought and microbes on estimated germination rates, intrinsic growth rates, and mortality rates. Pointranges represent the median and 95% credible intervals of the contrast distributions for each parameter, separated by species, and are colored by treatment variable. Transparent points represent contrast distributions with credible intervals which overlap zero.

community after one hundred years using the vegan package v2.6-4 (Oksanen et al., 2022). For all stochastic simulations, we repeated each unique simulation one thousand times and report the distribution of diversity metrics.

4.4 Results

Both inoculation and drought conditions impacted plant demographic rates (Fig. 1). Germination rates generally responded positively to inoculation (Median = 0.0603; 95% CI[-0.0585, 0.1596]; PD = 0.8067). Although this was not true for *C. purpurea* specifically for which the germination rate decreased with inoculation,

all other species experienced boosted germination rates with microbial inoculation with PD values above 0.95.

Generally, both inoculation (Median = -85.3; 95% CI[-271.00, 49.6]; PD = 0.864) and drought (Median = -95.50; 95% CI[-256.00, 30.20]; PD = 0.9182) decreased the expected density-independent fecundity (estimated independent of mortality). While the median microbe effects and drought effects were negative for all species, species differed in both the strength and certainty of these estimated effects. While we did not detect any consistent drought-dependent microbial effect, *C. purpurea* experienced a negligible reduction in fecundity due to microbes in mesic conditions but suffered a much stronger reduction in the drought treatment (Median = -120.00; 95% CI[-245.00, 8.06]; PD = 0.9668). Somewhat similarly, though we less certainty, *G. capitata* had a more severe reduction in fecundity due to microbes in the drought than in mesic conditions (Median = -54.9; 95% CI[-168.00, 58.3]; PD = 0.834).

While we did not detect a consistent effect of inoculation on mortality rates, inoculation did increase the mortality rate of *C. grandiflora* (Median = 0.225; 95% CI[0.130, 0.315]; PD ¿ 0.9999) and likely decreased the mortality rate of *C. purpurea* (Median = -0.0663; 95% CI[-0.172, 0.0443]; PD = 0.872). Drought generally increased mortality rates (Median = 0.0868; 95% CI[-0.0457, 0.2569]; PD = 0.8315), though we found no evidence of a direct effect of drought on the mortality of *P. congesta*. We found no evidence of consistent interaction effects of microbes or drought on intrinsic growth rates nor mortality rates, but a few species exhibited drought-dependent inoculation effects on mortality. For *C. amoena*, inoculation slightly decreased the mortality rate in mesic conditions but slightly increased the mortality rate in drought conditions (Median = 0.101; 95% CI[-

0.0356, 0.232]; PD = .932). Conversely, drought likely increased the reduction in mortality conferred to *C. purpurea* by inoculation (Median = -0.0635; 95% CI[-0.193, 0.0645]; PD = 0.84). Interestingly, we detected such an interaction effect in *P. congesta*, the species with the lowest mortality such that inoculation only affected mortality rates in the drought conditions where they decreased relative to the uninoculated treatment (Median = -0.0500; 95% CI[-0.108, 0.0075]; PD = 0.959).

While we found no consistent effects of either inoculation or drought on plant interaction coefficients, we identified many species-specific effects (Appendix C.2). Similarly, when assessing the effect of microbes and drought on the SNDs and SFDs, we found few consistent trends (Fig 2). Although our confidence in these effects is low, we did notice that median SNDs and SFDs were both higher in uninoculated and sterile treatments. This is trend is partially supported by a slightly positive effect of both inoculation (Median = 3.33; 95% CI[-22.40, 34.54], PD = .6054) and drought (Median = 4.14; 95% CI[-25.08,35.61], PD = 0.6188) on SFDs. We found no evidence for a consistent effect of inoculation or drought on CPDs, CPOs, or feasibility.

Simulating the whole community dynamics under our four treatment levels revealed singular and interactive effects of inoculation and drought on both plant community composition and diversity (Fig 3). Deterministic simulations and those with demographic stochasticity resulted in lower Shannon diversity in inoculated and drought conditions. When simulating community dynamics with both stochastic and environmental stochasticity, we found that although increasing drought frequency generally decreased diversity, the shape of this relationship changed with inoculation. In the uninoculated simulations, diversity linearly

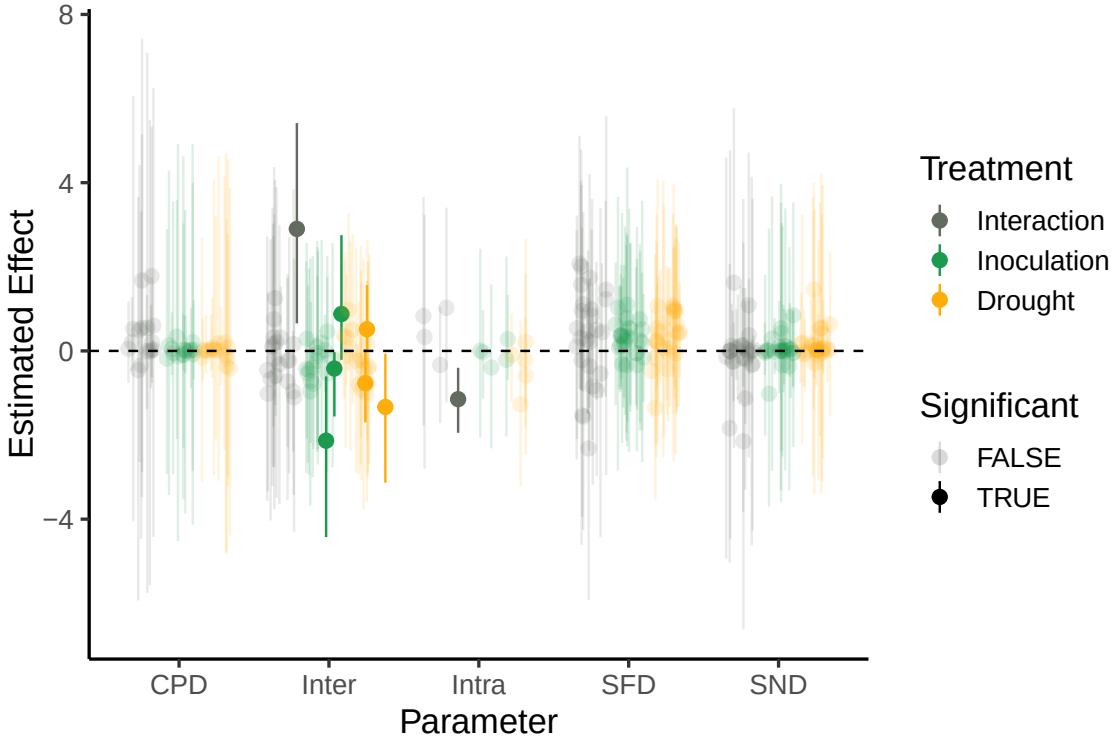

Figure 9. Scaled singular and interactive effects of drought and microbes on intra- and inter-specific competition, strucutral niche & fitness differences, and community-pair differentials. Pointranges represent the median and 95% credible intervals of the contrast distributions for each parameter, separated by species pair or combination, and are colored by treatment variable. Transparent points represent contrast distributions with credible intervals which overlap zero.

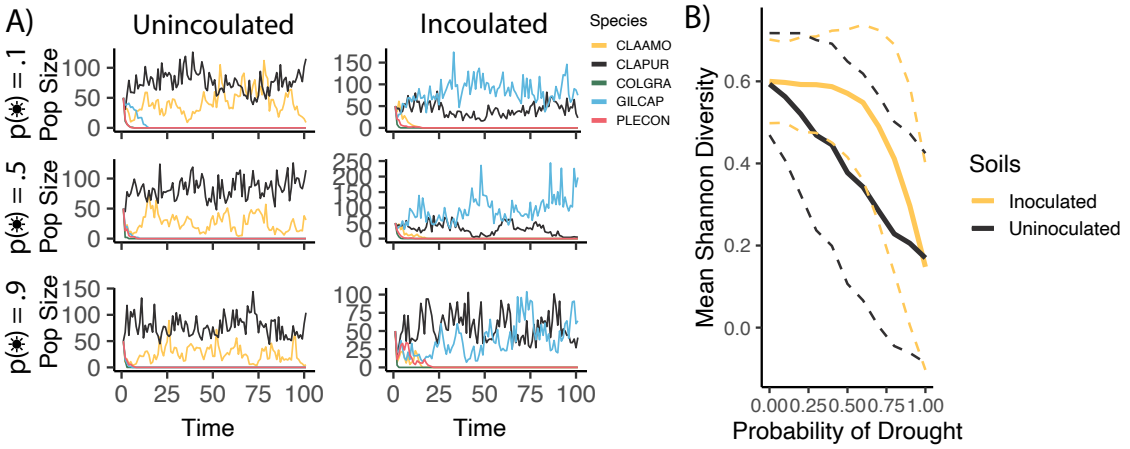

Figure 10. Results from the stochastic multispecies simulations across a range of drought probabilities and between inoculated and uninoculated conditions. A) Example time series in either inoculated or uninoculated conditions at low, medium, and high drought probabilities. B) Shannon diversity, averaged across all one thousand iterations, across the range of drought probabilities. Lines are colored by soil condition, and dashed lines represent one standard deviation above and below the mean.

decreased with drought frequency. In the inoculated simulations, increasing drought frequency had a meager effect on diversity until a frequency of about 0.5, at which point diversity precipitously dropped with increasing drought frequency. In all sets of simulations, inoculation generally resulted in communities dominated by *C. purpurea* and G. capitata as opposed to communities dominated by *C. purpurea* and *C. amoena* in uninoculated conditions. Further results from the simulations can be found in Appendix C.3.

4.5 Discussion

To better understand the effect of drought on microbe-mediated plant community dynamics, we conducted a two-phase plant-soil feedback experiment in both drought and mesic conditions. We used demographic data collected from this experiment to fit population models and estimate vital rates and species interaction strengths. Finally, we calculated a set of theory-informed metrics and conducted

a series of community-level simulations to summarize multispecies community dynamics. While both inoculation and drought had distinct effects on different vital rates that were relatively conserved across species, detectable responses of species interactions and downstream competition metrics to inoculation and drought were sparse and highly species (or species-combination) specific. Ultimately, however, these responses led to overall diversity-reducing effects of drought. We also identified a fluctuation-dependent interaction such that at intermediate frequencies of drought, inoculation buffered diversity from the effects of drought.

The potential positive effect of soil microbes on germination rates is well known and has been explored as a tool for increasing agricultural yield and restoration success (Barrera, Luera, Lavallee, & Soti, 2021; Cardarelli, Woo, Rouphael, & Colla, 2022). However, these effects do seem to be somewhat species-specific, and while microbes such as mycorrhizal fungi and rhizobia tend to increase germination rates in many species, other microbes may act as seed pathogens and decrease host germination rates Connolly, Carris, & Mack, 2018. In contrast to the largely positive effect of microbes on germination rates, we found a generally negative effect on seed output, congruent with other greenhouse studies that identify net-pathogenic effects on plant performance (Carlton, Duncritts, Chung, & Rudgers, 2018; R. H. Van Grunsven et al., 2007). Finally, we found rather species-specific responses of mortality rates to inoculation, and found evidence for species-specific interaction effects where drought modified the effect of inoculation on mortality rates. Others have identified these ontogenetically dependent microbial effects on demography (J. Wang et al., 2023), including one study which identified a positive effects of soil microbes on germination while vegetative growth rates were independent of soil microbes David et al. (2019). Interestingly, the magnitude and

at times the sign of these effects varied by species. This was especially true for the degree of context-dependency of the microbial effects. Quantifying the co-variance structure of vital-rate specific microbial effects on a variety of plant species may help explain emergent microbial effects at the community level.

In contrast to vital rates, we found that the impact of microbes and drought on species interactions and downstream competition metrics were highly variable across species pairs. Further, our uncertainty in these species interaction parameters was rather high, challenging our ability to detect such effects. These results are consistent with many other studies and highlight the difficulty of identifying general responses of species interactions to environmental covariates (Bimler, Stouffer, Martyn, & Mayfield, 2024; S. Liu et al., 2022). New methods for accurately estimating responses of species interactions to covariates are being developed (Bimler, Mayfield, Martyn, & Stouffer, 2023; Weiss-Lehman et al., 2022), and trait-based approaches have been proposed to explain observed variability in the sensitivity of species interactions to covariates (Mauro, Shah, Martin, & Ghalambor, 2022). However, we still lack a general theory of context-dependent species interactions. This problem is exacerbated in plant-soil feedbacks as researchers try to study the net effect of hyper-diverse communities of microbes, as we have done in this study. Understanding the dynamics of hyper-diverse communities under global change may be one path forward for better understanding the downstream effects of context-dependent species interactions in plant-soil feedbacks.

Because many microbes have been implicated in conferring drought-resistance to host plants, many agricultural practices have been proposed for leveraging microbial inoculants to improve yield in light of increasing drought

frequency and intensity (Bittencourt et al., 2023; Kalamulla et al., 2022). When considering how microbes may aid in restoration efforts, especially those aimed at developing drought-resilient plant communities, predictions about the role of microbes become more difficult as what is good for any given plant may not be good for promoting plant diversity and stability. Much of the research on this topic has been dedicated to the restoration of particular populations of plant of concern (Azizi et al., 2022; Valliere, Wong, Nevill, Zhong, & Dixon, 2020) and not whole communities. Our results suggest that while drought may likely decrease diversity of annual prairie plants, microbes may buffer this loss at intermediate drought frequencies, suggesting a potential role for microbial inoculants in restoration efforts. However, we did find that after a drought frequency of about 0.5, diversity precipitously crashed in inoculated conditions. This suggests that microbes may buffer plant communities from droughts up until some tipping point, at which point drought begins to have stronger negative impacts on diversity for inoculated communities. Identifying the degree to which this pattern is common in other systems, and if so, what frequency of droughts leads to this tipping point phenomenon would be crucial next steps for assessing the efficacy of inoculation in promoting drought-resistant plant communities.

Fluctuation dependent mechanisms of coexistence have been at the core of coexistence theory since its origins, but empirical tests of these mechanisms have been historically difficult (Chesson, 1994; Connell, 1978; Hutchinson, 1961). Much of our knowledge of these mechanisms come from theoretical investigations, but invasion growth rate analyses, including those described by Ellner et al. 2019, have made the quantification of these mechanisms more practical. We identified fluctuation-dependent mechanisms which promoted coexistence at intermediate

drought frequencies moreso in inoculated conditions. This microbally-mediated fluctuation-dependent coexistence is a novel phenomenon, seldom discussed in either the plant-soil feedback or coexistence theory literature. However, nuances regarding the temporal dynamics of plant-soil feedbacks complicate our ability to infer how general this phenomenon may be. Our approach, for tractability, obscures the differences between plants and microbes in their temporal scale, which may be at the heart of these fluctuation-dependent mechanisms. Ultimately, it is unlikely that microbes are always at some stationary equilibrium determined by the plant community composition, as explored recently with respect to plant-soil feedback decay rates (Ke & Levine, 2021; Ke et al., 2021; Thakur et al., 2021). These nuances, as well as the specific mechanisms by which microbially demography is impacted by drought, may be essential to further explaining the role of microbes in fluctuation-dependent coexistence. Thus, further integration of theory and empirical investigations such as this study, as well as studies leveraging new molecular techniques, will likely illuminate the complexity by which microbes contribute to the observed diversity and composition of plant communities.

CHAPTER V

CONCLUSION

A substantial body of work suggests that interactions between plants and soil microbes are important for structuring many plant communities. However, after decades of studying such interactions, plant ecologists still struggle to make sense of seemingly idiosyncratic experimental results that seldom translate to field dynamics. Coming to a generalizable understanding of plant-microbe community dynamics may require critical examination of the underlying theory framing our research, such as that offered by the integration of modern coexistence theory with plant-soil feedback theory. Further, I propose that leveraging molecular techniques to test theoretically grounded questions (as I have done in Chapter 2) and attempting to embrace idiosyncratic community dynamics by acknowledging and modeling context-dependent species interactions (as I have done in Chapters 3 & 4) are likely essential steps for the field as a whole to come to a more satisfying understanding of these mind-numbingly complex phenomena.

In my second chapter, I characterized species-specific fungal communities, framing dissimilarity in these host-associated mycobiomes as an extension of the host's phenotype and thus as a species level trait, analogous to SLA or root:shoot ratios. In tandem, I tested an frequently assumed but seldom tested assumption regarding the role of species-specific cultivation of microbial communities in plant-soil feedbacks, and I extended the body of work that attempts to identify how differences in species contribution to the stabilization of competition and ultimately coexistence. The results of my study offer some support for the idea that species cultivate distinct microbial communities, and that the dissimilarity of these communities may be related to increased niche & fitness differences,

ultimately having a net positive effect on the probability of coexistence. However, I was unable to identify differences in these trends between major functional groups of fungi (ie pathotrophs v.s. saprotrophs). This is counter to theory that suggests that pathogens and mutualists should play very distinct roles in mediating competitive dynamics, but I suspect that this is far more indicative of our limited fungal natural history rather than some true equivalency among symbionts. While approaches as I have presented here are able to reveal interesting and novel nuance to our understanding of microbe-mediated coexistence, we will likely need more direct measurements of microbial function to better explain these processes mechanistically.

In my third and fourth chapters, I incorporated context-dependent interactions between plants and microbes into my investigation of PSF-mediated coexistence. First, by pairing simulation-based and analytical methods, I demonstrated the potential for such context-dependencies to alter PSF dynamics and shift the outcome of competition. I also identified a unique role of plant-microbe interactions in shifting fitness differences and niche differences, an insight that has interesting implications for the mechanisms of context-dependent PSFs but that would not have been possible to identify using traditional theoretical frameworks. By applying these ideas to a greenhouse study, I was able to identify some drought-dependent microbial effects on demography and plant competition, but estimating such effects was especially difficult at the level of plant interactions. This contrast between relatively strong signals of demographic responses to microbes and drought v.s. relatively weak signals of species interaction responses likely reflects the immense complexity of species interactions. Ultimately, many species of microbes exist in the soil, each with their unique functional relationship

to host plants and with their unique sensitivity to environmental gradients such as drought. Our parameter estimates reflect the net consequence of these diverse networks of interactions on plant performance, which may ultimately be highly variable and seemingly idiosyncratic. Even still, I detected an interesting fluctuation-dependent buffering of drought effects on plant diversity conferred by soil microbes. Further research would be needed to identify whether such emergent properties of variable microbial effects is generalizable, but these results demonstrate the potential for variable responses at one level of complexity to generate important patterns at higher levels of complexity.

Each of my chapters implement quite novel methodological strategies for studying plant-microbial ecology. The integration of MCT and PSF theory is still in its nativity, but the approaches that I and others have developed enable us to examine plant-microbe interactions from a new angle and seem to be generated interesting insights. While each of my chapters highlight ongoing difficulties in the study of plant-microbe ecology (most of which I was unsuccessful at overcoming), I am hopeful that this work encourages both creative and critical use of ecological theory as well as a general embrace of the complexity of host-microbial systems. It was the hyper-diversity and plasticity of microbes that drew me to study plant-microbial ecology, and it is the hyper-diversity and plasticity that makes this field so challenging. I can only hope that more ecologists attempt new and innovative approaches to the study of plants and microbes supported by the insight of over a century of theoretical ecology.

APPENDIX A

SUPPLEMENTAL INFORMATION FOR CHAPTER 2

A.1 Demographic Model Selection and Interaction Coefficients

To estimate the intrinsic growth rates (λ_i) and pairwise competition coefficients (α_{ij}) for each of our eight species, we fit the following general model of population growth:

$$N_{i,t+1} = N_{i,t}F_{i,t} \tag{A.1}$$

where the fecundity at time t is a function of λ, α_{ii}, α_{ij}, $N_{i,t}$, and $N_{j,t}$. Because we did not collect data on interspecific variation in germination rates and survival rates, we assume that each of these parameters are equal to one. However, assuming any other constant germination and survival rates would not qualitatively alter the estimates of downstream fitness inequalities as the fitness inequalities describe relative differences between species. When testing the sensitivity to our fitness inequalities to this assumption, we found a negligible effect of the specific value for the shared germination and survival rate (Figure S1). Because these phenomenological competition parameters could influence the fecundity in any number of structural forms (Armitage, 2022), we fit three alternative structures: the linear Lotka-Volterra style function ($F_{i,t} = \lambda_i - \alpha_{ii}N_{i,t} - \alpha_{ij}N_{j,t}$), the Beverton-Holt function ($f_{i,t} = \lambda_i/\alpha_{ii}N_{i,t} + \alpha_{ij}N_{j,t}$), and the Ricker function ($f_{i,t} = \lambda_i e^{\alpha_{ii}N_{i,t}+\alpha_{ij}N_{j,t}}$). In Stan, we fit each of these models, as well as a null model with no competition, to our data and used the log-likelihood estimates to calculate the estimated log pointwise predictive density (ELPD), a measure of predictive accuracy used in model comparison with Bayesian parameter estimates, using the loo package in R (Vehtari et al., 2023).

Additionally, we used this model comparison procedure to assess the degree to which accounting for potential facilitative effects improved model predictive accuracy. While fitting the models mentioned above, we constrained the interaction coefficients to be competitive, so we additionally fit the Lotka-Volterra and Ricker forms without this constraint. Fitting the Beverton-Holt model without the constraint would be difficult as facilitative effects can quickly cause this model to predict negative fecundity.

The ELPD was highest for the unconstrained Ricker model and the constrained Beverton-Holt model. However, we were unable to confidently detect a difference in the predictive accuracy of these models ($\Delta ELPD < 2 \times \text{SE } ELPD$).

To further assess the performance of our final model (the fitted Beverton-Holt model), we performed a posterior predictive check using the posterior distributions for our λ and α values as well as the posterior distribution for the standard deviation around our predicted fecundity values to generate posterior prediction distributions for each of our data points. 95.77% of our fitness data fell within the 95% credible intervals of our posterior predictive distributions. These distributions, along with the actual fitness values, are presented by species below in Figures S1:S8.

Model	ELPD	SE ELPD	Δ ELPD
Ricker (Unconstrained)	-5728.12	-	-
Beverton-Holt	-5733.05	8.25	-4.92
Ricker	-5744.42	7.81	-16.30
Lotka-Volterra (Unconstrained)	-5757.63	9.61	-29.51
Lotka-Volterra	-5774.73	9.76	-46.61
Null	-5776.24	15.64	-48.11

Table A.1. Model Comparison.

	ACMAME	CALCIL	CLAAMO	CLAPUR
ACMAME	1.6 [0.48,3.28]	0.06 [0,0.32]	0.2 [0.04,0.74]	0.14 [0,2.02]
CALCIL	1.25 [0.24,2.99]	1.33 [0.31,3.04]	0.9 [0.25,2.5]	0.76 [0.02,2.69]
CLAAMO	1.46 [0.4,3.17]	0.65 [0.09,2.42]	1.62 [0.75,3.04]	1.07 [0.08,2.89]
CLAPUR	1.6 [0.39,3.3]	1.14 [0.2,2.94]	1.75 [0.71,3.33]	1.27 [0.21,3.01]
COLGRA	1.4 [0.29,3.1]	1.27 [0.27,2.98]	1.23 [0.34,2.89]	0.49 [0.02,2.42]
NAVINT	1.26 [0.31,2.91]	0.9 [0.15,2.73]	0.1 [0.01,0.33]	0.48 [0.01,2.55]
PLANOT	0.83 [0.16,2.49]	0.12 [0.01,1.3]	0.55 [0.19,1.77]	0.12 [0,1.76]
PLECON	0.62 [0.12,2.15]	0.12 [0.01,1.05]	0.18 [0.04,0.53]	0.53 [0.02,2.54]
	COLGRA	NAVINT	PLANOT	PLECON
ACMAME	0.09 [0,0.42]	0.06 [0,1.4]	0.98 [0.07,2.84]	1.24 [0.13,3.04]
CALCIL	1.16 [0.2,2.97]	0.44 [0.01,2.56]	0.77 [0.01,2.81]	0.28 [0.01,2.06]
CLAAMO	0.43 [0.08,1.91]	1.24 [0.15,3]	1.33 [0.21,3.07]	1.17 [0.09,3.03]
CLAPUR	1.73 [0.67,3.36]	1.22 [0.14,2.99]	0.14 [0,2.02]	1.29 [0.15,3.07]
COLGRA	1.53 [0.47,3.18]	1.17 [0.1,3]	1.23 [0.14,3]	1.2 [0.08,3.04]
NAVINT	1.42 [0.41,3.1]	0.46 [0.02,2.54]	0.7 [0.04,2.57]	1.09 [0.07,2.92]
PLANOT	0.15 [0.02,0.89]	1.2 [0.13,3.03]	0.56 [0.02,2.63]	1.25 [0.11,3.03]
PLECON	1.2 [0.1,3.05]	1.21 [0.1,3.04]	0.06 [0,1.88]	0.77 [0.02,2.73]

Table A.2. Median and 95% Credible Intervals for α estimates from constrained Beverton-Holt model.

	ACMAME	CALCIL	CLAAMO	CLAPUR
ACMAME	1.48 [0.43,3.13]	0.04 [0,0.18]	0.12 [0.02,0.33]	0.07 [0,2.04]
CALCIL	1.14 [0.17,3.03]	1.15 [0.22,3.04]	0.42 [0.15,2.26]	0.72 [0.01,2.7]
CLAAMO	1.31 [0.35,3.01]	0.35 [0.05,2.25]	1 [0.46,2.5]	1.03 [0.06,2.94]
CLAPUR	1.52 [0.43,3.21]	0.92 [0.15,2.77]	1.39 [0.49,3.14]	1.19 [0.18,3.03]
COLGRA	1.38 [0.27,3.13]	1.15 [0.19,2.99]	0.93 [0.23,2.9]	0.24 [0.01,2.41]
NAVINT	0.97 [0.24,2.68]	0.62 [0.1,2.82]	0.07 [0.01,0.18]	0.28 [0.01,2.51]
PLANOT	0.54 [0.12,2.02]	0.07 [0,0.44]	0.28 [0.12,0.83]	0.06 [0,1.33]
PLECON	0.4 [0.1,1.35]	0.08 [0.01,0.35]	0.13 [0.03,0.31]	0.28 [0.01,2.55]
	COLGRA	NAVINT	PLANOT	PLECON
ACMAME	0.06 [0,0.23]	0.04 [0,0.95]	0.91 [0.05,2.93]	1.19 [0.13,3]
CALCIL	0.93 [0.17,2.82]	0.25 [0,2.71]	0.8 [0.01,2.81]	0.16 [0.01,1.63]
CLAAMO	0.22 [0.05,1.09]	1.24 [0.13,3.02]	1.25 [0.18,3.09]	1.2 [0.09,3.02]
CLAPUR	1.55 [0.52,3.2]	1.17 [0.12,2.98]	0.08 [0,1.93]	1.25 [0.16,3.01]
COLGRA	1.37 [0.39,3.13]	1.15 [0.09,3.04]	1.17 [0.12,3.04]	1.21 [0.08,3.01]
NAVINT	1.24 [0.3,3.03]	0.24 [0.01,2.6]	0.51 [0.02,2.51]	0.99 [0.06,2.92]
PLANOT	0.09 [0.01,0.3]	1.12 [0.11,2.95]	0.34 [0.01,2.67]	1.23 [0.11,3.05]
PLECON	1.21 [0.08,3.03]	1.17 [0.11,2.97]	0.03 [0,1.89]	0.58 [0.02,2.78]

Table A.3. Median and 95% Credible Intervals for α estimates from constrained Ricker model.

	ACMAME	CALCIL	CLAAMO	CLAPUR
ACMAME	1.06 [0.31,2.42]	0 [-0.09,0.14]	0.12 [0.02,0.3]	-0.02 [-0.09,0.27]
CALCIL	0.65 [0.09,2.24]	0.72 [0.16,2.26]	0.35 [0.13,1.46]	0.02 [-0.13,1.44]
CLAAMO	0.91 [0.24,2.32]	0.24 [0.02,1.39]	0.84 [0.42,1.91]	0.32 [-0.08,2.01]
CLAPUR	1.11 [0.24,2.56]	0.6 [0.1,1.95]	1.03 [0.42,2.41]	0.68 [0.07,2.18]
COLGRA	0.88 [0.15,2.34]	0.71 [0.13,2.23]	0.62 [0.18,2.01]	-0.02 [-0.19,0.8]
NAVINT	0.7 [0.18,2]	0.34 [0.07,1.81]	0.06 [-0.01,0.17]	-0.05 [-0.14,0.48]
PLANOT	0.41 [0.09,1.37]	0.03 [-0.07,0.25]	0.26 [0.12,0.69]	-0.06 [-0.13,0.11]
PLECON	0.35 [0.07,1.01]	0.05 [-0.03,0.27]	0.12 [0.02,0.3]	0.06 [-0.08,1.07]
	COLGRA	NAVINT	PLANOT	PLECON
ACMAME	0.03 [-0.07,0.19]	-0.09 [-0.17,0.05]	0.28 [-0.04,1.92]	0.7 [0.04,2.23]
CALCIL	0.59 [0.1,2.04]	-0.1 [-0.18,0.17]	-0.12 [-0.2,0.86]	-0.04 [-0.3,0.65]
CLAAMO	0.2 [0.03,0.64]	0.7 [0.02,2.24]	0.76 [0.06,2.28]	0 [-1.92,1.9]
CLAPUR	1.14 [0.4,2.54]	0.68 [0.03,2.2]	-0.08 [-0.19,0.14]	0.72 [-0.08,2.26]
COLGRA	0.97 [0.29,2.45]	0.61 [0.02,2.21]	0.63 [0.04,2.19]	0.01 [-1.91,1.94]
NAVINT	0.82 [0.22,2.24]	0.08 [-0.04,1.31]	0.18 [-0.04,1.35]	0.2 [-0.82,1.81]
PLANOT	0.08 [-0.01,0.26]	0.62 [0.03,2.15]	0.04 [-0.1,1.21]	0.61 [-0.31,2.21]
PLECON	0.01 [-1.99,1.99]	0.56 [-0.28,2.13]	**-0.11 [-0.17,-0.02]**	0.05 [-0.27,1.56]

Table A.4. Median and 95% Credible Intervals for α estimates from unconstrained Ricker model. Bolded text represents confidently facilitative interactions.

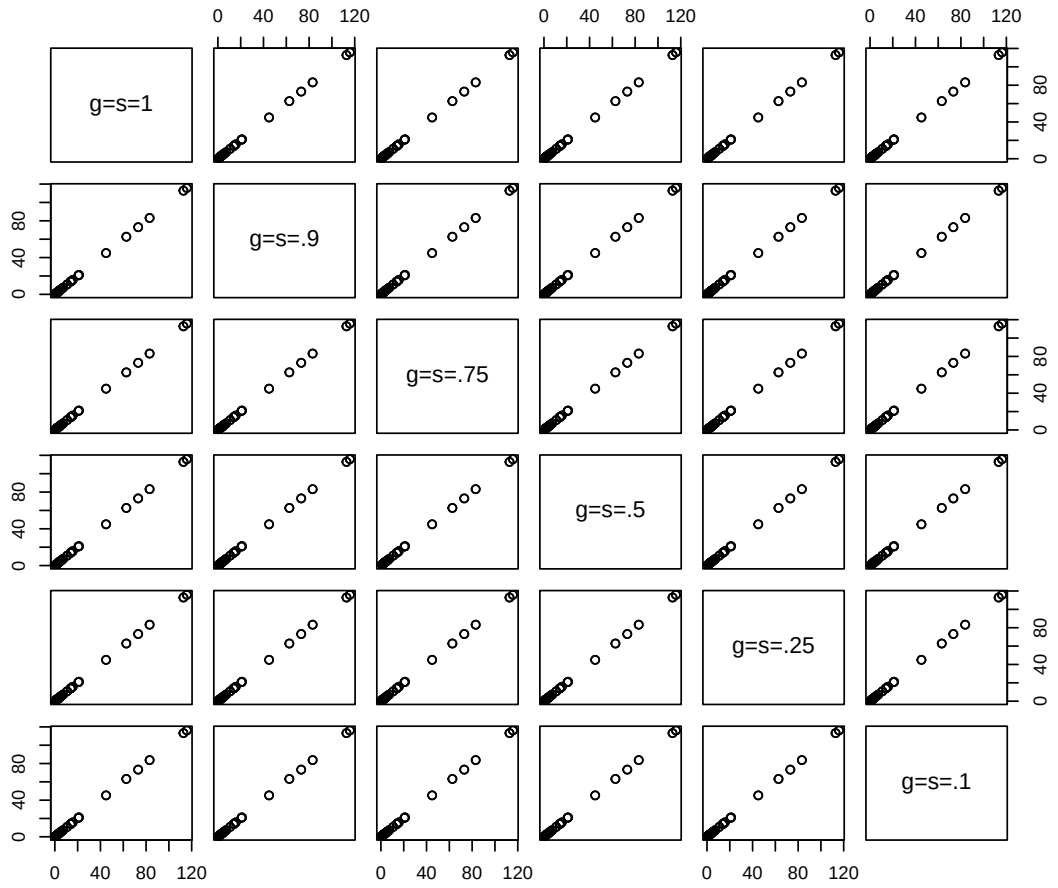

Figure S1. Median fitness inequality estimates for all species pairs under different assumptions for germination and survival rates.

A.2 Phylogenetic Analyses

A.2.1 Methods. To assess the degree to which each species' soil mycobiome is phylogenetically constrained, and to account for this potential phylogenetic signature while assessing relationships between fungal community similarity and competitive dynamics, we first fit linear models predicting fungal community dissimilarity as a function of phylogenetic distance. Phylogenetic distance between our eight species were retrieved from published phylogenetic trees of vascular plants using the V.PhyloMaker package in R (Jin & Qian, 2019). Mean

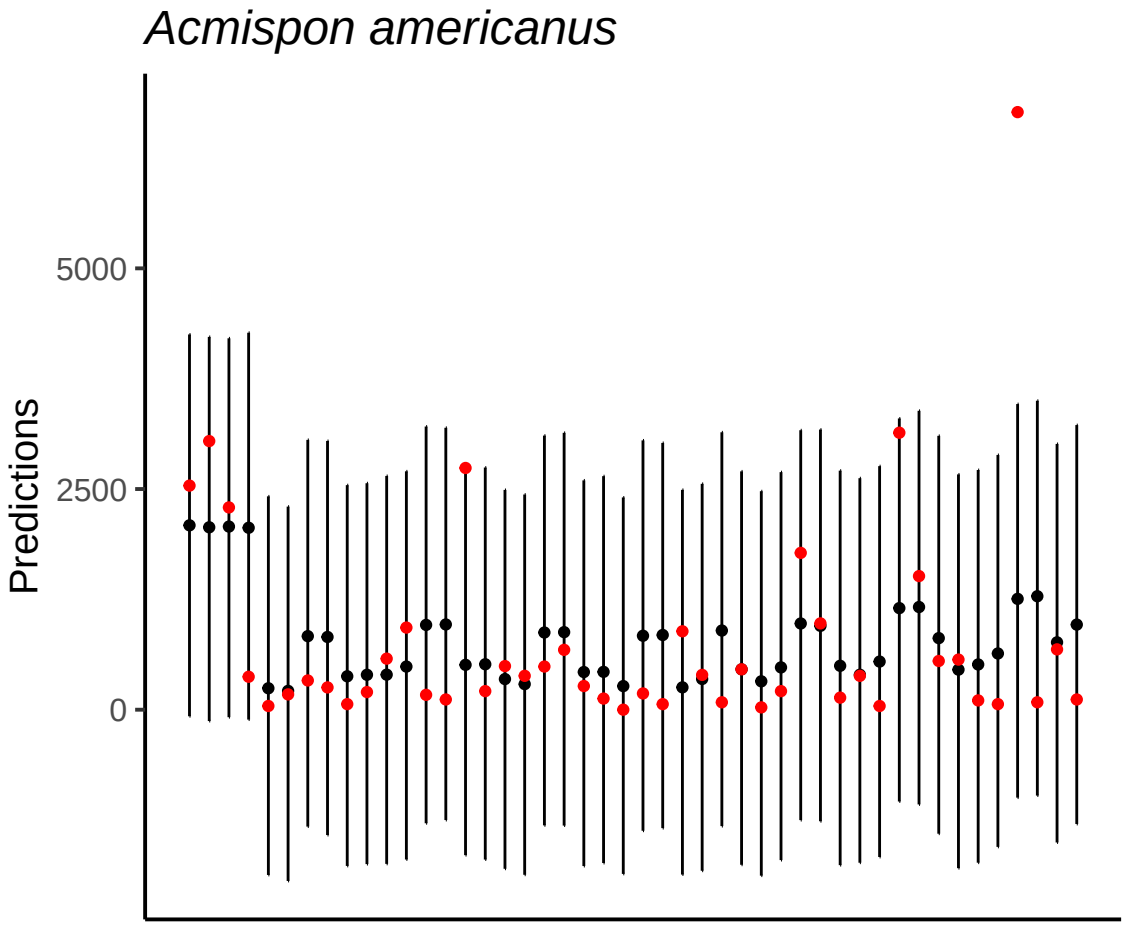

Figure S2. Posterior predictive distributions for fitness measurements from each *Acmispon americanus* plant. Black points represent median posterior predictions and error bars represent the 95% credible intervals of the posterior predictive distribution. Red points represent the true fitness values.

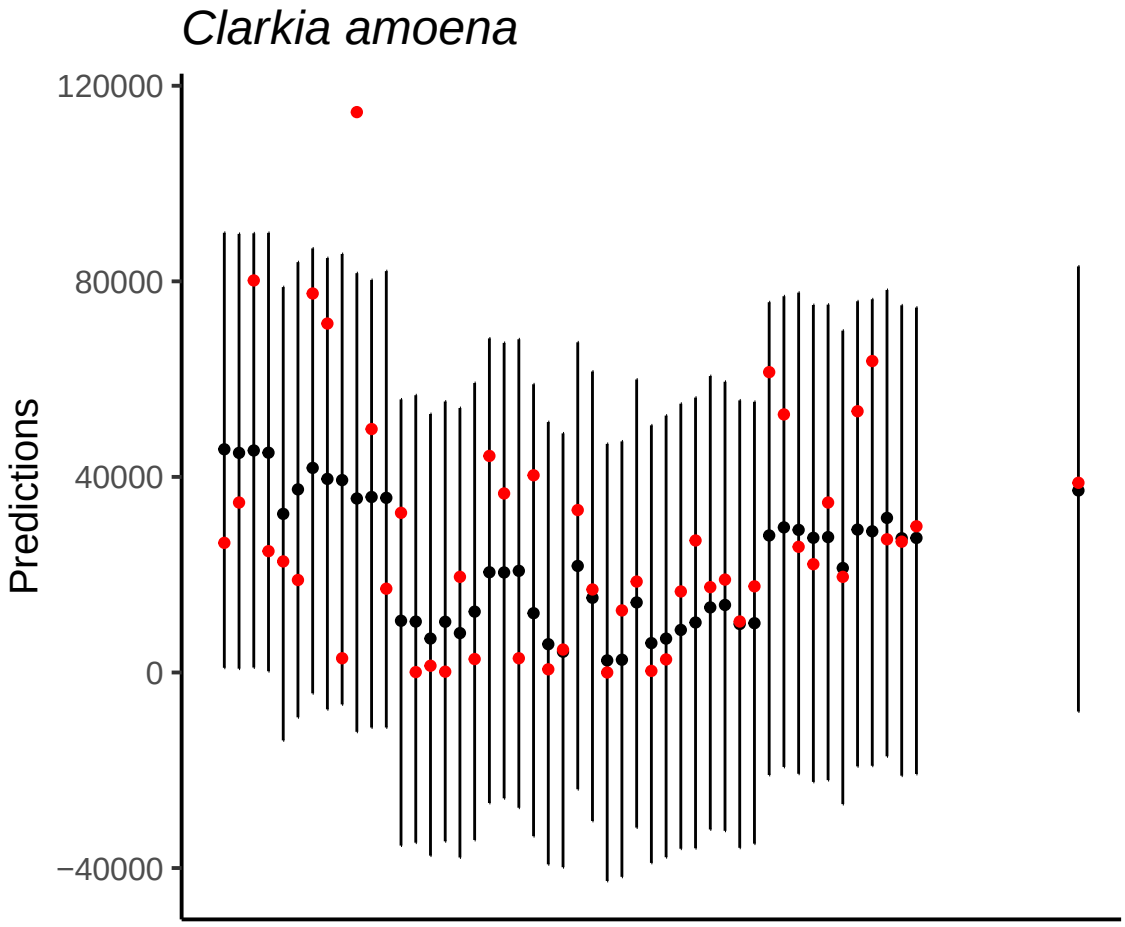

Figure S3. Posterior predictive distributions for fitness measurements from each *Clarkia amoena* plant. Black points represent median posterior predictions and error bars represent the 95% credible intervals of the posterior predictive distribution. Red points represent the true fitness values.

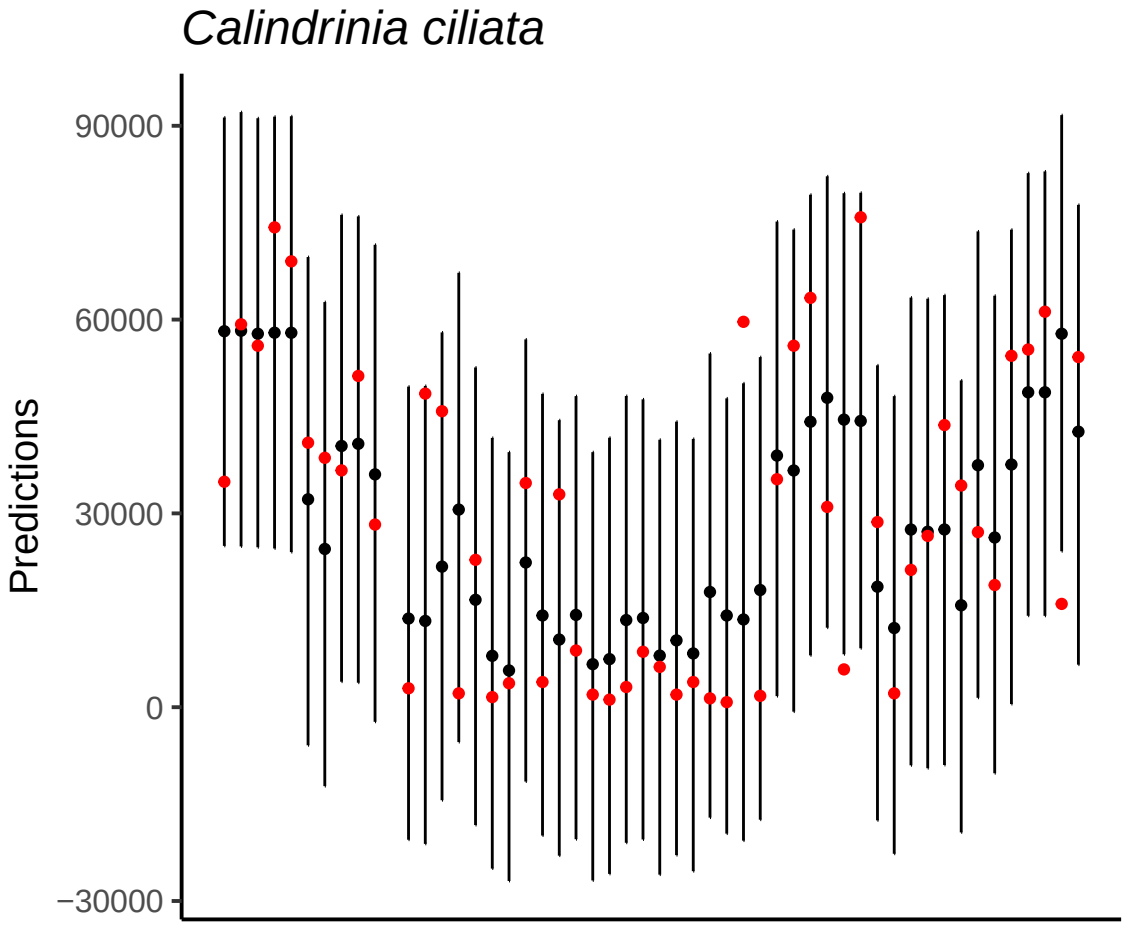

Figure S4. Posterior predictive distributions for fitness measurements from each *Calindrinia ciliata* plant. Black points represent median posterior predictions and error bars represent the 95% credible intervals of the posterior predictive distribution. Red points represent the true fitness values.

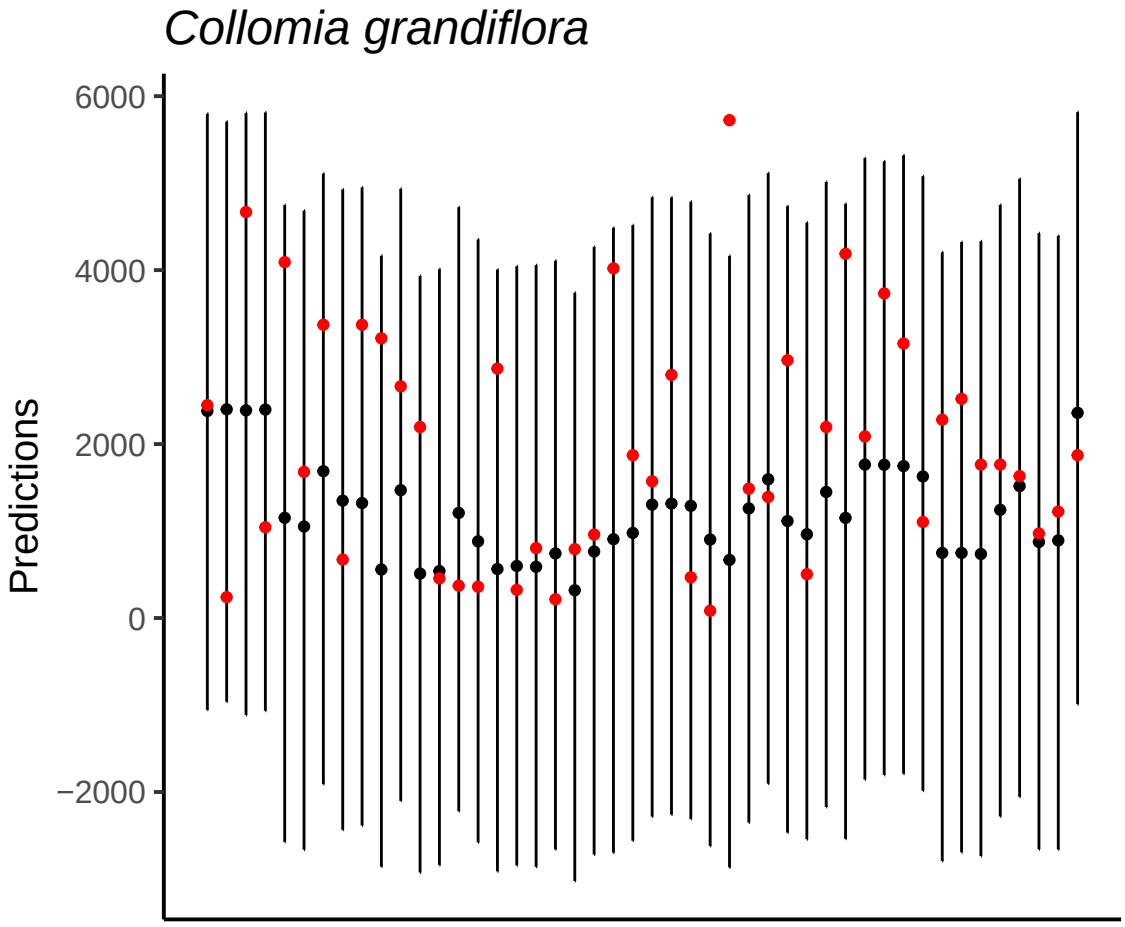

Figure S5. Posterior predictive distributions for fitness measurements from each *Collomia grandiflora* plant. Black points represent median posterior predictions and error bars represent the 95% credible intervals of the posterior predictive distribution. Red points represent the true fitness values.

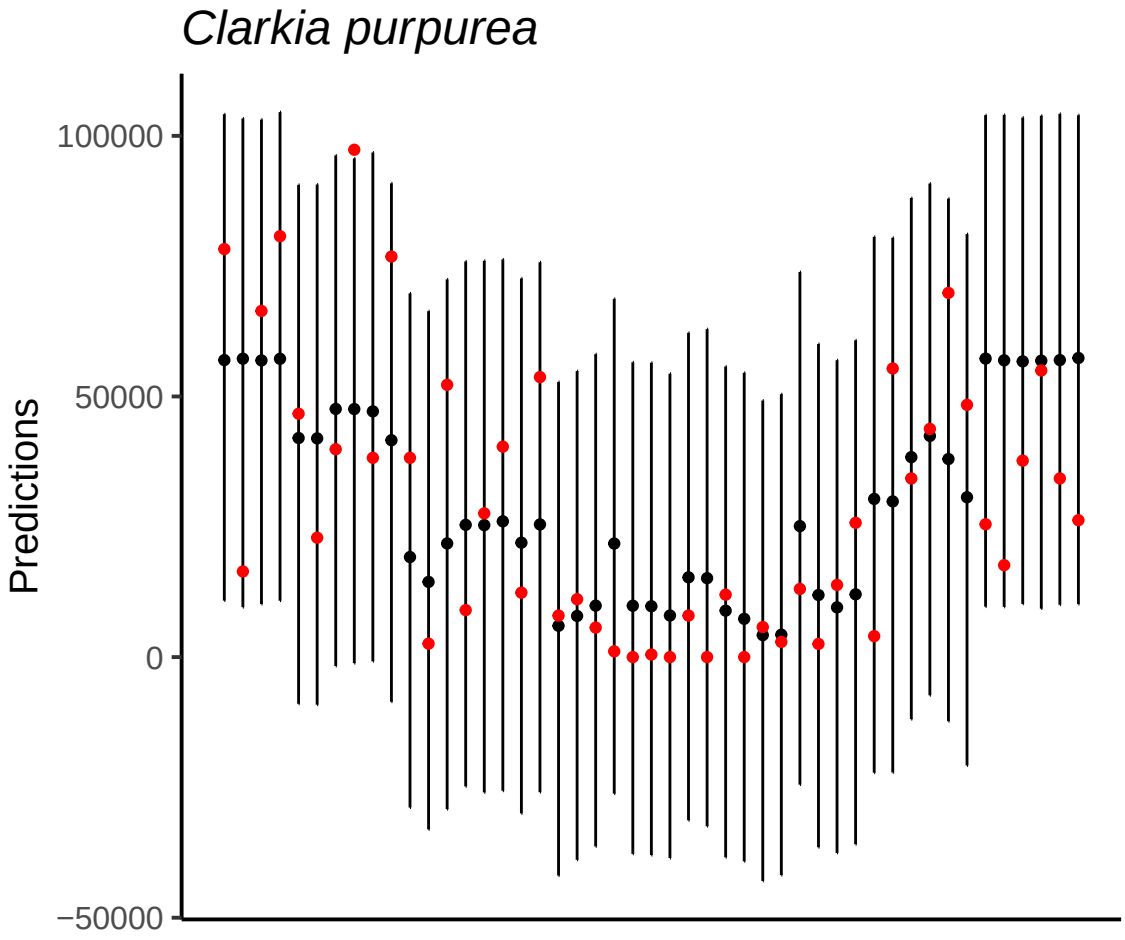

Figure S6. Posterior predictive distributions for fitness measurements from each *Clarkia purpurea* plant. Black points represent median posterior predictions and error bars represent the 95% credible intervals of the posterior predictive distribution. Red points represent the true fitness values.

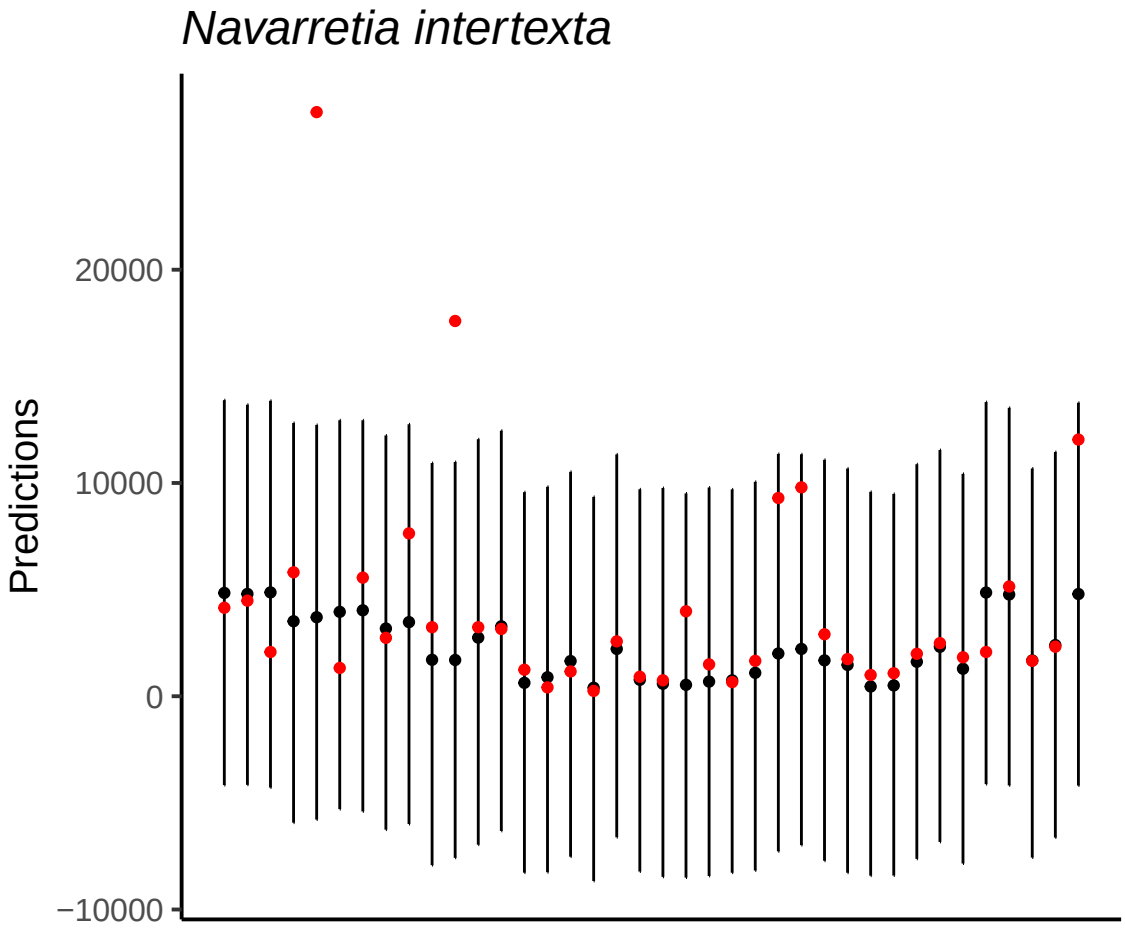

Figure S7. Posterior predictive distributions for fitness measurements from each *Navarretia intertexta* plant. Black points represent median posterior predictions and error bars represent the 95% credible intervals of the posterior predictive distribution. Red points represent the true fitness values.

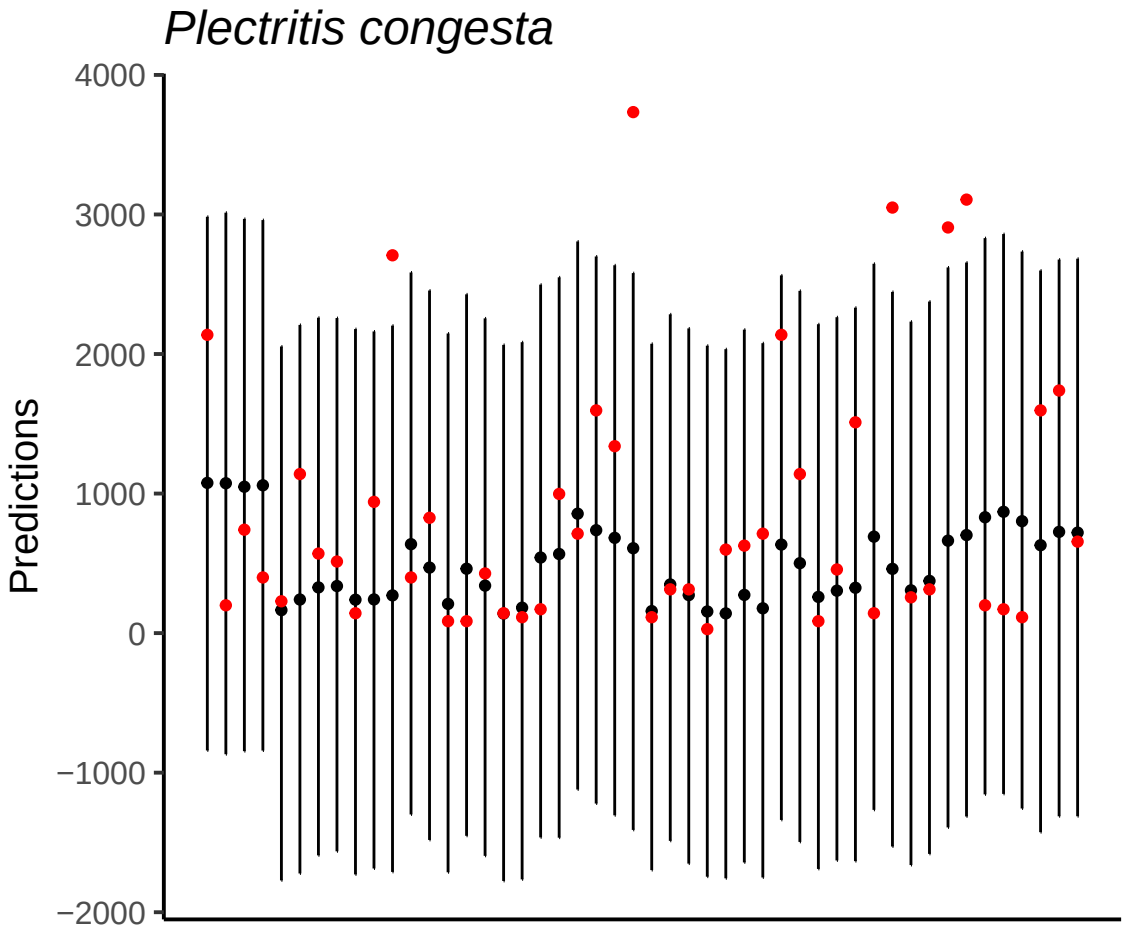

Figure S8. Posterior predictive distributions for fitness measurements from each *Plectritis congesta* plant. Black points represent median posterior predictions and error bars represent the 95% credible intervals of the posterior predictive distribution. Red points represent the true fitness values.

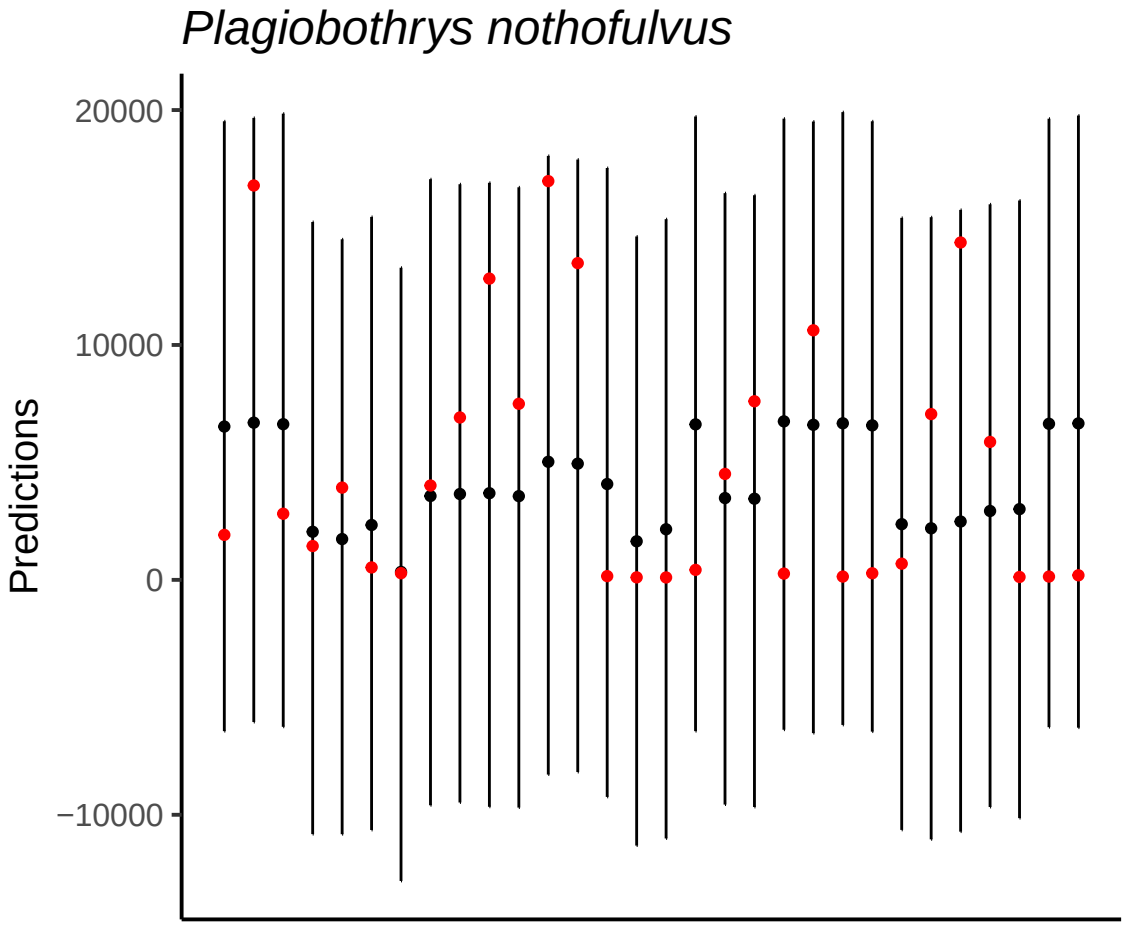

Figure S9. Posterior predictive distributions for fitness measurements from each *Plagiobothrys nothofulvus* plant. Black points represent median posterior predictions and error bars represent the 95% credible intervals of the posterior predictive distribution. Red points represent the true fitness values.

bray-curtis dissimilarity between species' soil mycobiome were estimated from the sample dissimilarity matrix as described in the main text.

Phylogenetic distance was used to fit a single random sample from the posterior distribution of mean fungal dissimilarity, and the coefficients of this model were saved. This process was repeated with 5000 random samples from the posterior, resulting in a distribution of coefficients that represent, given our data, our certainty in the relationship between phylogenetic distance and fungal community dissimilarity.

In addition to the coefficients from these linear models, we also retained the residuals of these models which were used in place of fungal community dissimilarity in additional analyses. We repeated the main analyses in the text with these residuals to assess how niche differences, fitness inequalities, and the probability of coexistence were related to fungal community dissimilarity after accounting for the phylogenetic autocorrelation of species pairs.

A.2.2 Results. When fitting these models with all species pairs, we found no relationship between fungal community dissimilarity and phylogenetic dissimilarity. However, this was due to two species pairs (*Clarkia amoena* & *Clarkia purpurea*; *Collomia grandiflora* & *Navarrettia intertexta*) having extremely low phylogenetic distance relative to the remaining 26 species pairs. Excluding these two pairs of sister taxa, we did find evidence of a phylogenetic signature within fungal community composition such that all of our coefficients from our linear models were positive (Figure S1; Median = 0.0019; 95% CI[0.0016,0.0022]).

When using the residuals of these models in place of fungal community dissimilarity, their general relationships with niche differences, fitness inequalities, and coexistence probabilities all remained the same as those reported in the main

text. However the exact parameter estimates did vary. With these residuals, 90.69% of the growth rate estimates in the exponential niche difference models predicted a positive relationship between fungal community dissimilarity and niche differences (Figure S2; Median = -6.08; 95% CI[-15.57, 3.97]). When fitting models for fitness inequalities, 88.90% of the growth rate estimates predicted a positive relationship with fungal community dissimilarity (Figure S3; Median = 4.21; 95% CI[-2.23, 10.64]). Still, these functions of niche and fitness differences suggest that coexistence could not be predicted by the residual variation in fungal community dissimilarity after accounting for phylogeny per se. Finally, 99.82% of the coefficients from the binomial models predicted a positive relationship between fungal community dissimilarity and coexistence probability (Figure S4; Median = 7.27; 95% CI[2.70,12.50]).

Overall, although we found support for a relationship between phylogenetic distance and fungal community dissimilarity, when accounting for this relationship, the remaining variation in fungal community dissimilarity was still predictive of competitive dynamics between species pairs. Because the models using the residuals predicted similar trends to those with the fungal community dissimilarity estimates, we chose to report the more latter, more simplified models in the main text.

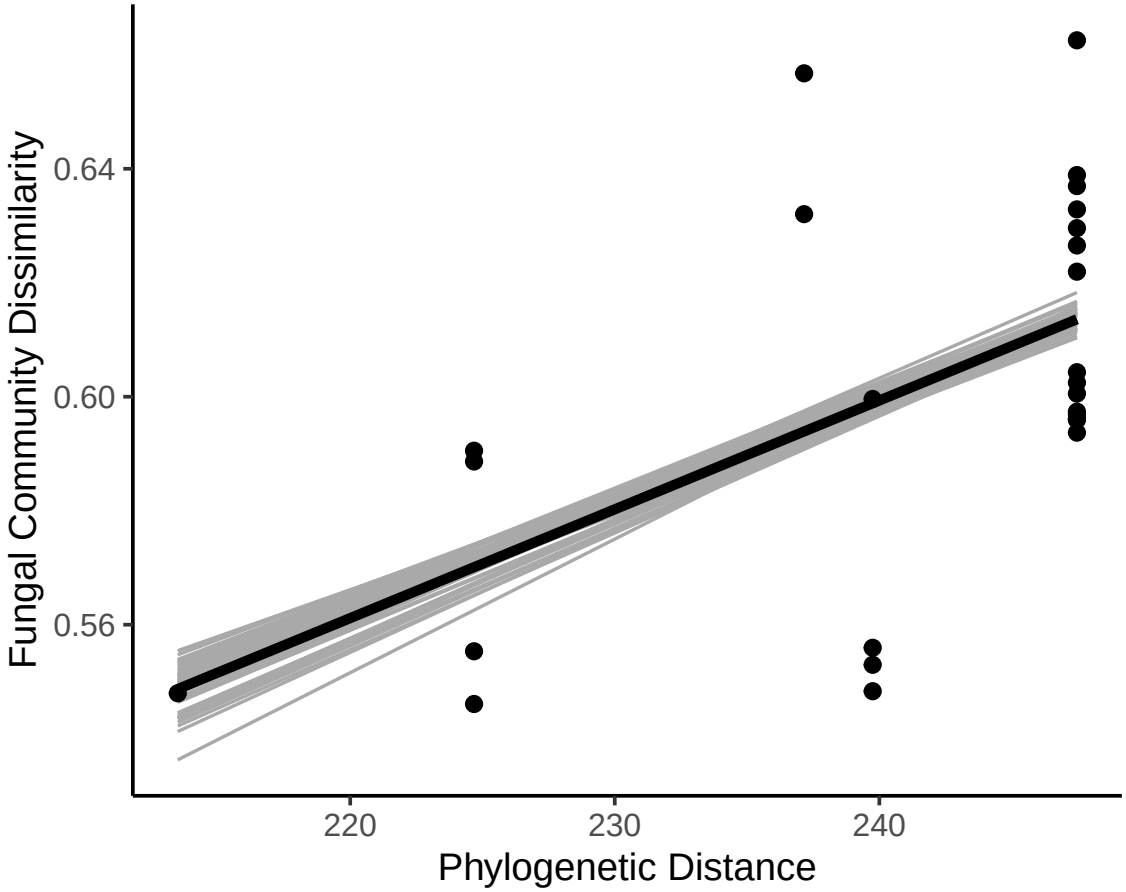

Figure S10. Median pairwise dissimilarity in species associated fungal communities as a function of pairwise phylogenetic distance. Black line represents the median parameter estimates from 5000 lines fit with random pulls from our estimates of average fungal community dissimilarity. Grey lines represent 50 random pulls from the total distribution of 5000 lines.

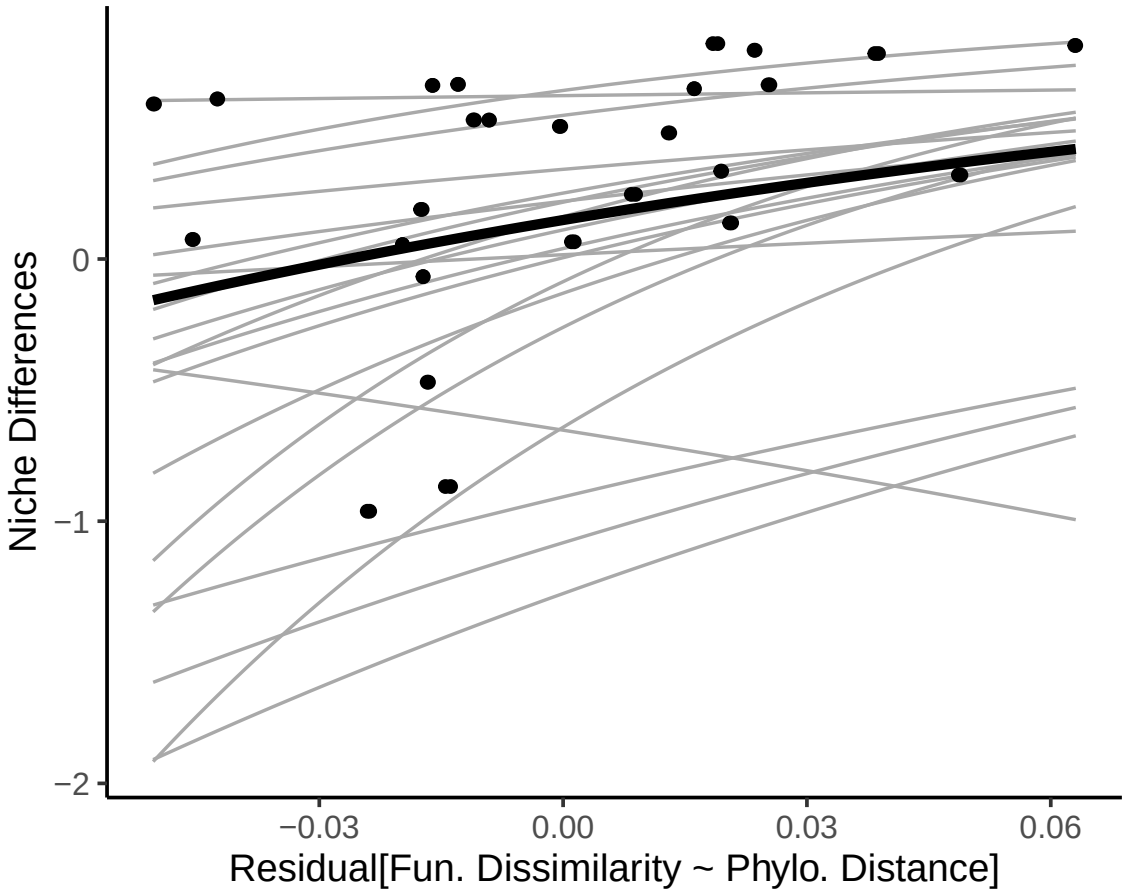

Figure S11. Relationship between niche differences and the residual variation in fungal community dissimilarity after accounting for phylogentic distance. Points are the median niche difference estimates and median residual values. Black curve represents the median parameter estimates from 5000 exponential curves fit with random pulls from the distibutions of niche differences and residuals. Gray curves represent 50 random pulls from the 5000 exponential curves.

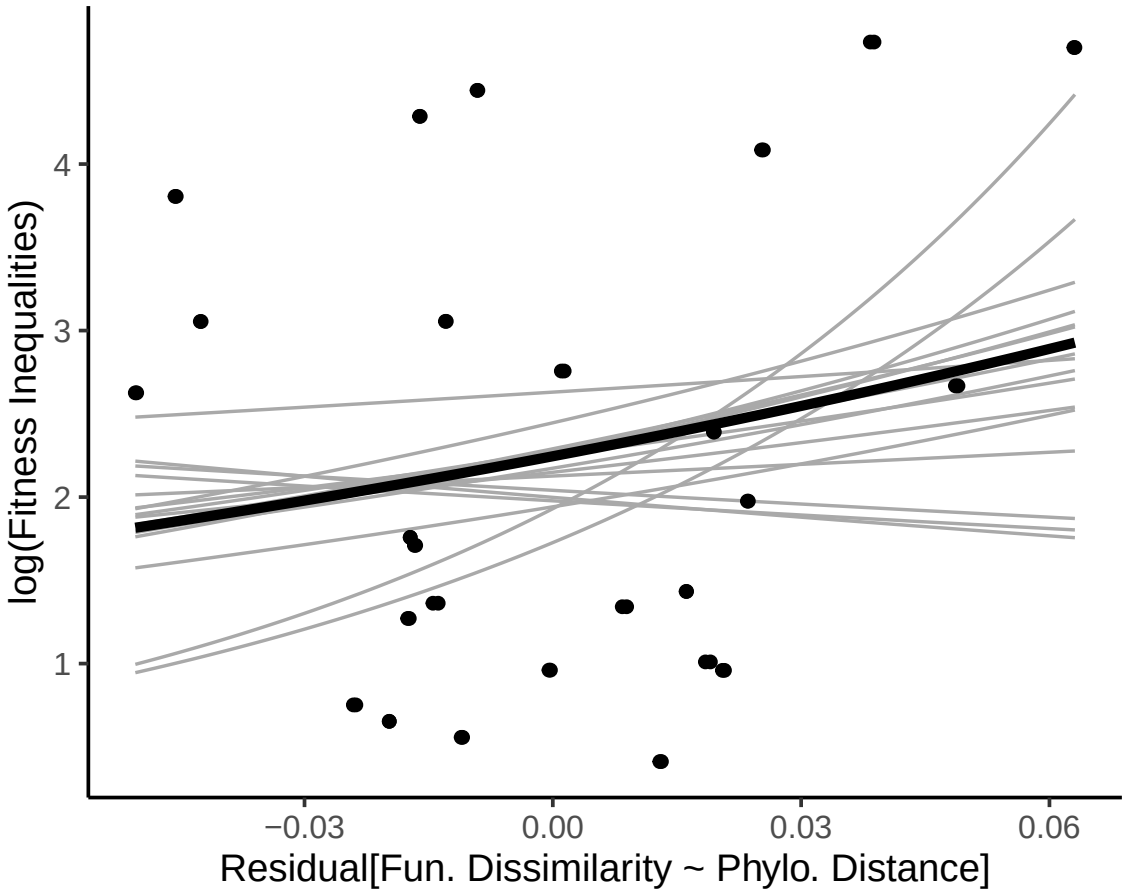

Figure S12. Relationship between fitness inequalities and the residual variation in fungal community dissimilarity after accounting for phylogentic distance. Points are the median fitness inequality estimates and median residual values. Black curve represents the median parameter estimates from 5000 exponential curves fit with random pulls from the distibution of fitness inequalities and residuals. Gray curves represent 50 random pulls from the 5000 exponential curves.

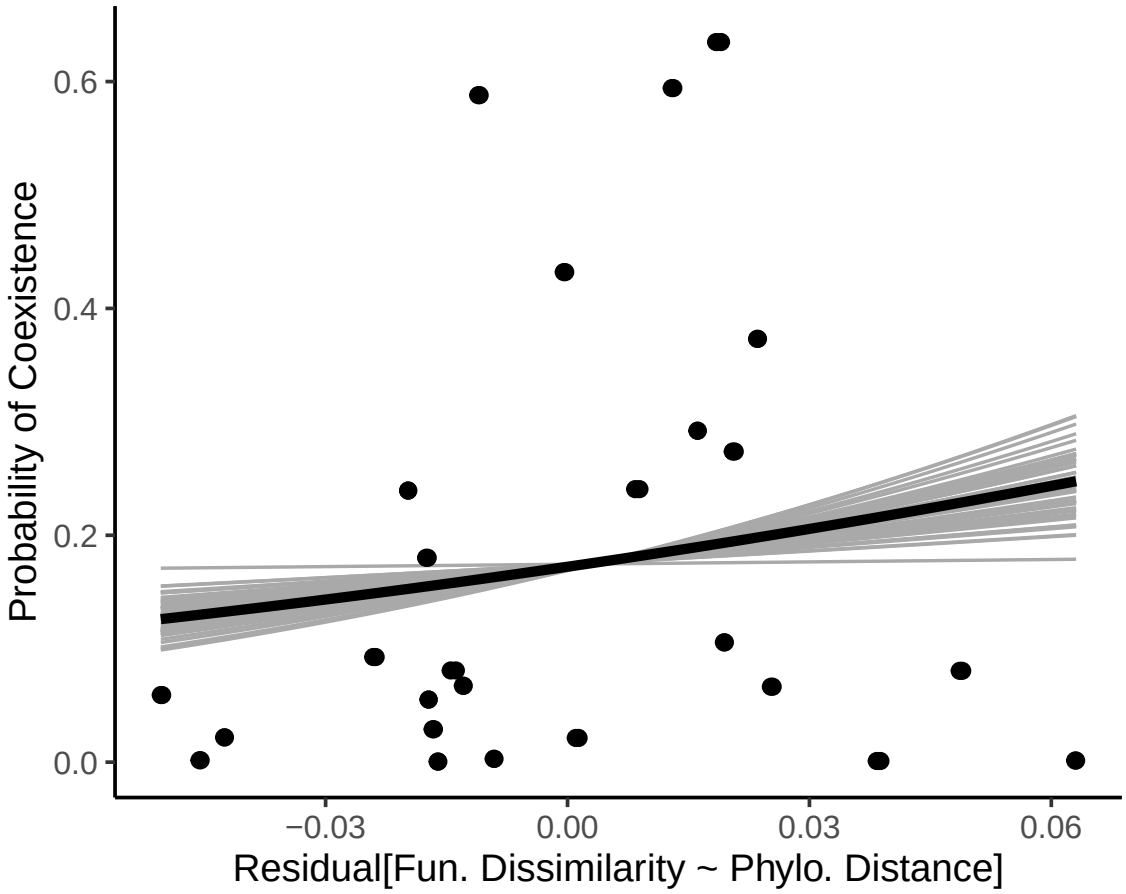

Figure S13. Coexistence probability as a function of the residual variation in fungal community dissimilarity after accounting for phylogenetic distance. Points are the coexistence probailities and median residuals. The black curve represents the median parameter estimate from the 5000 binomial regressions with random pulls from the distribution of the residuals. Gray curves represent 50 random pulls from the 5000 binomial curves.

A.3 Asymptotic Functions

A.3.1 Form of Equations. One could quantify the relationship between a functional trait difference and the pairwise niche differences and fitness differences by fitting a linear model of niche and fitness difference estimates and mean trait differences. However, predictions of such a model may quickly become unreasonable because there are natural asymptotes imposed by the calculation of niche and fitness differences. The value of these asymptotes will vary depending on the exact definition of niche and fitness differences, but using the definitions from the main text, niche differences can range from $-\infty$ to 1 whereas fitness differences can range from 0 to ∞. Because the goal was not only to quantify the relationship between fungal community dissimilarity and niche and fitness differences (for which linear models may suffice), but to evaluate the downstream consequences for coexistence, we have chosen to fit asymptotic functions that yield more reasonable predictions along a hypothetical dissimilarity gradient similar to those used by Godoy et al. 2014.

We began with a general form of an exponential equation:

$$y = ae^{kd} \tag{A.2}$$

where a is the x-intercept and k is the rate of change of our response variable (y) with fungal community dissimilarity (d). This general form has an asymptote at 0, and if a is constrained to be positive, will never predict values of y less than 0. Thus, our equation for fitness differences looked very similar to Eq. 1:

$$FI(d) = a_{FI}e^{k_{FI}d} \tag{A.3}$$

which we fit to our data while constraining a_{FI} to be positive. Conversely, to impose an asymptote of 1, we fit the following equation for niche differences:

$$ND(d) = 1 + a_{ND}e^{k_{FI}d} \tag{A.4}$$

To ensure that the predictions of this equation remain below the asymptote, we constrained a_{ND} to be negative while fitting this equation. Notably, this flips the interpretation of k_{ND} such that negative values represent decaying growth toward 1 and positive values represent exponential decrease away from 1.

A.3.2 Interpretation of Equations.

A.3.2.1 Parameter Interpretation. The rate parameters k_{FI} and k_{ND} represent the magnitude and direction of the change in fitness inequalities and niche differences respectively with fungal community dissimilarity. Importantly, these parameters differ in interpretation from standard slope parameters in a linear mode in two ways. First, as stated above, positive values of k_{ND} would suggest a negative correlation between niche differences and fungal community dissimilarity whereas negative values of k_{ND} would correspond to our hypothesized positive correlation. Secondly, comparing values of k_{FI} and k_{ND} may be inform us of how the *overall* rate of change varies between these quantities along a dissimilarity gradient from $-\inf$ to $\inf$, but alone, these values do *not* inform us of differences in the instantaneous growth rate (value of first derivative) between these two quantities at any given value of fungal dissimilarity. It is thus important, when discussing the relative rate of increase in fitness differences v.s. niche differences to distinguish the overall rate of increase from the rate of increase at some focal point or some focal range.

A.3.2.2 Evaluating Coexistence. To make predictions about coexistence using these functions, we can derive a new equation for the minimum required niche differences for coexistence ($rND(d)$) such that a species pair is predicted to coexist if $rND(d) < ND(d)$. The minimum required niche differences for coexistence is determined by the fitness inequalities according to the coexistence criterion from Chesson & Kuang 2008, which assuming that the niche overlap is equal to $1 - ND$, can be written as:

$$1 - ND < \frac{\kappa_j}{\kappa_i} < \frac{1}{1 - ND} \tag{A.5}$$

where $\frac{\kappa_j}{\kappa_i}$ is the fitness ratio. Because we calculated the fitness inequality as the maximum fitness ratio (or the fitness ratio calculated with where species i is the inferior competitor), we can simplify this criterion to:

$$FI < \frac{1}{1 - ND} \tag{A.6}$$

Solving this inequality for ND and deeming this the minimum required niche differences for coexistence (rND), we get:

$$rND = 1 - \frac{1}{FI} \tag{A.7}$$

Finally, substituting FI(d) for FI, we get the function for rND along a fungal community dissimilarity gradient:

$$rND = 1 - \frac{1}{a_{FI} e^{k_{FI} d}} \tag{A.8}$$

A.3.2.3 Possible Model Behaviors. By constraining the values of a in Eq. 2 and Eq. 3, the predictions from these functions will remain below

and above their asymptotes respectively. This does not constrain the sign of the relationship between dissimilarity and either ND or FI as k is free to be positive or negative. Thus, ND may increase toward or decrease from 1, and FI may increase from or decrease toward 0. Assuming that our hypotheses of increasing ND and FI with dissimilarity (hypotheses supported by our results), there are five possible outcomes with distinct implications for coexistence: 1) FI exceed ND within the focal range of dissimilarity (or possible universally), suggesting that species are never predicted to coexist along the dissimilarity gradient. 2) ND exceed FI within the focal range of dissimilarity, suggesting that species are always predicted to coexist along the gradient. 3) At some point within the focal range, ND begin to exceed FI, suggesting that there is a single minimum dissimilarity, above which species may coexist. 4) At some point within the focal range, FI begin to exceed ND, suggesting that there is a single maximum dissimilarity, under which species may coexist. 5) The two functions intersect twice within the focal range, suggesting that their is some range of dissimilarity values within which species may coexist. These scenarios are shown in Figure S1.

A.3.3 Relation to Coexistence Probability. These parameterized equations make deterministic predictions about coexistence for any value of fungal community dissimilarity. However, uncertainty exists in this system in the form of 1) intraspecific variation in associated fungal communities, 2) intraspecific variation in unmeasured traits, 3) interactions between fungal community dissimilarity and intraspecific variation, and 4) measurement error. Thus, in addition to understanding how these functions make single predictions about the outcome of competition, we may also wish to understand how, given variation around model predictions, these functions relate to the probability of any given species pair

coexisting. Ultimately, we propose that there should be a positive relationship between $ND(d) - rND(d)$ and the coexistence probability, regardless of whether the deterministic models predict coexistence along an underlying gradient in species dissimilarity. To demonstrate this, we present the results of some stochastic simulations which introduce uncertainty into our parameterized models of niche and fitness differences.

A.3.3.1 Stochastic Simulations. To demonstrate the relationship between $ND(d) - rND(d)$ and the probability of coexistence, we used our parameterized niche and fitness differences models (which do not predict coexistence at any point along our observed range of fungal community dissimilarity) to simulate the niche differences and required niche differences of theoretical species pairs that vary in their mean fungal community dissimilarity. For every hundredth value of the Bray-Curtis dissimilarity ranging from 0 to 1, we pulled 1000 random values for niche differences and required niche differences from truncated normal distributions (Mersmann, Trautmann, Steuer, & Bornkamp, 2023). The mean of each distribution was defined as the predicted value according to our parameterized models using the median parameter estimates. The standard deviation of the truncated normal distributions was defined as the standard deviation of the observed median niche difference and required niche difference estimates from our 64 species pairs (0.47 and 0.21 respectively). For each dissimilarity value, we calculated the probability that a species pair would coexist by taking the proportion of iterations in which $ND > rND$.

Overall, we found a sigmoidal relationship between fungal community dissimilarity and our simulated coexistence probability (Figure S2). At low fungal community dissimilarity (where the $ND - rND$ is high), there is virtually

no chance of coexistence. However, at some critical dissimilarity value (a bit over 0.5), the coexistence probability increases up to a point and levels off at a maximum value as fungal community dissimilarity approaches 1. Importantly, within our range of estimated mean dissimilarities between species, the simulated coexistence probability shows a near linear increase with increasing community dissimilarity. This finding corroborates the findings that the estimated coexistence probability among our species pairs is positively correlated with fungal community dissimilarity. Further, these results suggest that even when deterministic models of niche and fitness differences along the dissimilarity gradient predict universal exclusion, ambient stochasticity may lead to a positive relationship between dissimilarity and the probability of coexistence.

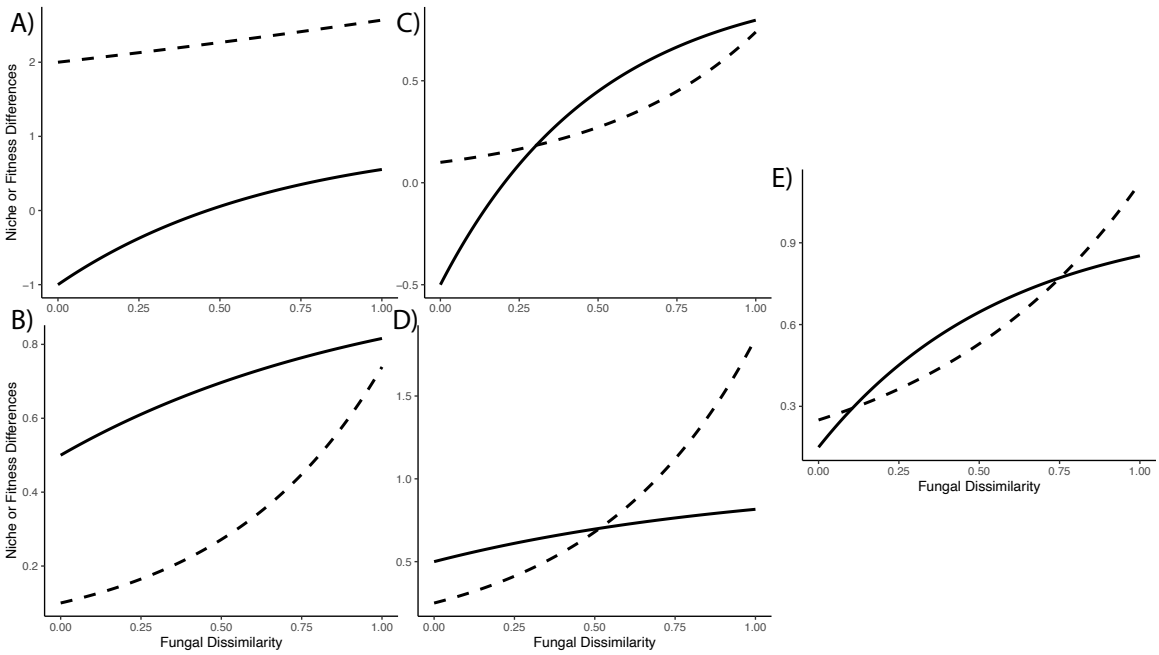

Figure S14. Example parameterizations for the five possible model behaviors, assuming that both niche and fitness differences increase with fungal community dissimilarity. The solid line represents niche differences and the dashed line represents fitness inequalities. Coexistence is predicted with the solid line exceeds the dashed line. A) Coexistence is never predicted ($a_{ND} = -2$, $k_{ND} = -1.5$, $a_{FI} = 2$, $k_{FI} = 0.25$). B) Coexistence is always predicted ($a_{ND} = -0.5$, $k_{ND} = -1$, $a_{FI} = 0.1$, $k_{FI} = 2$). C) A minimum dissimilarity point exists, above which coexistence is predicted ($a_{ND} = -1.5$, $k_{ND} = -2$, $a_{FI} = 0.1$, $k_{FI} = 2$). D) A maximum dissimilarity point exists, below which coexistence is predicted ($a_{ND} = -0.5$, $k_{ND} = -1$, $a_{FI} = 0.25$, $k_{FI} = 2$). E) A range of dissimilarity values exists within which coexistence is predicted ($a_{ND} = -0.85$, $k_{ND} = -1.75$, $a_{FI} = 0.25$, $k_{FI} = 1.5$).

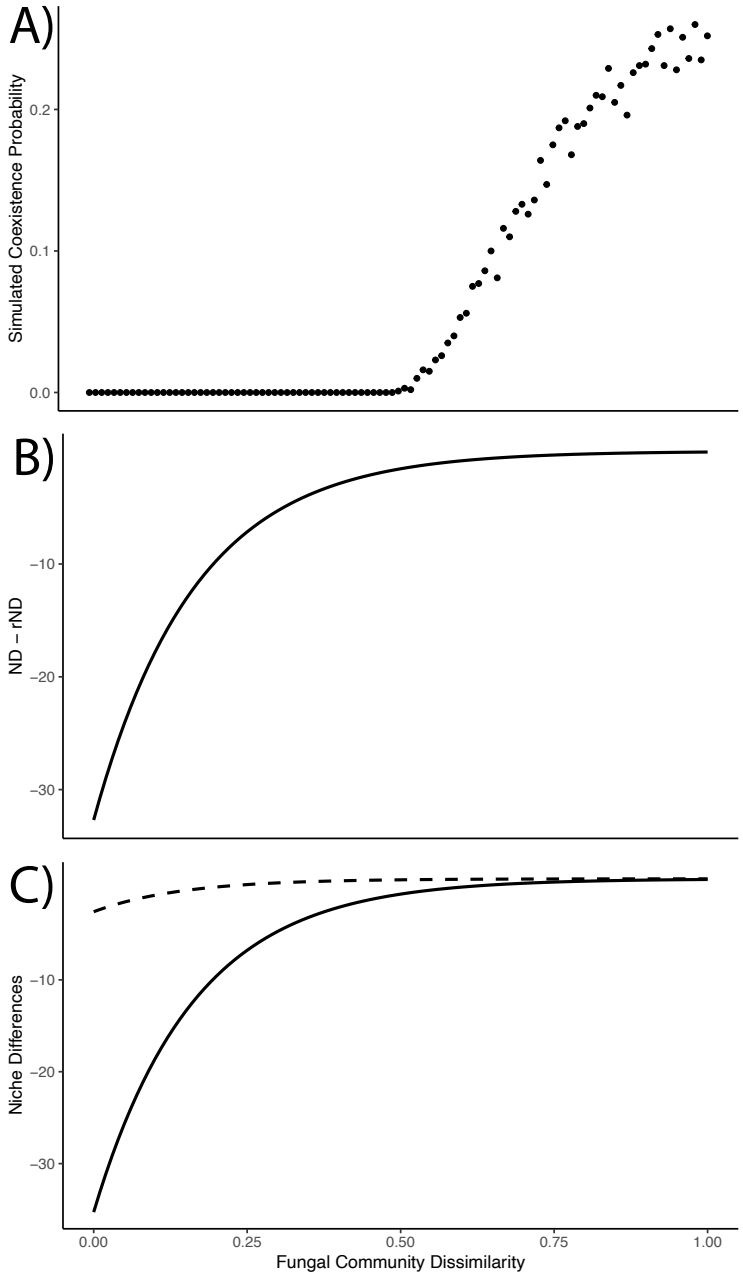

Figure S15.]

A) Simulated coexistence probability from our fit niche and fitness differences models along a fungal community dissimilarity gradient. Points represent the proportion of iterations in which randomly generated niche differences exceeded the randomly generated required niche differences for coexistence. B) Difference between the predicted niche differences and required niche differences for coexistence along the fungal community dissimilarity gradient. C) Predicted niche differences (solid) and required niche differences for coexistence (dashed) along a fungal community dissimilarity from our asymptotic models with median parameter estimates.

A.4 Results from Experimental and Monoculture Samples

A.4.1 Fungal Community Composition. Among the samples from the competition experiment, we still found a species effect on fungal community composition (PERMANOVA; $p = 0.035$; $R^2 = 0.11936$; Figure S1A). Much moreso than with the experimental samples, the samples from the monoculture beds displayed a strong species signature in fungal community composition (PERMANOVA; $p = 0.001$; $R^2 = 0.30545$; Figure S1B).

A.4.2 Competition Strength. We found some evidence of a negative relationship between overall competition strength and fungal community dissimilarity in both experimental (Median = 0.74; 95% CI[-3.93, 2.25]; 72.06% of distribution < 0) and monoculture (Median = -0.89; 95% CI[-2.97, 0.94]; 81.50% of distribution < 0) samples. Unlike the results from using both sample types combined, when divided into intra- and interspecific competition, fungal community dissimilarity did not vary with interspecific competition or with intraspecific competition for either experimental samples or monoculture samples.

A.4.3 Niche and Fitness Differences. We found a positive association between fungal community dissimilarity from our experimental samples and both niche differences and fitness inequalities (Figure S2A). 77.92% of the samples from our distribution predict a positive association between dissimilarity and niche differences (Median = -3.06; 95% CI[-14.24,5.20]). 85.41% of the samples from our distribution predict a positive association between dissimilarity and fitness inequalities (Median = 1.79; 95% CI[-1.51,5.55]). When using dissimilarity estimates from our monoculture samples, we found strong evidence supporting a positive relationship between dissimilarity and fitness inequalities, but only marginal support for a positive relationship with niche differences (Figure S2B).

69.28% samples predict a positive association between dissimilarity and niche differences (Median = -1.40; 95% CI[-9.89,4.70]). 86.03% of the samples from our distribution predict a positive association between dissimilarity and fitness inequalities (Median = 3.09; 95% CI[-2.04,10.10]).

A.4.4 Coexistence Probability. Similar to the main results with the full dataset, the results from our fractional logistic regression with just the experimental samples suggest that there is a positive association between fungal dissimilarity and the probability of coexistence (Figure S3B). 70.52% of the samples from our distribution were positive (Median = 0.62, 95% CI[-1.67,3.04]). Conversely, the results from our binomial regression with just the monoculture samples suggest that there is little evidence for any association between fungal dissimilarity and the probability of coexistence (Figure S3B).

A.5 Results from Different Fungal Guilds

A.5.1 Community Composition. When dividing the total fungal community dataset into subsets by containing only taxa of a particular trophic mode (pathotrophs, saprotrophs, and symbiotrophs), we still found an interactive effect of plant species and sample type on fungal community composition for each subset (Table S1). To assess whether mean species-level dissimilarity estimated from these subsets differed from the total dataset and one another, we performed 500 mantel tests from random pulls from the posterior distributions of the mean species-level dissimilarity. These mantel tests suggested that mean dissimilarity did vary across trophic modes (Figure S1) except for the symbiotrophes which were not dissimilar from the means estimated from the total dataset or the means estimated from either the pathotroph or saprotroph datasets (Table S2).

A.5.2 Competition Strength. When quantifying the potential relationship between dissimilarity of particular trophic modes and competition strength, we found that neither pathotroph (Median = -0.80; 95% CI[-5.45,3.70]) nor saptroptroph (Median = -0.91; 95% CI[-4.60,2.50]) dissimilarity were correlated with overall competition strength. However, we did find some support for a negative relationship between competition strength and symbiotroph dissimilarity (Median = -1.77; 95% CI[-5.55,1.73]). Similar to the results from the total fungal community dissimilarity, we found some support for a positive correlation between intraspecific dissimilarity and intraspecific competition. Pathotrophs showed the strongest signal of this relationship (Median = 4.55; 95% CI[-8.67,17.81]), followed by saprotrophs (Median = 3.14; 95% CI[-6.76.13.02]) and symbiotrophs (Median = 2.38; 95% CI[-7.23,12.49]). Of the three guilds, we only found a relationship

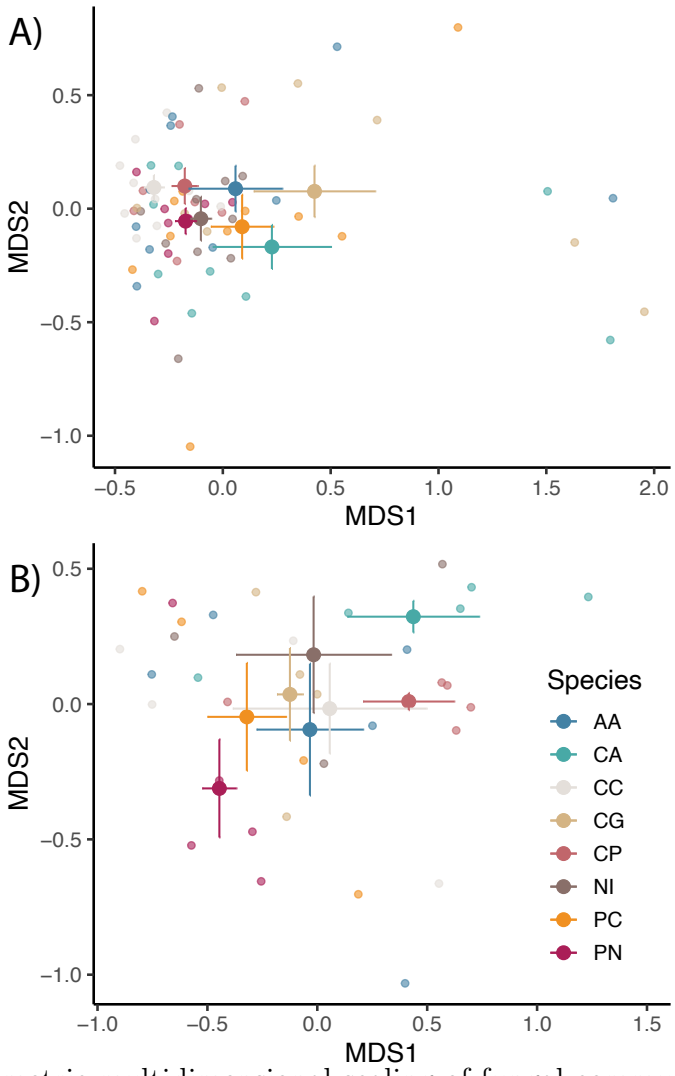

Figure S16. Nonmetric multidimensional scaling of fungal communities within either experimental samples (A) or monoculture samples (B). Small transparent points represent sample scores; larger solid points represent the average scores with errorbars equal to one standard error. Color represents the plant species associated with each sample.

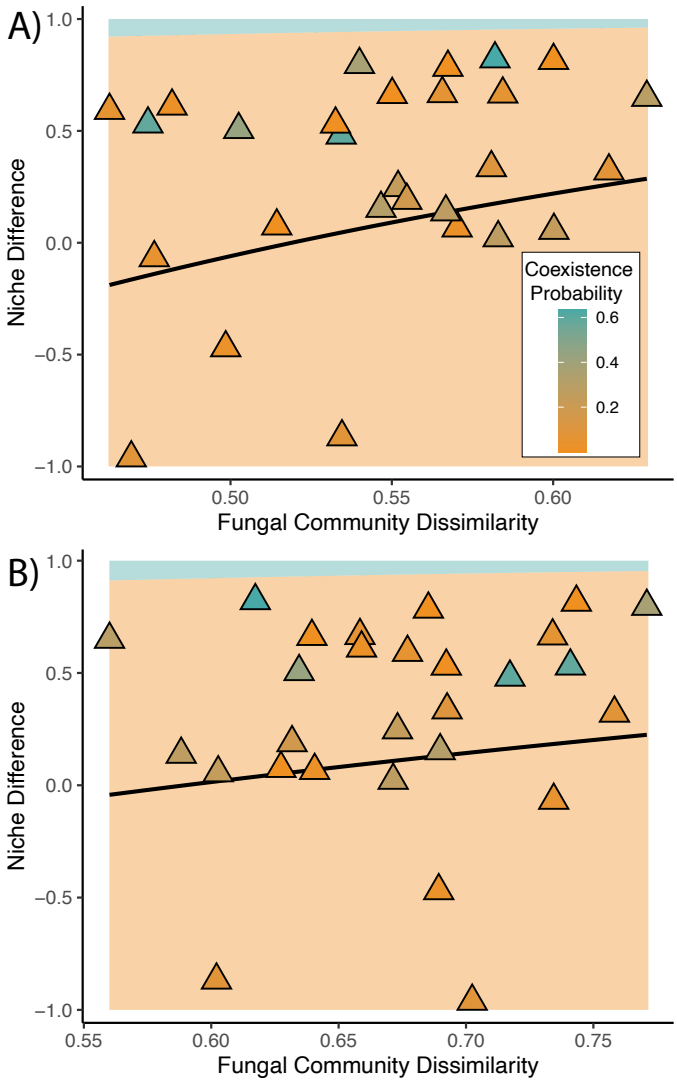

Figure S17. Niche differences as a function of fungal community dissimilarity in the experimental samples (A) and monoculture samples (B). All points represent the median of the posterior distribution for their respective quantities, and their color indicates that species pair's probability of coexistence. The black curve is the fit asymptotic equation relating niche differences to fungal community dissimilarity. The blue shaded area represents the coexistence domain when including the fit asymptotic function of fitness inequalities into the inequality statements derived from our criterion for coexistence. Similarly, the orange shaded area represents the area at which species pairs would not be expected to coexist based off of our estimated fitness inequalities as a function of fungal community dissimilarity.

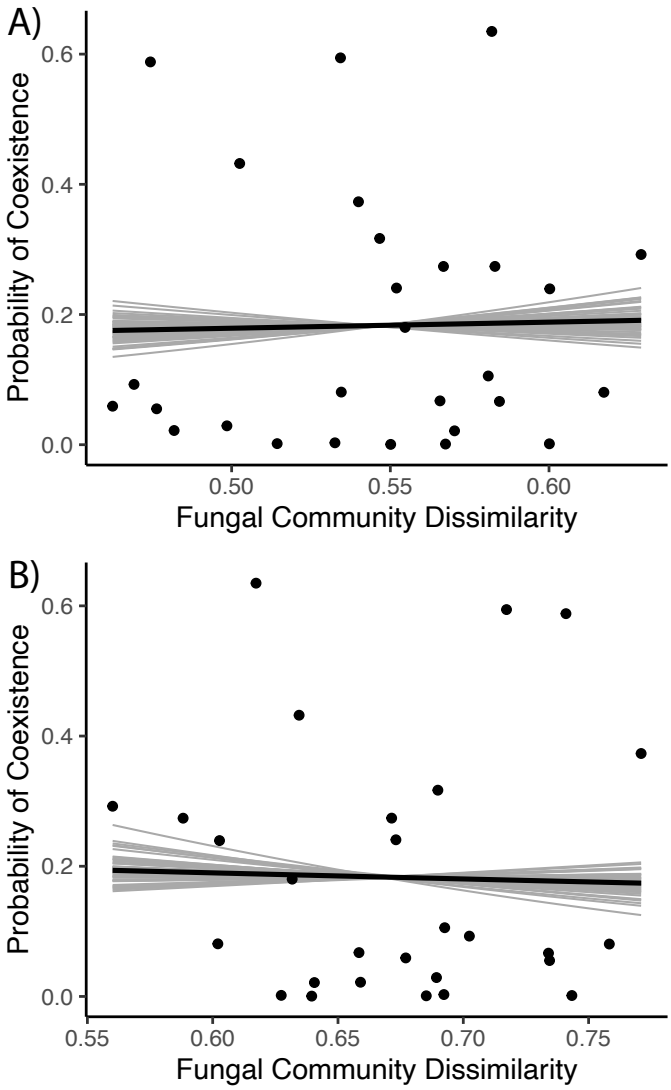

Figure S18. Probability of coexistence as a function of fungal dissimilarity for experimental samples (A) and monoculture samples (B). Dissimilarity values correspond to the median posterior distributions for species pair dissimilarities. Probability of coexistence was calculated as the proportion of samples from the posterior distribution that were predicted to coexist. The black curve is the binomial regression using the median slope and intercept parameters. Grey curves are 50 random draws from the distributions of slope and intercept parameters.

between dissimilarity and interspecific competition for symbiotrophs which appeared to have a negative correlation (Median = -1.81; 95% CI[-6.34;2.60]).

A.5.3 Niche and Fitness Differences. We found similar trends across all trophic modes when quantifying their relationship with niche and fitness differences. Symbiotrophs had the most positive relationship with niche differences (Median = -6.16; 95% CI[-16.63,4.50]), followed by pathotrophs (Median = -5.55; 95% CI[-15.21,4.66]) and saprotrophs (Median = -5.39; 95% CI[-14.65,3.90]). Pathotrophs had the most positive relationship with fitness inequalities (Median = 3.97; 95% CI[-1.98,9.47]), followed by symbiotrophs (Median = 2.96; 95% CI[-1.95,8.16]) and saprotrophs (Median = 2.69; 95% CI[-1.54,7.62]). No guild displayed any association between dissimilarity and competitive ratios. Pathotrophs had the most positive relationship with demographic ratios (Median = 4.01; 95% CI[-1.96,10.21]), followed by symbiotrophs (Median = 3.39; 95% CI[-2.34,10.16]) and saprotrophs (Median = 2.26; 95% CI[-1.71,8.27]).

A.5.4 Coexistence Probability. Among the three guilds, dissimilarity was positively correlated with coexistence probability. All guilds displayed similar trends with pathotrophs having a median coefficient of 2.76 (95% CI[-0.21,5.80]), saprotrophs having a median of 2.77 (95% CI[-0.22,5.91]) and symbiotrophs having a median of 2.76 (95% CI[-0.21,5.83]).

Predictor Variable	Total	Pathotrophs	Saptrophs	Symbiotrophs
Plant Species	$p = 0.002; R^2 = 0.088$	$p = 0.006; R^2 = 0.080$	$p = 0.011; R^2 = 0.083$	$p = 0.004; R^2 = 0.093$
Sample Type	$p < 0.001; R^2 = 0.058$	$p < 0.001; R^2 = 0.051$	$p < 0.001; R^2 = 0.065$	$p = 0.003; R^2 = 0.026$
Interaction	$p < 0.001; R^2 = 0.098$	$p = 0.008; R^2 = 0.083$	$p = 0.004; R^2 = 0.087$	$p = 0.051; R^2 = 0.077$

Table A.5. Table S5: Results from PERMANOVA for each trophic mode's fungal community dataset.

	Total	Pathotrophs	Saptrophs
Pathotrophs	92.8%		
Saprotrophs	99.8%	97.2%	
Symbiotrophs	9.6%	4.0%	1.8%

Table A.6. Table S6: Percent of mantel tests (out of 500 pulls from posterior distributions) that came out significant ($p < 0.05$) between estimates derived from four trophic mode datasets.

Response Variable	Total	Pathotrophs	Saptrophs	Symbiotrophs
Overall Competition Strength	None	None	None	Negative (83.70%)
Intraspecific Competition	Positive (80.60%)	Positive (76.42%)	Positive (73.88%)	Positive (69.60%)
Interspecific Competition	None	None	None	Negative (79.46%)
Niche Differences	Positive (86.49%)	Positive (83.63%)	Positive (87.75%)	Positive (86.49%)
Competitive Ratio	None	None	None	None
Log Demographic Ratio	Positive (88.40%)	Positive (90.35%)	Positive (86.15%)	Positive (88.40%)
Fitness Inequalities	Positive (90.03%)	Positive (90.57%)	Positive (88.81%)	Positive (88.37%)
Coexistence Probablity	Positive (96.36%)	Positive (96.66%)	Positive (96.50%)	Positive (96.50%)

Table A.7. Table S7: Relationships between fungal community dissimilarity and each of the competitive dynamic response variables across trophic modes. We considered dissimilarity to be related to a response variable if over 70% of the samples from our distributions of parameter estimates supported this relationship. These percentages are provided in parentheticals.

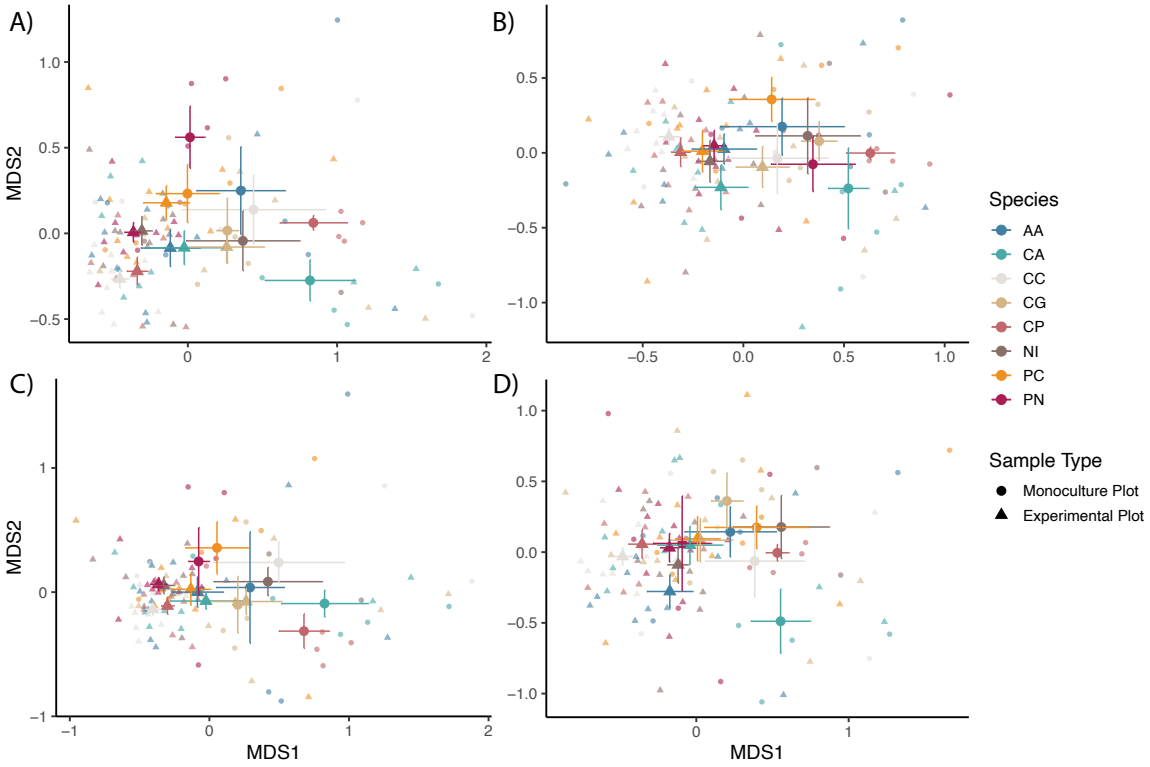

Figure S19. Non-metric multidimensional scaling using Bray-Curtis dissimilarities of total fungal (A), pathotroph (B), saprotroph (C), and symbiotroph (D) community composition across all samples. Small transparent points represent sample scores; larger solid points represent the average scores with errorbars equal to one standard error. Shape of points represents which plots samples came from, and color represents which species samples are associated with.

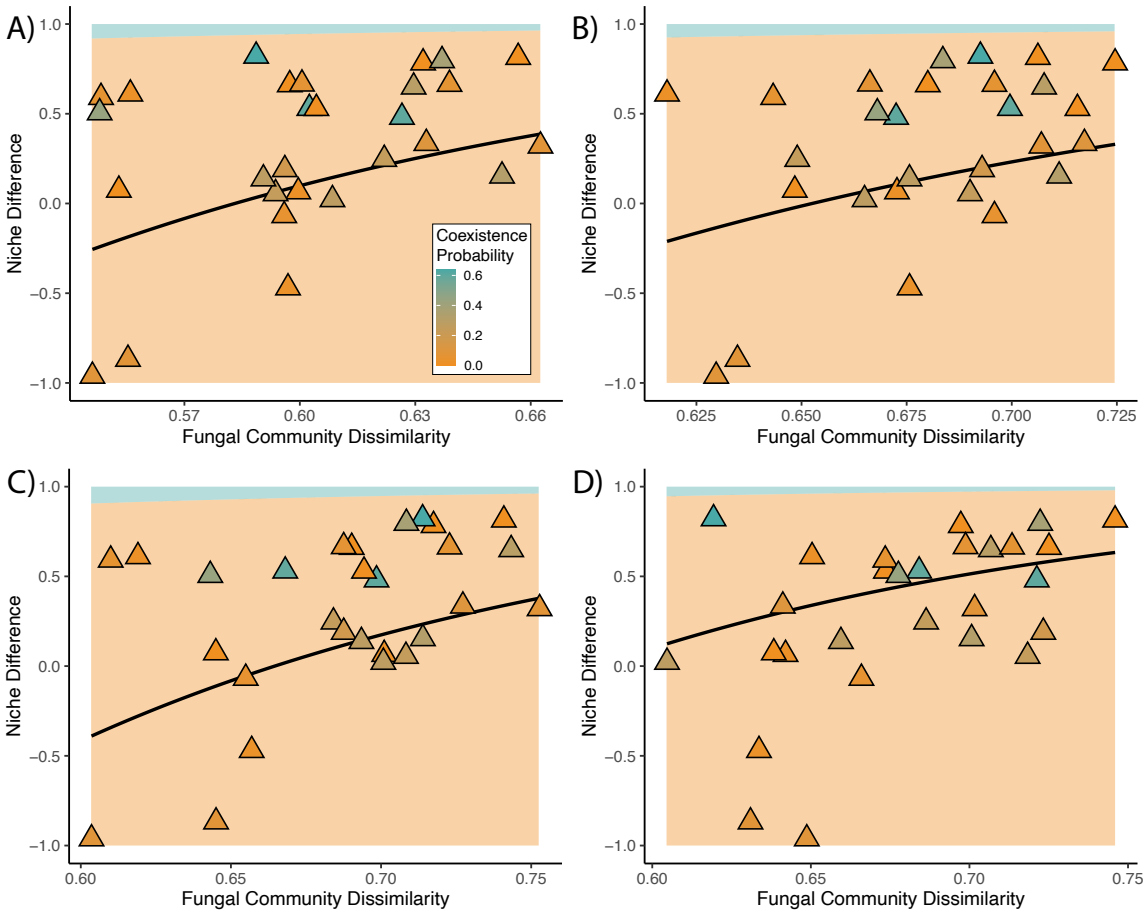

Figure S20. Niche differences as a function of total fungal (A), pathotroph (B), saprotroph (C), and symbiotroph (D) community dissimilarity. All points represent the median of the posterior distribution for their respective quantities, and their color indicates that species pair's probability of coexistence. The black curve is the fit asymptotic equation relating niche differences to fungal community dissimilarity. The blue shaded area represents the coexistence domain when including the fit asymptotic function of fitness inequalities into the inequality statements derived from our criterion for coexistence. Similarly, the orange shaded area represents the area at which species pairs would not be expected to coexist based off of our estimated fitness inequalities as a function of fungal community dissimilarity.

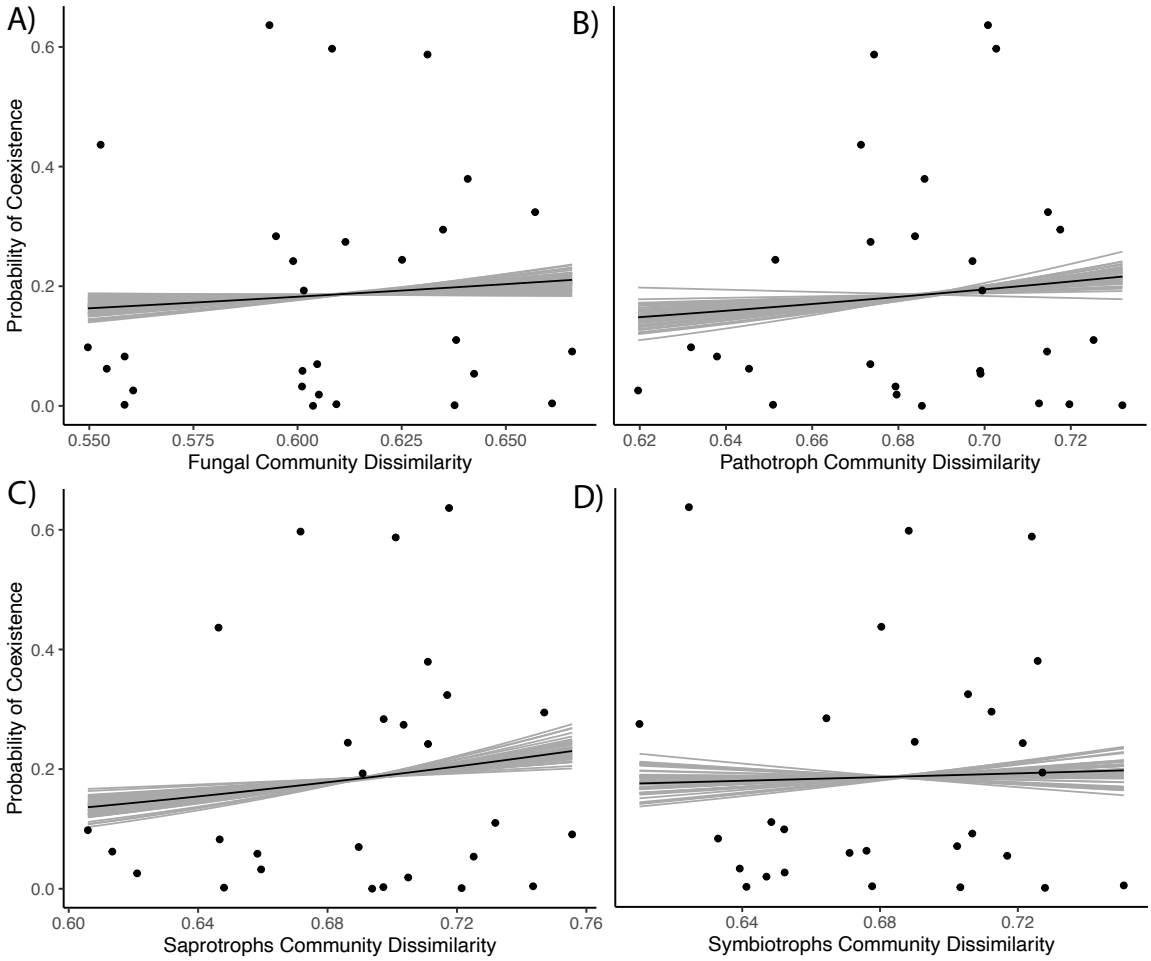

Figure S21. Probability of coexistence as a function of total fungal (A), pathotroph (B), saprotroph (C), and symbiotroph (D) community dissimilarity. Dissimilarity values correspond to the median posterior distributions for species pair dissimilarities. Probability of coexistence was calculated as the proportion of samples from the posterior distribution that were predicted to coexist. The black curve is the binomial regression using the median slope and intercept parameters. Grey curves are 50 random draws from the distributions of slope and intercept parameters.

A.6 Multispecies Coexistence Analyses

As an attempt to contextualize potential discrepancies between the predicted pairwise species coexistence from our population models and co-occurance patterns in the field, we have investigated the potential for indirect species interactions to stabilize multispecies coexistence. To do this, we used the structural approach to investigating multispecies coexistence presented in Saavedra et al. 2017. This approach avoids the pitfalls of multispecies competition models by investigating the conditions for feasible coexistence (as opposed to stable coexistence). Thus, to assess whether taking a multispecies approach would better capture observed co-occurance patterns, we have calculated the number of species combinations which may feasibly coexist across each value of species richness. If emergent properties of multispecies competition are necessary for recreating know co-occurance patterns, then we should see an increase in the percent of feasible combinations as species richness increases past 2. We have also paired this analysis with a quantification of the role of indirect interactions in mediating multispecies coexistence by calculating the community-pair differential. This metric represents the difference between the feasibility of coexistence of a multispecies combination and that of the component pairwise combinations. Positive values of the community-pair differential suggest that indirect interactions promote multispecies coexistence whereas negative values suggest that indirect interactions decrease the feasibility of multispecies coexistence. If we find generally high values of this metric, it is likely that a multispecies approach is necessary to capture known co-occurance patterns.

Because our pairwise approach predicts very little coexistence (Figure 2 in the main text), the results from this set of multispecies coexistence are important

for isolating the potential cause of the generally low probabilities of coexistence. However, our results suggest that indirect interactions are unlikely to be the cause of the discrepancy between our model predictions and community dynamics in the field. We generally found community-pair differentials to be close to zero, with most 95% credible intervals overlapping with zero. Additionally, we found that the percent of feasible combinations sharply decreased with species richness after pairwise combinations (Figure S2).Thus, we explore other potential reasons for which we might predict lower rates of coexistence (namely, fluctuation-dependent stabilization) in the discussion of the main text.

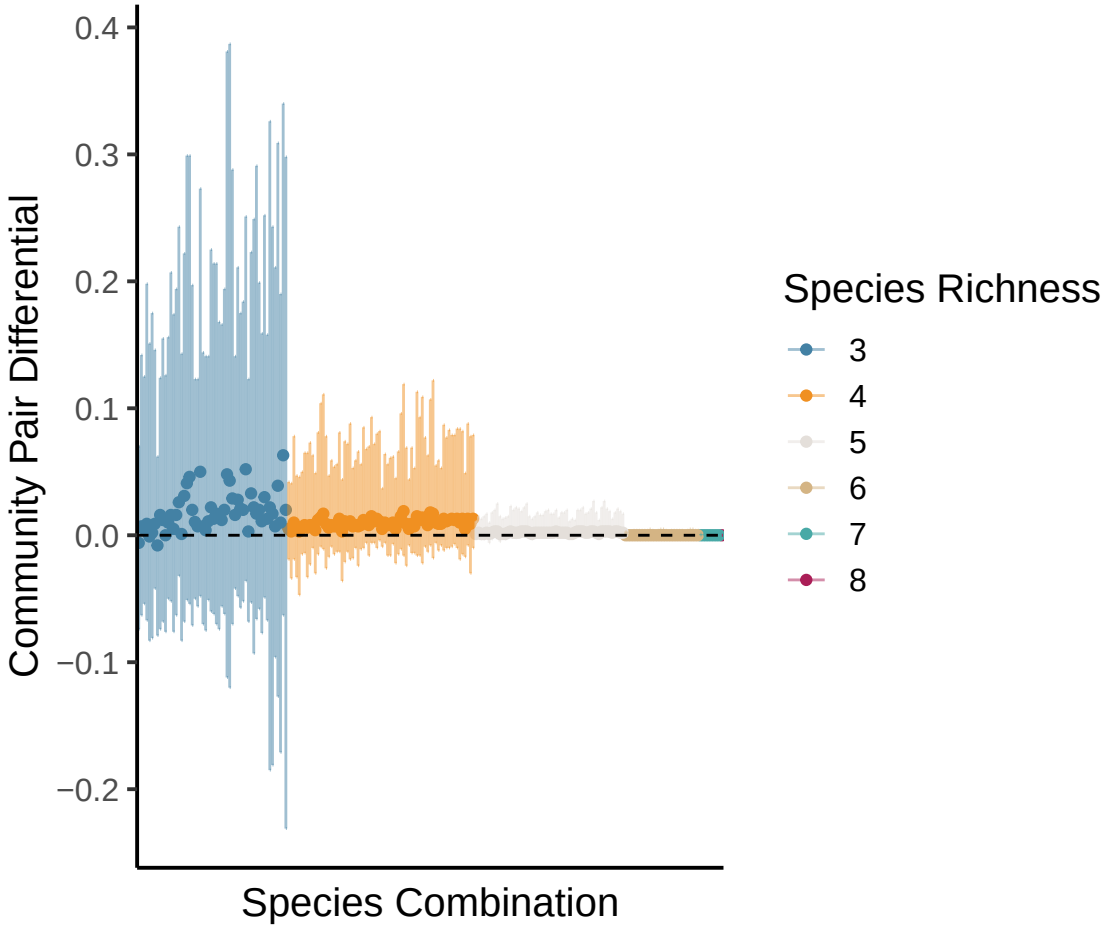

Figure S22. Community-pair differentials for each species combination colored by species richness of the combination. Negative values represent combinations for which indirect interactions lower the feasibility of coexistence whereas positive values represent combinations for which indirect interactions increase the feasibility of coexistence. Points represent the median estimate and error bars represent the 95% credible intervals from the posterior distribution of population parameters.

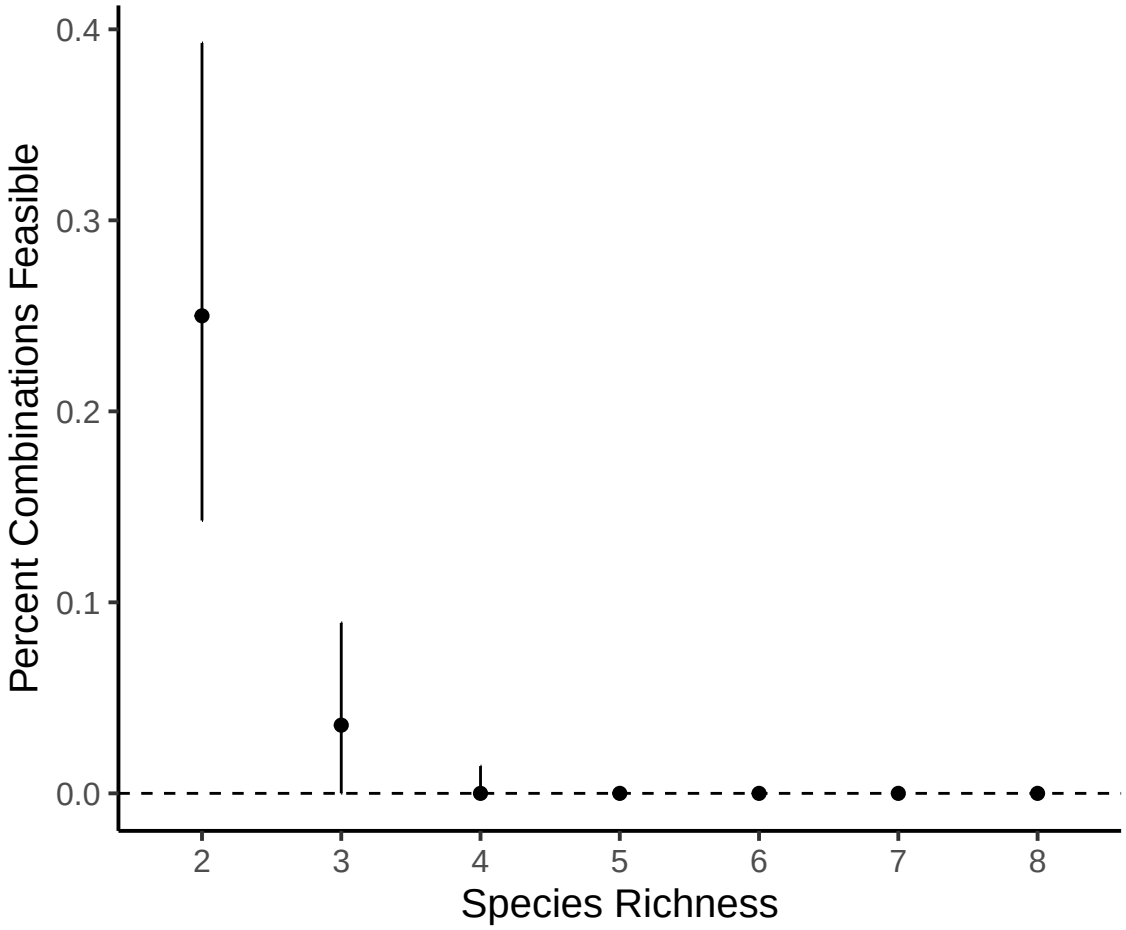

Figure S23. Percent of species combinations which could feasibly coexist for each species richness category. Points represent medians and error bars represent 95% credible intervals from the posterior distribution of population parameters.

APPENDIX B

SUPPLEMENTAL INFORMATION FOR CHAPTER 3

B.1 Non-linear Responses to Environmental Variables

In the core simulations in this study, we assumed linear relationship between the environment and species interactions. However, it's possible that species interactions have saturating or parabolic functional responses to relevant environmental variables. If some environmental variable monotonically affects the interaction strength, it is possible that some upper or lower limit imposes a saturating functional relationship. Alternatively, optimum environmental conditions may impose a parabolic function relationship. Here, we explore these relationships and assess the consequences of nonlinearity in the models described in the main text.

B.1.1 Methods. To assess how nonlinear responses of plant-microbial interactions to the environment may affect plant coexistence, we reran the baseline empirical invasion scenario with three forms of the scaling functions (linear, sigmoidal, and parabolic) for both the cultivation rate of the pathogen ϕ_{XA} and the microbial effect on the pathogen on the invasive plant σ_{AX}. To further explore non-monotonic scaling functions, we also examined scaling functions of σ_{AX} that span both sides of the parabola in three different scenarios.

B.1.1.1 Comparison of Nonlinear Forms. For each of these simulations, two plant species are competing with one another, and the competitively dominant plant species cultivates a species-specific pathogen. The microbe-independent competition coefficients are set as $c_{AA} = -0.5$, $c_{BA} = -0.8$, $c_{BB} = -0.8$, and $c_{AB} = -0.5$. We then proceeded to sequentially replace static parameter values for ϕ_{XA} and σ_{AX} with linear, sigmoidal, and parabolic functions

of an environmental gradient, while keeping the value of the other plant-microbe interactions static at a baseline value. When σ_{AX} was scaled by the environmental gradient, ϕ_{XA} was held constant at 0.2, When ϕ_{XA} was scaled, σ_{AX} was held constant at -0.2. Sigmoidal and parabolic scaling functions were designed to have similar minimum and maximum values along the range of the moisture gradient to that of the linear scaling functions (Table S1).

Function	Parameter	Equation
Linear	ϕ_{XA}	$\phi_{XA} = .2 + v$
	σ_{AX}	$\sigma_{AX} = -.2 - v$
Sigmoidal	ϕ_{XA}	$\phi_{XA} = \frac{2}{1+e^{-2v}}$
	σ_{AX}	$\sigma_{AX} = \frac{4}{1+e^{2v}} - 2.2$
Parabolic	ϕ_{XA}	$\phi_{XA} = -.5(v-2)^2 + 2.2$
	σ_{AX}	$\sigma_{AX} = .25(v-2)^2 - 2.2$

Table B.1. Table S1: Equations for Comparisons of Nonlinear Scaling Functions

B.1.1.2 Further Exploration of Parabolic Scaling. For the additional parabolic scaling functions of σ_{AX}, we began with a scaling function of the one species-specific pathogen's effect on the competitively dominant plant species with the vertex (i.e. the point along the rainfall gradient where the pathogencity is the lowest) at zero:

$$\sigma_{XA} = .25v^2 - 2.2 \tag{B.1}$$

We then added an additional species-specific pathogen on the competitively inferior species that is scaled identically to the first pathogen. Finally, we reran these simulations after adjusting the new pathogen's scaling function to offset its minimum pathogencity from the original pathogen:

$$\sigma_{YB} = .25(v-1)^2 - 2.2 \tag{B.2}$$

For all simulations, the cultivation rate was kept positive by dropping negative outputs of the ϕ_{XA} and ϕ_{YB} scaling functions from subsequent calculations. After scaling, we calculated the overall competition coefficients as $\alpha_{ij} = c_{ij} + \sigma_{iX}\phi_{Xj}$. Across all scenarios, we calculated niche and fitness differences along the environmental gradient to quantify the downstream effects of these different forms of environmental context dependency on coexistence dynamics.

B.1.2 Results and Discussion. Sigmoidal and half-parabolic scaling functions did not dramatically differ in their downstream effects on niche and fitness ratios from those of the linear scaling functions (Figure S1). Importantly, when these scaling functions are monotonic and span a similar range of parameter values, the overall trajectory through niche and fitness ratios space is similar. However, non-linearities do shift the rate of change in these values such that the sensitivity of the context-dependent parameter (and thus the competitive dynamics) is dependent on the position along the environmental gradient.

In our exploration of full parabolic functions, we do find novel shifts in the trajectory which were not observed in other sets of our simulations (Figure S2). When one pathogen's infleunce on a host species is parabolically dependent on rainfall, the plant competitive dynamics move parabolically through niche/fitness space such that they move into coexistence space at the vertex of the scaling function and then retrace the initial trajectory in reverse (Figure S2a). This behavior is similarly seen when two species have rainfall-dependent sensitivities to pathogens, but only when these scaling functions share a vertex (Figure S2b). When these scaling functions do not share a vertex, the trajectory is not retraced,

and at each point along the environmental gradient, the species pair exists at a unique point in niche/fitness space (Figure S2c).

This brief case study in these nonlinear context-dependencies highlights an important consideration for the modeling of context-dependent species interactions: the form of these models is determined, in part, by the scale along the environmental gradient. This points to two seemingly simple but nonetheless useful insights. First, across a small enough range along an environmental gradient, linear approximations can make nearly identical predictions about the behavior of the community. Thus, effort should be focused on assessing parameter values across the environmental gradient, but determining the exact functional form may be a lower priority. Second, general information about the form of the scaling function at larger scales can inform our expectations about shifts in the velocity and trajectory of system dynamics. For example, parameters with saturation scaling functions will likely have a smaller rate of change with respect to the environmental variable at high extremes of the gradient. Alternatively, parameters with a local optimum are likely to shift in their velocity as well as the trajectory of the competitive dynamics through niche and fitness difference space as the environmental variable changes.

B.2 List of Model Structures in Main Text

In this paper, we explore multiple structures of coupled plant-microbe communities. Ignoring the exact magnitude and sign of the species interactions, these structures vary in the taxonomic richness of the microbial community as well as the specificity of particular plant-microbe interactions. Actual plant-microbe community structures are incredibly diverse, due in part to the incredible diversity of microbes (Dundore-Arias, Michalska-Smith, Millican, & Kinkel, 2023), and a large set of structures can be defined even with our greatly simplified communities with at most three microbial taxa. As a demonstrative example, we might constrain the set of network structures for our purposes to include only those with 1) two plant species which directly compete with one another as well as themselves, 2) at least one microbe which is both cultured by some plant (ie assuming all microbes require the presence of at least one plant) and affects the fitness of some plant (ie ignoring microbes which do not affect the fitness of either plant species). We can further reduce the set of all unique structures by ignoring the identity of the plants or the microbes. Just considering such directed, unweighted graphs produces 5, 25, and 85 unique structures for 1, 2, and 3 microbe species systems.

Our results demonstrate that the structure of these networks may impact plant community dynamics. Though not central to the goal of this paper, we do attempt to address this structural sensitivity by exploring multiple network structures in each of our simulations as well as in our sensitivity analysis. Here, we present a list of network structures used in the main text.

Diagram	Description	Name	Analysis
	No plant-microbe interactions	ThSi I	Theoretical Simulations
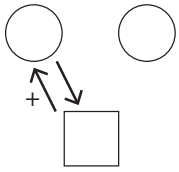	One specialist mutualist	ThSi II	Theoretical Simulations
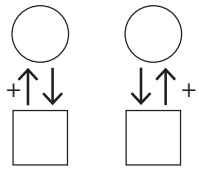	One specialist mutualist per species	ThSi III	Theoretical Simulations
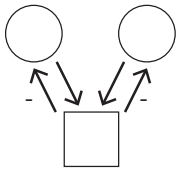	One generalist pathogen	SeAn	Sensitivity Analysis

Diagram	Description	Name	Analysis
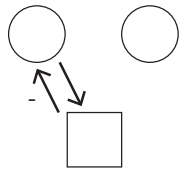	One specialist pathogen	InSi I	Invasion Simulations
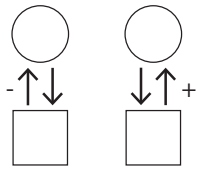	One specialist pathogen and one specialist mutualist	InSi II	Invasion Simulations
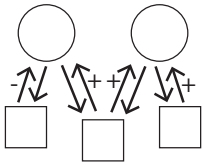	One specialist pathogen, one specialist mutualist, and one generalist mutualist/decomposer	InSi III	Invasion Simulations

Table B.2. Table S2: Description of Various Model Forms Used in Main Text

B.3 Additional Sensitivity Analyses

Here, we present the methods and results from an analytical local stability analysis as well as a partial-rank correlation coefficient (PRCC) based global sensitivity analysis. Our analytical local sensitivity analysis evaluates the sensitivity of niche differences and fitness ratios to these direct and indirect species interactions at a given point in parameter space. Conversely, our global sensitivity analysis evaluates the sensitivity of niche differences and fitness ratios to species interactions across some defined finite parameter space and includes the interactive impacts of parameters on the niche differences and fitness ratios. Our simulation-based local sensitivity analysis presented in the main text does not include the interactive effects of parameters, but does show how sensitivity to a given species interaction term changes as we move along it's axis in parameter space. Lastly, we use the analytical local sensitivity analysis to explore the potential for model structure (ie plant-microbe network topology) to influence the results of our sensitivity analysis. Specifically, we examined how the sensitivity of particular parameters shifts as additional microbial taxa are included in the model.

Based on our definition of overall competition coefficients (Eq. 6), we can define extended equations for the niche differences, fitness ratios, and fitness inequalities.

The niche differences can be defined as:

$$ND = 1 - \sqrt{\frac{(c_{ij} + \sigma_{ix}\phi_{xj})(c_{ji} + \sigma_{jx}\phi_{xi})}{(c_{ii} + \sigma_{ix}\phi_{xi})(c_{jj} + \sigma_{jx}\phi_{xj})}} \tag{B.3}$$

The fitness ratio can be defined as:

$$FR = \sqrt{\frac{(c_{ij} + \sigma_{ix}\phi_{xj})(c_{ii} + \sigma_{ix}\phi_{xi})}{(c_{ji} + \sigma_{jx}\phi_{xi})(c_{jj} + \sigma_{jx}\phi_{xj})}} \tag{B.4}$$

Finally, the fitness inequalities can be defined as the maximum value of the two fitness ratios, or the fitness ratio where species i is the competitively inferior species.

To better understand the role of c, σ and ϕ parameters in determining the value of the niche differences, fitness ratios, and fitness inequalities, we performed three types of sensitivity analyses: a local stability analysis (presented in the main text), an analytical sensitivity analysis, and a partial rank correlation coefficient (PRCC) based sensitivity analysis. Here, we provide the results of the local stability analysis for the fitness ratios as well as the methods and results for the analytical and PRCC-based sensitivity analyses. We also repeat this process to look instead at the differential roles of direct plant competition, c, and microbial feedbacks, m, which are defined as the product of ϕ and σ in our one species model. The maximum value function introduces additional mathematical and statistical complexity to calculating the sensitivity of the fitness inequalities, so we did not apply these additional methods to the sensitivity of the fitness inequalities, and instead analyzed the sensitivity of the fitness ratios and niche differences. The baseline parameterization for all of these analyses was the same as that used for the local sensitivity analysis: $c_{ii} = -0.06$, $c_{ij} = -0.055$, $c_{jj} = -0.075$, $c_{ji} = -0.05$, $\sigma_{ix} = 0.002$, $\sigma_{jx} = 0.00225$, $\phi_{xi} = 10.5$, $\phi_{xj} = 10$.

B.3.1 Local Sensitivity Analysis. The local sensitivity analysis for the niche differences and fitness ratios are displayed in Figure 3 in the main text. Here, we show the local sensitivity analysis for the fitness inequalities (Figure S1). The maximum value function within the calculation of the fitness inequalities

creates relationships between parameter values and fitness inequalities that contain a single minimum value and that are asymmetric about this inflection point . The sensitivity of the fitness inequalities to each parameter can thus be assessed by inspecting the steepness on either side of the inflection point. In contrast to the niche differences, fitness inequalities were most sensitive to microbial effects on plants (σ) and least sensitive to plant cultivation rates (ϕ), with intermediate sensitivity to plant-plant interaction coefficients and microbial feedback terms.

B.3.2 Analytical Sensitivity Analysis. We conducted a derivative-based analytical sensitivity analysis by calculating the partial derivatives of the full niche differences and fitness ratio equations (Eq S1 & S2) and then computed the value of these partial derivatives at the baseline parameterization (Figure S2). Again, we repeat this process to calculate the sensitivity of niche differences and fitness ratios to microbial feedbacks (Figure S3). Here, we report the equations for the partial derivatives and present their values at the baseline. Notably, the partial derivatives for the microbial feedback terms are the same as those of their respective microbe-independent plant competition coefficients (e.g. the partial derivative of the niche differences with respect to c_{ij} is the same as that with respect to m_{ij}). Congruent with the local sensitivity analysis reported in the main text and above, we find that plant competition terms (c) and microbial feedback terms (m) similarly influence niche and fitness difference. Conversely, fitness ratios are more sensitive to the microbial effects on plants (σ) than niche differences, and both metrics are much more sensitive to σ terms than the cultivation terms (ϕ) in this parameterization.

B.3.2.1 Partial Derivatives.

ϕ & σ Parameterization

Niche Differences

$$\frac{\partial ND}{\partial c_{ij}} = -\frac{c_{\mathrm{ji}} + \sigma_{\mathrm{jx}}\phi_{\mathrm{xi}}}{2\left(c_{\mathrm{ii}} + \sigma_{\mathrm{ix}}\phi_{\mathrm{xi}}\right)\left(c_{\mathrm{jj}} + \sigma_{\mathrm{jx}}\phi_{\mathrm{xj}}\right)\sqrt{\frac{\left(c_{\mathrm{ij}}+\sigma_{\mathrm{ix}}\phi_{\mathrm{xj}}\right)\left(c_{\mathrm{ji}}+\sigma_{\mathrm{jx}}\phi_{\mathrm{xi}}\right)}{\left(c_{\mathrm{ii}}+\sigma_{\mathrm{ix}}\phi_{\mathrm{xi}}\right)\left(c_{\mathrm{jj}}+\sigma_{\mathrm{jx}}\phi_{\mathrm{xj}}\right)}}} \tag{B.5}$$

$$\frac{\partial ND}{\partial c_{ji}} = -\frac{c_{\mathrm{ij}} + \sigma_{\mathrm{ix}}\phi_{\mathrm{xj}}}{2\left(c_{\mathrm{ii}} + \sigma_{\mathrm{ix}}\phi_{\mathrm{xi}}\right)\left(c_{\mathrm{jj}} + \sigma_{\mathrm{jx}}\phi_{\mathrm{xj}}\right)\sqrt{\frac{\left(c_{\mathrm{ij}}+\sigma_{\mathrm{ix}}\phi_{\mathrm{xj}}\right)\left(c_{\mathrm{ji}}+\sigma_{\mathrm{jx}}\phi_{\mathrm{xi}}\right)}{\left(c_{\mathrm{ii}}+\sigma_{\mathrm{ix}}\phi_{\mathrm{xi}}\right)\left(c_{\mathrm{jj}}+\sigma_{\mathrm{jx}}\phi_{\mathrm{xj}}\right)}}} \tag{B.6}$$

$$\frac{\partial ND}{\partial c_{ii}} = \frac{\left(c_{\mathrm{ij}} + \sigma_{\mathrm{ix}}\phi_{\mathrm{xj}}\right)\left(c_{\mathrm{ji}} + \sigma_{\mathrm{jx}}\phi_{\mathrm{xi}}\right)}{2\left(c_{\mathrm{ii}} + \sigma_{\mathrm{ix}}\phi_{\mathrm{xi}}\right)^{2}\left(c_{\mathrm{jj}} + \sigma_{\mathrm{jx}}\phi_{\mathrm{xj}}\right)\sqrt{\frac{\left(c_{\mathrm{ij}}+\sigma_{\mathrm{ix}}\phi_{\mathrm{xj}}\right)\left(c_{\mathrm{ji}}+\sigma_{\mathrm{jx}}\phi_{\mathrm{xi}}\right)}{\left(c_{\mathrm{ii}}+\sigma_{\mathrm{ix}}\phi_{\mathrm{xi}}\right)\left(c_{\mathrm{jj}}+\sigma_{\mathrm{jx}}\phi_{\mathrm{xj}}\right)}}} \tag{B.7}$$

$$\frac{\partial ND}{\partial c_{jj}} = \frac{\left(c_{\mathrm{ij}} + \sigma_{\mathrm{ix}}\phi_{\mathrm{xj}}\right)\left(c_{\mathrm{ji}} + \sigma_{\mathrm{jx}}\phi_{\mathrm{xi}}\right)}{2\left(c_{\mathrm{ii}} + \sigma_{\mathrm{ix}}\phi_{\mathrm{xi}}\right)\left(c_{\mathrm{jj}} + \sigma_{\mathrm{jx}}\phi_{\mathrm{xj}}\right)^{2}\sqrt{\frac{\left(c_{\mathrm{ij}}+\sigma_{\mathrm{ix}}\phi_{\mathrm{xj}}\right)\left(c_{\mathrm{ji}}+\sigma_{\mathrm{jx}}\phi_{\mathrm{xi}}\right)}{\left(c_{\mathrm{ii}}+\sigma_{\mathrm{ix}}\phi_{\mathrm{xi}}\right)\left(c_{\mathrm{jj}}+\sigma_{\mathrm{jx}}\phi_{\mathrm{xj}}\right)}}} \tag{B.8}$$

$$\frac{\partial ND}{\partial \sigma_{ix}} = -\frac{\frac{\phi_{\mathrm{xj}}\left(c_{\mathrm{ji}}+\sigma_{\mathrm{jx}}\phi_{\mathrm{xi}}\right)}{\left(c_{\mathrm{ii}}+\sigma_{\mathrm{ix}}\phi_{\mathrm{xi}}\right)\left(c_{\mathrm{jj}}+\sigma_{\mathrm{jx}}\phi_{\mathrm{xj}}\right)} - \frac{\phi_{\mathrm{xi}}\left(c_{\mathrm{ij}}+\sigma_{\mathrm{ix}}\phi_{\mathrm{xj}}\right)\left(c_{\mathrm{ji}}+\sigma_{\mathrm{jx}}\phi_{\mathrm{xi}}\right)}{\left(c_{\mathrm{ii}}+\sigma_{\mathrm{ix}}\phi_{\mathrm{xi}}\right)^{2}\left(c_{\mathrm{jj}}+\sigma_{\mathrm{jx}}\phi_{\mathrm{xj}}\right)}}{2\sqrt{\frac{\left(c_{\mathrm{ij}}+\sigma_{\mathrm{ix}}\phi_{\mathrm{xj}}\right)\left(c_{\mathrm{ji}}+\sigma_{\mathrm{jx}}\phi_{\mathrm{xi}}\right)}{\left(c_{\mathrm{ii}}+\sigma_{\mathrm{ix}}\phi_{\mathrm{xi}}\right)\left(c_{\mathrm{jj}}+\sigma_{\mathrm{jx}}\phi_{\mathrm{xj}}\right)}}} \tag{B.9}$$

$$\frac{\partial ND}{\partial \sigma_{jx}} = -\frac{\frac{\phi_{\mathrm{xi}}\left(c_{\mathrm{ij}}+\sigma_{\mathrm{ix}}\phi_{\mathrm{xj}}\right)}{\left(c_{\mathrm{ii}}+\sigma_{\mathrm{ix}}\phi_{\mathrm{xi}}\right)\left(c_{\mathrm{jj}}+\sigma_{\mathrm{jx}}\phi_{\mathrm{xj}}\right)} - \frac{\phi_{\mathrm{xj}}\left(c_{\mathrm{ij}}+\sigma_{\mathrm{ix}}\phi_{\mathrm{xj}}\right)\left(c_{\mathrm{ji}}+\sigma_{\mathrm{jx}}\phi_{\mathrm{xi}}\right)}{\left(c_{\mathrm{ii}}+\sigma_{\mathrm{ix}}\phi_{\mathrm{xi}}\right)\left(c_{\mathrm{jj}}+\sigma_{\mathrm{jx}}\phi_{\mathrm{xj}}\right)^{2}}}{2\sqrt{\frac{\left(c_{\mathrm{ij}}+\sigma_{\mathrm{ix}}\phi_{\mathrm{xj}}\right)\left(c_{\mathrm{ji}}+\sigma_{\mathrm{jx}}\phi_{\mathrm{xi}}\right)}{\left(c_{\mathrm{ii}}+\sigma_{\mathrm{ix}}\phi_{\mathrm{xi}}\right)\left(c_{\mathrm{jj}}+\sigma_{\mathrm{jx}}\phi_{\mathrm{xj}}\right)}}} \tag{B.10}$$

$$\frac{\partial ND}{\partial \phi_{xi}} = -\frac{\frac{\sigma_{\mathrm{jx}}\left(c_{\mathrm{ij}}+\sigma_{\mathrm{ix}}\phi_{\mathrm{xj}}\right)}{\left(c_{\mathrm{ii}}+\sigma_{\mathrm{ix}}\phi_{\mathrm{xi}}\right)\left(c_{\mathrm{jj}}+\sigma_{\mathrm{jx}}\phi_{\mathrm{xj}}\right)} - \frac{\sigma_{\mathrm{ix}}\left(c_{\mathrm{ij}}+\sigma_{\mathrm{ix}}\phi_{\mathrm{xj}}\right)\left(c_{\mathrm{ji}}+\sigma_{\mathrm{jx}}\phi_{\mathrm{xi}}\right)}{\left(c_{\mathrm{ii}}+\sigma_{\mathrm{ix}}\phi_{\mathrm{xi}}\right)^{2}\left(c_{\mathrm{jj}}+\sigma_{\mathrm{jx}}\phi_{\mathrm{xj}}\right)}}{2\sqrt{\frac{\left(c_{\mathrm{ij}}+\sigma_{\mathrm{ix}}\phi_{\mathrm{xj}}\right)\left(c_{\mathrm{ji}}+\sigma_{\mathrm{jx}}\phi_{\mathrm{xi}}\right)}{\left(c_{\mathrm{ii}}+\sigma_{\mathrm{ix}}\phi_{\mathrm{xi}}\right)\left(c_{\mathrm{jj}}+\sigma_{\mathrm{jx}}\phi_{\mathrm{xj}}\right)}}} \tag{B.11}$$

$$\frac{\partial ND}{\partial \phi_{xj}} = -\frac{\frac{\sigma_{\mathrm{ix}}\left(c_{\mathrm{ji}}+\sigma_{\mathrm{jx}}\phi_{\mathrm{xi}}\right)}{\left(c_{\mathrm{ii}}+\sigma_{\mathrm{ix}}\phi_{\mathrm{xi}}\right)\left(c_{\mathrm{jj}}+\sigma_{\mathrm{jx}}\phi_{\mathrm{xj}}\right)} - \frac{\sigma_{\mathrm{jx}}\left(c_{\mathrm{ij}}+\sigma_{\mathrm{ix}}\phi_{\mathrm{xj}}\right)\left(c_{\mathrm{ji}}+\sigma_{\mathrm{jx}}\phi_{\mathrm{xi}}\right)}{\left(c_{\mathrm{ii}}+\sigma_{\mathrm{ix}}\phi_{\mathrm{xi}}\right)\left(c_{\mathrm{jj}}+\sigma_{\mathrm{jx}}\phi_{\mathrm{xj}}\right)^{2}}}{2\sqrt{\frac{\left(c_{\mathrm{ij}}+\sigma_{\mathrm{ix}}\phi_{\mathrm{xj}}\right)\left(c_{\mathrm{ji}}+\sigma_{\mathrm{jx}}\phi_{\mathrm{xi}}\right)}{\left(c_{\mathrm{ii}}+\sigma_{\mathrm{ix}}\phi_{\mathrm{xi}}\right)\left(c_{\mathrm{jj}}+\sigma_{\mathrm{jx}}\phi_{\mathrm{xj}}\right)}}} \tag{B.12}$$

Fitness Ratio

$$\frac{\partial FR}{\partial c_{ij}} = \frac{c_{\mathrm{ii}} + \sigma_{\mathrm{ix}}\phi_{\mathrm{xi}}}{2\left(c_{\mathrm{ji}} + \sigma_{\mathrm{jx}}\phi_{\mathrm{xi}}\right)\left(c_{\mathrm{jj}} + \sigma_{\mathrm{jx}}\phi_{\mathrm{xj}}\right)\sqrt{\frac{\left(c_{\mathrm{ii}}+\sigma_{\mathrm{ix}}\phi_{\mathrm{xi}}\right)\left(c_{\mathrm{ij}}+\sigma_{\mathrm{ix}}\phi_{\mathrm{xj}}\right)}{\left(c_{\mathrm{ji}}+\sigma_{\mathrm{jx}}\phi_{\mathrm{xi}}\right)\left(c_{\mathrm{jj}}+\sigma_{\mathrm{jx}}\phi_{\mathrm{xj}}\right)}}} \tag{B.13}$$

$$\frac{\partial FR}{\partial c_{ji}} = -\frac{\left(c_{\mathrm{ii}} + \sigma_{\mathrm{ix}}\phi_{\mathrm{xi}}\right)\left(c_{\mathrm{ij}} + \sigma_{\mathrm{ix}}\phi_{\mathrm{xj}}\right)}{2\left(c_{\mathrm{ji}} + \sigma_{\mathrm{jx}}\phi_{\mathrm{xi}}\right)^2\left(c_{\mathrm{jj}} + \sigma_{\mathrm{jx}}\phi_{\mathrm{xj}}\right)\sqrt{\frac{\left(c_{\mathrm{ii}}+\sigma_{\mathrm{ix}}\phi_{\mathrm{xi}}\right)\left(c_{\mathrm{ij}}+\sigma_{\mathrm{ix}}\phi_{\mathrm{xj}}\right)}{\left(c_{\mathrm{ji}}+\sigma_{\mathrm{jx}}\phi_{\mathrm{xi}}\right)\left(c_{\mathrm{jj}}+\sigma_{\mathrm{jx}}\phi_{\mathrm{xj}}\right)}}} \tag{B.14}$$

$$\frac{\partial FR}{\partial c_{ii}} = \frac{c_{\mathrm{ij}} + \sigma_{\mathrm{ix}}\phi_{\mathrm{xj}}}{2\left(c_{\mathrm{ji}} + \sigma_{\mathrm{jx}}\phi_{\mathrm{xi}}\right)\left(c_{\mathrm{jj}} + \sigma_{\mathrm{jx}}\phi_{\mathrm{xj}}\right)\sqrt{\frac{\left(c_{\mathrm{ii}}+\sigma_{\mathrm{ix}}\phi_{\mathrm{xi}}\right)\left(c_{\mathrm{ij}}+\sigma_{\mathrm{ix}}\phi_{\mathrm{xj}}\right)}{\left(c_{\mathrm{ji}}+\sigma_{\mathrm{jx}}\phi_{\mathrm{xi}}\right)\left(c_{\mathrm{jj}}+\sigma_{\mathrm{jx}}\phi_{\mathrm{xj}}\right)}}} \tag{B.15}$$

$$\frac{\partial FR}{\partial c_{jj}} = -\frac{\left(c_{\mathrm{ii}} + \sigma_{\mathrm{ix}}\phi_{\mathrm{xi}}\right)\left(c_{\mathrm{ij}} + \sigma_{\mathrm{ix}}\phi_{\mathrm{xj}}\right)}{2\left(c_{\mathrm{ji}} + \sigma_{\mathrm{jx}}\phi_{\mathrm{xi}}\right)\left(c_{\mathrm{jj}} + \sigma_{\mathrm{jx}}\phi_{\mathrm{xj}}\right)^2\sqrt{\frac{\left(c_{\mathrm{ii}}+\sigma_{\mathrm{ix}}\phi_{\mathrm{xi}}\right)\left(c_{\mathrm{ij}}+\sigma_{\mathrm{ix}}\phi_{\mathrm{xj}}\right)}{\left(c_{\mathrm{ji}}+\sigma_{\mathrm{jx}}\phi_{\mathrm{xi}}\right)\left(c_{\mathrm{jj}}+\sigma_{\mathrm{jx}}\phi_{\mathrm{xj}}\right)}}} \tag{B.16}$$

$$\frac{\partial FR}{\partial \sigma_{ix}} = \frac{\frac{\phi_{\mathrm{xj}}\left(c_{\mathrm{ii}}+\sigma_{\mathrm{ix}}\phi_{\mathrm{xi}}\right)}{\left(c_{\mathrm{ji}}+\sigma_{\mathrm{jx}}\phi_{\mathrm{xi}}\right)\left(c_{\mathrm{jj}}+\sigma_{\mathrm{jx}}\phi_{\mathrm{xj}}\right)} + \frac{\phi_{\mathrm{xi}}\left(c_{\mathrm{ij}}+\sigma_{\mathrm{ix}}\phi_{\mathrm{xj}}\right)}{\left(c_{\mathrm{ji}}+\sigma_{\mathrm{jx}}\phi_{\mathrm{xi}}\right)\left(c_{\mathrm{jj}}+\sigma_{\mathrm{jx}}\phi_{\mathrm{xj}}\right)}}{2\sqrt{\frac{\left(c_{\mathrm{ii}}+\sigma_{\mathrm{ix}}\phi_{\mathrm{xi}}\right)\left(c_{\mathrm{ij}}+\sigma_{\mathrm{ix}}\phi_{\mathrm{xj}}\right)}{\left(c_{\mathrm{ji}}+\sigma_{\mathrm{jx}}\phi_{\mathrm{xi}}\right)\left(c_{\mathrm{jj}}+\sigma_{\mathrm{jx}}\phi_{\mathrm{xj}}\right)}}} \tag{B.17}$$

$$\frac{\partial FR}{\partial \sigma_{jx}} = \frac{-\frac{\phi_{\mathrm{xi}}\left(c_{\mathrm{ii}}+\sigma_{\mathrm{ix}}\phi_{\mathrm{xi}}\right)\left(c_{\mathrm{ij}}+\sigma_{\mathrm{ix}}\phi_{\mathrm{xj}}\right)}{\left(c_{\mathrm{ji}}+\sigma_{\mathrm{jx}}\phi_{\mathrm{xi}}\right)^2\left(c_{\mathrm{jj}}+\sigma_{\mathrm{jx}}\phi_{\mathrm{xj}}\right)} - \frac{\phi_{\mathrm{xj}}\left(c_{\mathrm{ii}}+\sigma_{\mathrm{ix}}\phi_{\mathrm{xi}}\right)\left(c_{\mathrm{ij}}+\sigma_{\mathrm{ix}}\phi_{\mathrm{xj}}\right)}{\left(c_{\mathrm{ji}}+\sigma_{\mathrm{jx}}\phi_{\mathrm{xi}}\right)\left(c_{\mathrm{jj}}+\sigma_{\mathrm{jx}}\phi_{\mathrm{xj}}\right)^2}}{2\sqrt{\frac{\left(c_{\mathrm{ii}}+\sigma_{\mathrm{ix}}\phi_{\mathrm{xi}}\right)\left(c_{\mathrm{ij}}+\sigma_{\mathrm{ix}}\phi_{\mathrm{xj}}\right)}{\left(c_{\mathrm{ji}}+\sigma_{\mathrm{jx}}\phi_{\mathrm{xi}}\right)\left(c_{\mathrm{jj}}+\sigma_{\mathrm{jx}}\phi_{\mathrm{xj}}\right)}}} \tag{B.18}$$

$$\frac{\partial FR}{\partial \phi_{xi}} = \frac{\frac{\sigma_{\mathrm{ix}}\left(c_{\mathrm{ij}}+\sigma_{\mathrm{ix}}\phi_{\mathrm{xj}}\right)}{\left(c_{\mathrm{ji}}+\sigma_{\mathrm{jx}}\phi_{\mathrm{xi}}\right)\left(c_{\mathrm{jj}}+\sigma_{\mathrm{jx}}\phi_{\mathrm{xj}}\right)} - \frac{\sigma_{\mathrm{jx}}\left(c_{\mathrm{ii}}+\sigma_{\mathrm{ix}}\phi_{\mathrm{xi}}\right)\left(c_{\mathrm{ij}}+\sigma_{\mathrm{ix}}\phi_{\mathrm{xj}}\right)}{\left(c_{\mathrm{ji}}+\sigma_{\mathrm{jx}}\phi_{\mathrm{xi}}\right)^2\left(c_{\mathrm{jj}}+\sigma_{\mathrm{jx}}\phi_{\mathrm{xj}}\right)}}{2\sqrt{\frac{\left(c_{\mathrm{ii}}+\sigma_{\mathrm{ix}}\phi_{\mathrm{xi}}\right)\left(c_{\mathrm{ij}}+\sigma_{\mathrm{ix}}\phi_{\mathrm{xj}}\right)}{\left(c_{\mathrm{ji}}+\sigma_{\mathrm{jx}}\phi_{\mathrm{xi}}\right)\left(c_{\mathrm{jj}}+\sigma_{\mathrm{jx}}\phi_{\mathrm{xj}}\right)}}} \tag{B.19}$$

$$\frac{\partial FR}{\partial \phi_{xj}} = \frac{\frac{\sigma_{\mathrm{ix}}\left(c_{\mathrm{ii}}+\sigma_{\mathrm{ix}}\phi_{\mathrm{xi}}\right)}{\left(c_{\mathrm{ji}}+\sigma_{\mathrm{jx}}\phi_{\mathrm{xi}}\right)\left(c_{\mathrm{jj}}+\sigma_{\mathrm{jx}}\phi_{\mathrm{xj}}\right)} - \frac{\sigma_{\mathrm{jx}}\left(c_{\mathrm{ii}}+\sigma_{\mathrm{ix}}\phi_{\mathrm{xi}}\right)\left(c_{\mathrm{ij}}+\sigma_{\mathrm{ix}}\phi_{\mathrm{xj}}\right)}{\left(c_{\mathrm{ji}}+\sigma_{\mathrm{jx}}\phi_{\mathrm{xi}}\right)\left(c_{\mathrm{jj}}+\sigma_{\mathrm{jx}}\phi_{\mathrm{xj}}\right)^2}}{2\sqrt{\frac{\left(c_{\mathrm{ii}}+\sigma_{\mathrm{ix}}\phi_{\mathrm{xi}}\right)\left(c_{\mathrm{ij}}+\sigma_{\mathrm{ix}}\phi_{\mathrm{xj}}\right)}{\left(c_{\mathrm{ji}}+\sigma_{\mathrm{jx}}\phi_{\mathrm{xi}}\right)\left(c_{\mathrm{jj}}+\sigma_{\mathrm{jx}}\phi_{\mathrm{xj}}\right)}}} \tag{B.20}$$

m Parameterization

Niche Differences

$$\frac{\partial ND}{\partial c_{ij}} = -\frac{c_{\mathrm{ji}} + m_{\mathrm{ji}}}{2\left(c_{\mathrm{ii}} + m_{\mathrm{ii}}\right)\left(c_{\mathrm{jj}} + m_{\mathrm{jj}}\right)\sqrt{\frac{\left(c_{\mathrm{ij}}+m_{\mathrm{ij}}\right)\left(c_{\mathrm{ji}}+m_{\mathrm{ji}}\right)}{\left(c_{\mathrm{ii}}+m_{\mathrm{ii}}\right)\left(c_{\mathrm{jj}}+m_{\mathrm{jj}}\right)}}} \tag{B.21}$$

$$\frac{\partial ND}{\partial c_{ji}} = -\frac{c_{\mathrm{ij}} + m_{\mathrm{ij}}}{2\left(c_{\mathrm{ii}} + m_{\mathrm{ii}}\right)\left(c_{\mathrm{jj}} + m_{\mathrm{jj}}\right)\sqrt{\frac{\left(c_{\mathrm{ij}}+m_{\mathrm{ij}}\right)\left(c_{\mathrm{ji}}+m_{\mathrm{ji}}\right)}{\left(c_{\mathrm{ii}}+m_{\mathrm{ii}}\right)\left(c_{\mathrm{jj}}+m_{\mathrm{jj}}\right)}}} \tag{B.22}$$

$$\frac{\partial ND}{\partial c_{ii}} = \frac{\left(c_{\mathrm{ij}} + m_{\mathrm{ij}}\right)\left(c_{\mathrm{ji}} + m_{\mathrm{ji}}\right)}{2\left(c_{\mathrm{ii}} + m_{\mathrm{ii}}\right)^{2}\left(c_{\mathrm{jj}} + m_{\mathrm{jj}}\right)\sqrt{\frac{\left(c_{\mathrm{ij}}+m_{\mathrm{ij}}\right)\left(c_{\mathrm{ji}}+m_{\mathrm{ji}}\right)}{\left(c_{\mathrm{ii}}+m_{\mathrm{ii}}\right)\left(c_{\mathrm{jj}}+m_{\mathrm{jj}}\right)}}} \tag{B.23}$$

$$\frac{\partial ND}{\partial c_{jj}} = \frac{\left(c_{\mathrm{ij}} + m_{\mathrm{ij}}\right)\left(c_{\mathrm{ji}} + m_{\mathrm{ji}}\right)}{2\left(c_{\mathrm{ii}} + m_{\mathrm{ii}}\right)\left(c_{\mathrm{jj}} + m_{\mathrm{jj}}\right)^{2}\sqrt{\frac{\left(c_{\mathrm{ij}}+m_{\mathrm{ij}}\right)\left(c_{\mathrm{ji}}+m_{\mathrm{ji}}\right)}{\left(c_{\mathrm{ii}}+m_{\mathrm{ii}}\right)\left(c_{\mathrm{jj}}+m_{\mathrm{jj}}\right)}}} \tag{B.24}$$

$$\frac{\partial ND}{\partial m_{ij}} = -\frac{c_{\mathrm{ji}} + m_{\mathrm{ji}}}{2\left(c_{\mathrm{ii}} + m_{\mathrm{ii}}\right)\left(c_{\mathrm{jj}} + m_{\mathrm{jj}}\right)\sqrt{\frac{\left(c_{\mathrm{ij}}+m_{\mathrm{ij}}\right)\left(c_{\mathrm{ji}}+m_{\mathrm{ji}}\right)}{\left(c_{\mathrm{ii}}+m_{\mathrm{ii}}\right)\left(c_{\mathrm{jj}}+m_{\mathrm{jj}}\right)}}} \tag{B.25}$$

$$\frac{\partial ND}{\partial m_{ji}} = -\frac{c_{\mathrm{ij}} + m_{\mathrm{ij}}}{2\left(c_{\mathrm{ii}} + m_{\mathrm{ii}}\right)\left(c_{\mathrm{jj}} + m_{\mathrm{jj}}\right)\sqrt{\frac{\left(c_{\mathrm{ij}}+m_{\mathrm{ij}}\right)\left(c_{\mathrm{ji}}+m_{\mathrm{ji}}\right)}{\left(c_{\mathrm{ii}}+m_{\mathrm{ii}}\right)\left(c_{\mathrm{jj}}+m_{\mathrm{jj}}\right)}}} \tag{B.26}$$

$$\frac{\partial ND}{\partial m_{ii}} = \frac{\left(c_{\mathrm{ij}} + m_{\mathrm{ij}}\right)\left(c_{\mathrm{ji}} + m_{\mathrm{ji}}\right)}{2\left(c_{\mathrm{ii}} + m_{\mathrm{ii}}\right)^{2}\left(c_{\mathrm{jj}} + m_{\mathrm{jj}}\right)\sqrt{\frac{\left(c_{\mathrm{ij}}+m_{\mathrm{ij}}\right)\left(c_{\mathrm{ji}}+m_{\mathrm{ji}}\right)}{\left(c_{\mathrm{ii}}+m_{\mathrm{ii}}\right)\left(c_{\mathrm{jj}}+m_{\mathrm{jj}}\right)}}} \tag{B.27}$$

$$\frac{\partial ND}{\partial m_{jj}} = \frac{\left(c_{\mathrm{ij}} + m_{\mathrm{ij}}\right)\left(c_{\mathrm{ji}} + m_{\mathrm{ji}}\right)}{2\left(c_{\mathrm{ii}} + m_{\mathrm{ii}}\right)\left(c_{\mathrm{jj}} + m_{\mathrm{jj}}\right)^{2}\sqrt{\frac{\left(c_{\mathrm{ij}}+m_{\mathrm{ij}}\right)\left(c_{\mathrm{ji}}+m_{\mathrm{ji}}\right)}{\left(c_{\mathrm{ii}}+m_{\mathrm{ii}}\right)\left(c_{\mathrm{jj}}+m_{\mathrm{jj}}\right)}}} \tag{B.28}$$

Fitness Ratio

$$\frac{\partial FR}{\partial c_{ij}} = \frac{c_{\mathrm{ii}} + m_{\mathrm{ii}}}{2\left(c_{\mathrm{ji}} + m_{\mathrm{ji}}\right)\left(c_{\mathrm{jj}} + m_{\mathrm{jj}}\right)\sqrt{\frac{\left(c_{\mathrm{ii}}+m_{\mathrm{ii}}\right)\left(c_{\mathrm{ij}}+m_{\mathrm{ij}}\right)}{\left(c_{\mathrm{ji}}+m_{\mathrm{ji}}\right)\left(c_{\mathrm{jj}}+m_{\mathrm{jj}}\right)}}} \tag{B.29}$$

$$\frac{\partial FR}{\partial c_{ji}} = -\frac{\left(c_{\mathrm{ii}} + m_{\mathrm{ii}}\right)\left(c_{\mathrm{ij}} + m_{\mathrm{ij}}\right)}{2\left(c_{\mathrm{ji}} + m_{\mathrm{ji}}\right)^{2}\left(c_{\mathrm{jj}} + m_{\mathrm{jj}}\right)\sqrt{\frac{\left(c_{\mathrm{ii}}+m_{\mathrm{ii}}\right)\left(c_{\mathrm{ij}}+m_{\mathrm{ij}}\right)}{\left(c_{\mathrm{ji}}+m_{\mathrm{ji}}\right)\left(c_{\mathrm{jj}}+m_{\mathrm{jj}}\right)}}} \tag{B.30}$$

$$\frac{\partial FR}{\partial c_{ii}} = \frac{c_{ij} + m_{ij}}{2\left(c_{ji} + m_{ji}\right)\left(c_{jj} + m_{jj}\right)\sqrt{\frac{\left(c_{ii}+m_{ii}\right)\left(c_{ij}+m_{ij}\right)}{\left(c_{ji}+m_{ji}\right)\left(c_{jj}+m_{jj}\right)}}} \tag{B.31}$$

$$\frac{\partial FR}{\partial c_{jj}} = -\frac{\left(c_{ii} + m_{ii}\right)\left(c_{ij} + m_{ij}\right)}{2\left(c_{ji} + m_{ji}\right)\left(c_{jj} + m_{jj}\right)^{2}\sqrt{\frac{\left(c_{ii}+m_{ii}\right)\left(c_{ij}+m_{ij}\right)}{\left(c_{ji}+m_{ji}\right)\left(c_{jj}+m_{jj}\right)}}} \tag{B.32}$$

$$\frac{\partial FR}{\partial m_{ij}} = \frac{c_{ii} + m_{ii}}{2\left(c_{ji} + m_{ji}\right)\left(c_{jj} + m_{jj}\right)\sqrt{\frac{\left(c_{ii}+m_{ii}\right)\left(c_{ij}+m_{ij}\right)}{\left(c_{ji}+m_{ji}\right)\left(c_{jj}+m_{jj}\right)}}} \tag{B.33}$$

$$\frac{\partial FR}{\partial m_{ji}} = -\frac{\left(c_{ii} + m_{ii}\right)\left(c_{ij} + m_{ij}\right)}{2\left(c_{ji} + m_{ji}\right)^{2}\left(c_{jj} + m_{jj}\right)\sqrt{\frac{\left(c_{ii}+m_{ii}\right)\left(c_{ij}+m_{ij}\right)}{\left(c_{ji}+m_{ji}\right)\left(c_{jj}+m_{jj}\right)}}} \tag{B.34}$$

$$\frac{\partial FR}{\partial m_{ii}} = \frac{c_{ij} + m_{ij}}{2\left(c_{ji} + m_{ji}\right)\left(c_{jj} + m_{jj}\right)\sqrt{\frac{\left(c_{ii}+m_{ii}\right)\left(c_{ij}+m_{ij}\right)}{\left(c_{ji}+m_{ji}\right)\left(c_{jj}+m_{jj}\right)}}} \tag{B.35}$$

$$\frac{\partial FR}{\partial m_{jj}} = -\frac{\left(c_{ii} + m_{ii}\right)\left(c_{ij} + m_{ij}\right)}{2\left(c_{ji} + m_{ji}\right)\left(c_{jj} + m_{jj}\right)^{2}\sqrt{\frac{\left(c_{ii}+m_{ii}\right)\left(c_{ij}+m_{ij}\right)}{\left(c_{ji}+m_{ji}\right)\left(c_{jj}+m_{jj}\right)}}} \tag{B.36}$$

B.3.3 PRCC Based Sensitivity Analysis. Finally, we conducted a partial-rank correlation coefficient (PRCC) sensitivity analysis drawing 100,000 combinations of parameter estimates from Uniform distributions and estimating the PRCC between each parameter and either the niche differences or fitness ratios (Wu, Dhingra, Gambhir, and Remais 2013; Figure S4). This analysis allows all parameters to vary uniformly at random across their given distributions; thus results are not dependent on all other parameters being fixed, such as occurs in the local sensitivity analysis. The minimun and maximum parameter values were the same as those for the local sensitivity analysis: $c_{ij}[-0.1, 0]$; cultivation rates $\phi_{xi}[0, 20]$; microbial effects on plants $\sigma_{ix}[-0.01, 0.01]$; and microbial feedbacks

$m_{ij}[-.2, .2]$. The PRCC was estimated using epiR version 2.0.7 (Stevenson, Sergeant, & Firestone, 2024). [This is where I will put the results of this analysis... they confuse me though...]

B.3.4 Role of Taxonomic Richness. To assess whether the taxonomic richness of the microbial system impacts the results of the sensitivity analysis, we repeated the analytical local sensitivity analysis three times, sequentially adding an additional pathogen taxon. All microbial taxa in this set of analyses were complete generalists, being cultivated by and affecting both plant species. We assumed microbial taxa had similar but unidentical interactions with each plant, so each additional pathogen was slightly more pathogenic and had a slightly higher cultivation rate by both species. Thus, in addition to the baseline parameterization used in the one species model, we used the following additional parameter for species interactions involving microbial taxa y and z: $\phi_{yi} = 10.6$, $\phi_{yj} = 10.1$, $\sigma_{iy} = -0.0021$, $\sigma_{jy} = -0.00235$, $\phi_{zi} = 10.7$, $\phi_{zj} = 10.2$, $\sigma_{iz} = -0.0022$, and $\sigma_{jz} = -0.00245$. We also ran these sensitivity analyses scaling the cultivation rates by species richness such that ϕ was the ratio of the values above and the number of microbial taxa in the system.

The key finding that plant-microbe interactions alter fitness ratios more so than niche differences, whereas plant-plant interactions seem to alter fitness ratios and niche differences similarly persists across the three models. The main difference across these three models was the relative magnitude sensitivity of fitness ratios and niche differences between plant-plant terms and plant-microbe terms. For the models in which we did not scale the cultivation rates by taxonomic richness, the sensitivity of these terms to plant-microbe interactions increased with taxonomic richness at a much faster rate than the that of the plant-plant terms. Conversely, in

the models where we scaled the cultivation rate by taxonomic richness, the relative differences between plant-plant interactions and plant-microbe interactions stayed the same across taxonomic richness.

B.4 Model Structure and Parameterization of Invasion Simulations

B.4.1 Species Specific Pathogen Model Structure. In our first set of simulations considering the invasive plant, *Alliaria petiolata* and containing only a species specific pathogen associated with the competitively dominant plant species, plant population growth was modeled as:

$$\frac{dN_A}{dt} = r_A N_A(1 + c_{AA}N_A + c_{AB}N_B + \sigma_{AX}S_X) \tag{B.37}$$

$$\frac{dN_B}{dt} = r_B N_B(1 + c_{BB}N_B + c_{BA}N_A) \tag{B.38}$$

The population growth of the pathogenic microbial taxon was modeled as:

$$\frac{dS_X}{dt} = g_X S_X(1 - \frac{S_X}{k_X}) \tag{B.39}$$

where the carrying capacity is modeled as:

$$k_X = \phi_{XA}N_A \tag{B.40}$$

Thus, applying a separation of timescales between plant and microbe population dynamics as performed by Ke and Wan (2020), we can calculate competition coefficients by assuming that the microbial taxon is always at carrying capacity and substituting this into the plant population growth models such that, for example, the population growth rate of *Alliaria petiolata* can be rewritten as

$$\frac{dN_A}{dt} = r_A N_A(1 + (c_{AA} + \sigma_{AX}\phi_{XA})N_A + c_{AB}N_B) \tag{B.41}$$

Thus, our competition coefficients for our models including only the species specific pathogen are:

$$\alpha_{AA} = c_{AA} + \sigma_{AX}\phi_{XA} \tag{B.42}$$

$$\alpha_{BA} = c_{BA} \tag{B.43}$$

$$\alpha_{BB} = c_{BB} \tag{B.44}$$

$$\alpha_{AB} = c_{AB} \tag{B.45}$$

B.4.2 Species Specific Mutualist Model Structure. Our next set of simulations included a species specific mutualist (Y) for the native competitor such that the population growth rate for *Alliaria petiolata* stayed the same, but the growth rate for the native competitor was modeled as:

$$\frac{dN_B}{dt} = r_B N_B(1 + c_{BB}N_B + c_{BA}N_A + \sigma_{BY}) \tag{B.46}$$

The incorporation of a mutualist that is both cultivated by and influencing the growth rate of the native competitor alters intraspecific competition for the native species such that:

$$\alpha_{BB} = c_{BB} + \sigma_{BY}\phi_{YB} \tag{B.47}$$

while all other competition coefficients are calculated similarly to the previous set of simulations.

B.4.3 Generalist Decomposer Model Structure. Our final set of simulations included a generalist decomposer (Z) that interacted with both *Alliaria petiolata* and the native competitor such that their population growth rates were modeled as:

$$\frac{dN_A}{dt} = r_A N_A(1 + c_{AA}N_A + c_{AB}N_B + \sigma_{AX}S_X + \sigma_{AZ}S_Z) \tag{B.48}$$

$$\frac{dN_B}{dt} = r_B N_B(1 + c_{BB}N_B + c_{BA}N_A + \sigma_{BY}S_Y + \sigma_{BZ}S_Z) \tag{B.49}$$

Incorporating a generalist microbial taxon alters all competition coefficients such that now, competition coefficients can be calculated as:

$$\alpha_{AA} = c_{AA} + \sigma_{AX}\phi_{XA} + \sigma_{AZ}\phi_{ZA} \tag{B.50}$$

$$\alpha_{BA} = c_{BA} + \sigma_{BZ}\phi_{ZA} \tag{B.51}$$

$$\alpha_{BB} = c_{BB} + \sigma_{BY}\phi_{YB} + \sigma_{BZ}\phi_{ZB} \tag{B.52}$$

$$\alpha_{AB} = c_{AB} + \sigma_{AZ}\phi_{ZB} \tag{B.53}$$

B.4.4 Parameterization. To start, we set the microbe-independent plant competition parameters such that *Alliaria petiolata* would competitively exclude the native competitor under sterile conditions where $c_{AA} = -0.005$, $c_{BA} = -0.008$, $c_{BB} = -0.008$, and $c_{AB} = -0.005$. Because niche and fitness differences are calculated with only the overall competition coefficients (α_{ij}), we

did not define parameter values for the plant growth rates (r_i). To incorporate microbial effects, we set the baseline per capita effect of the pathogen on *A. petiolata* as $\hat{\sigma}_{0,AX} = -0.002$ and the baseline cultivation rate of the pathogen by *A. petiolata* as $\hat{\phi}_{0,XA} = 0.2$. Finally, we scaled the cultivation rate of the pathogen by rainfall (v) such that the pathogen was cultivated more quickly with increased rainfall: $\phi_{XA} = 0.2 + v$.

When incorporating the mutualist, we kept the parameterization above and added new baseline $\hat{\sigma}_{0,iX}$ and $\hat{\phi}_{0,Xi}$ parameters where $\hat{\sigma}_{0,BY} = 0.002$ and $\hat{\phi}_{0,YB} = 0.2$. We then scaled ϕ_{YB} such that the cultivation rate of the mutualist decreased with increased rainfall: $\phi_{YB} = 0.2 - 0.5 * v$.

Finally, when incorporating the generalist decomposer, we added new baseline parameters where $\hat{\sigma}_{0,AZ} = 0.003$, $\hat{\phi}_{0,ZA} = 0.2$, $\hat{\sigma}_{0,BZ} = 0.001$, and $\hat{\phi}_{0,ZB} = 0.2$. We then scaled the cultivation of the decomposer by both plant species such that cultivation rates increased similarly with increased precipitation: $\phi_{ZA} = 0.2 + v$ and $\phi_{ZB} = 0.2 + v$.

For each simulation, we calculated competition coefficients as defined above and niche differences and fitness ratios as defined in the main text. The finding of Lozano et al. (2021) informed our decisions about how to scale the cultivation rates of each fungal guild in response to the precipitation gradient.

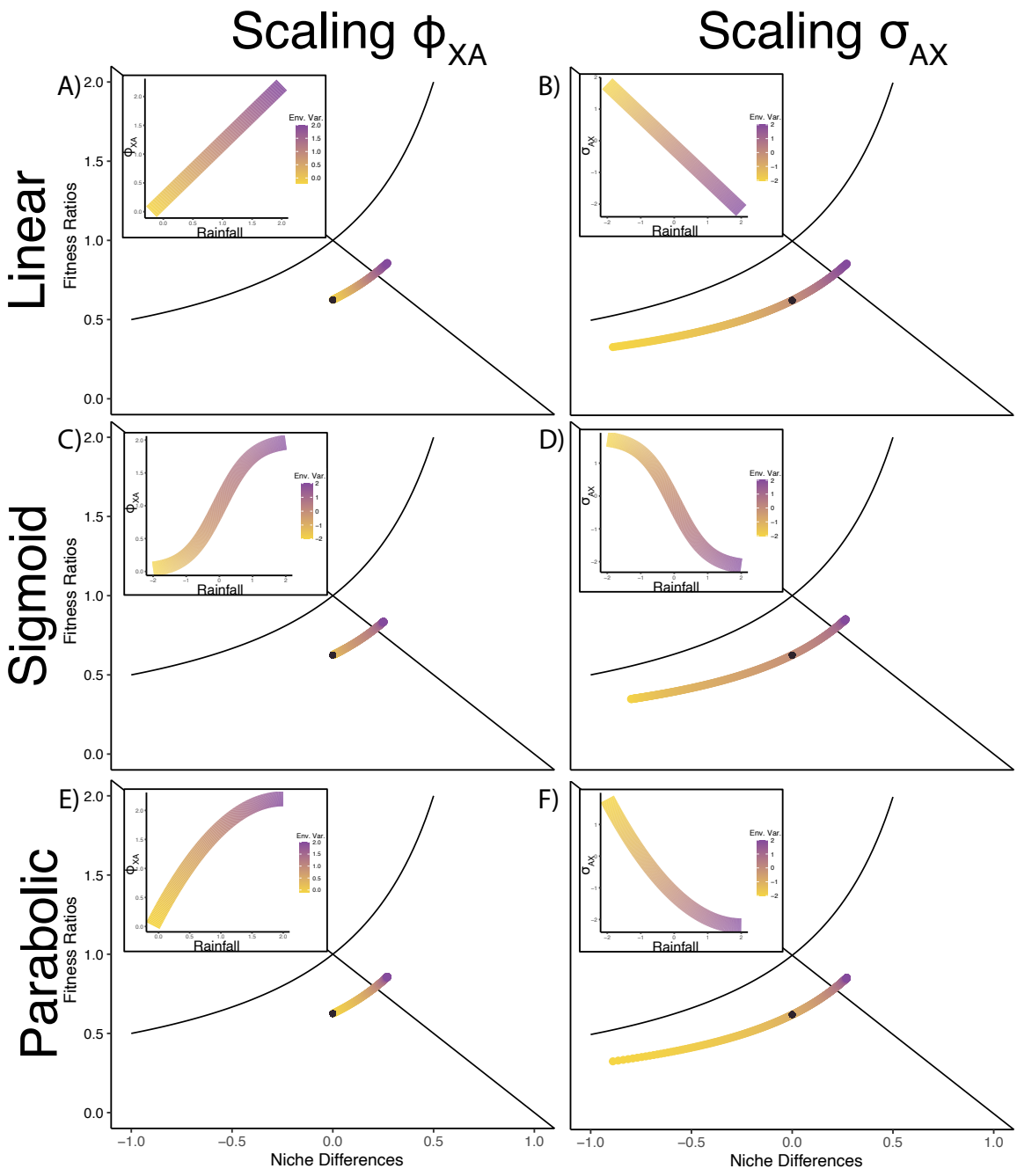

Figure S1. Results from linear (A & B), sigmoidal (C & D), and parabolic (E & F) scaling functions for ϕ_{XA} (first column; A, C, and E) and σ_{AX} (second column; B, D, and F). Graphs of the scaling functions are inlaid into each plot in niche difference and fitness ratio space.

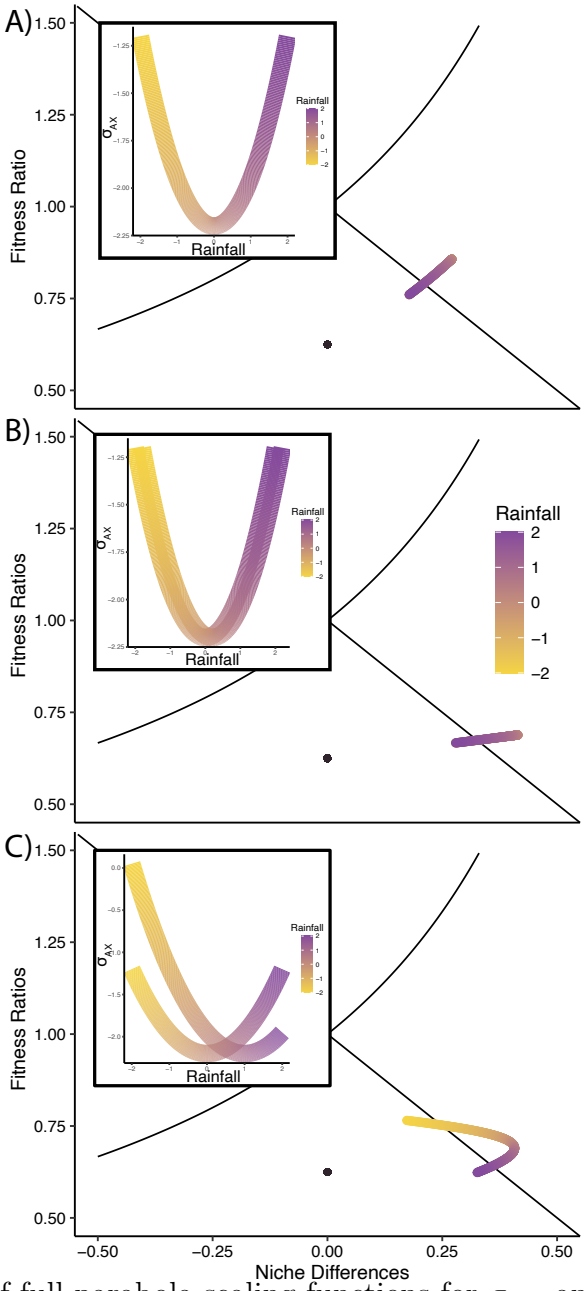

Figure S2. Effects of full parabola scaling functions for σ_{AX} and σ_{BY} on niche differences and fitness ratios. A) A single species-specific pathogen with a minimum pathogenicity on the competitively dominant species at 0 along the rainfall gradient. B) Two species-specific pathogens, one for each plant species, with identical scaling functions with a minimum pathogencitiy at 0 along the rainfall gradient. C) Two species-specific pathogens with offset minimum pathogenicity values. Graphs of the scaling functions are inlaid into each plot in niche difference and fitness ratio space.

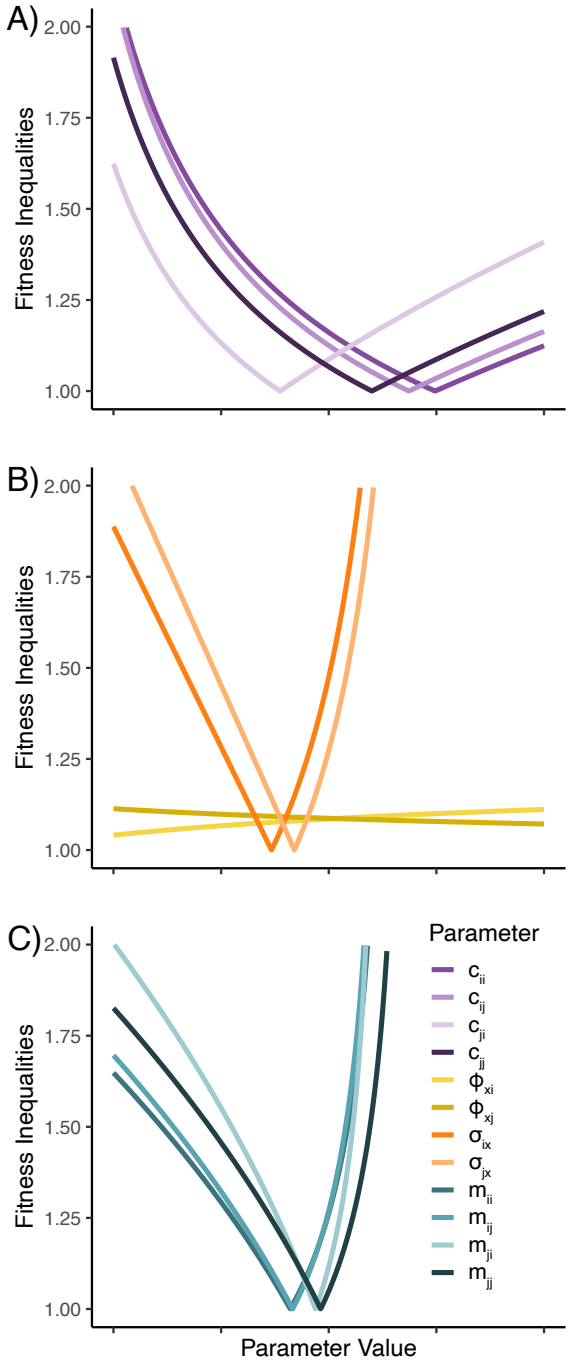

Figure S3. Local sensitivity analysis of the taxon specific plant-soil feedback Lotka-Volterra model. Lines represent the changes in fitness inequalities as the focal parameter varies from it's minimum to maximum value while all other parameters are held constant at their baseline values. Panels A, B, and C represent sensitivities to microbe-independent competition, plant-microbe interactions, and microbial feedbacks respectively

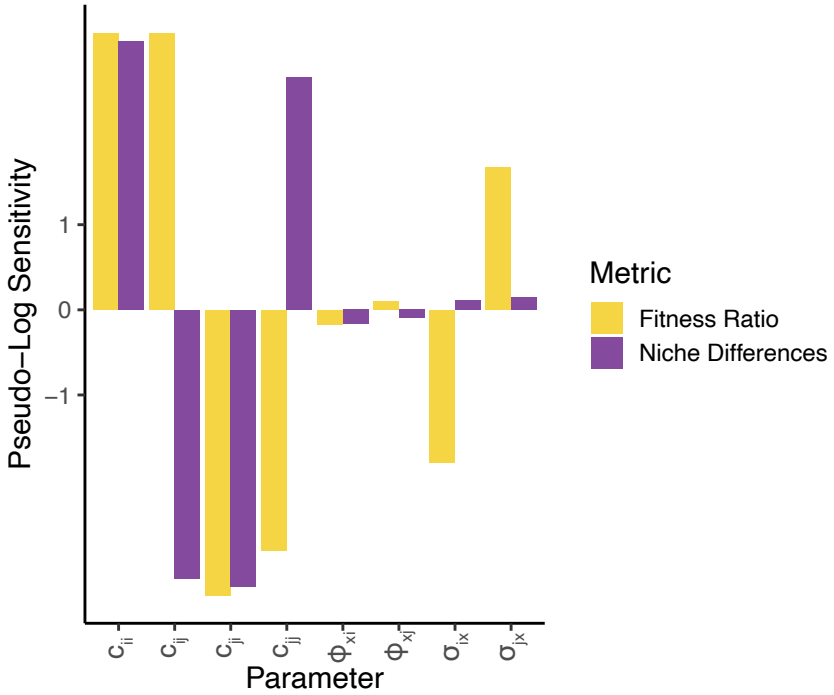

Figure S4. Comparison of microbe-independent plant competition and plant-microbe interaction term partial derivatives for the fitness ratio and niche differences calculated at the baseline parameter values.

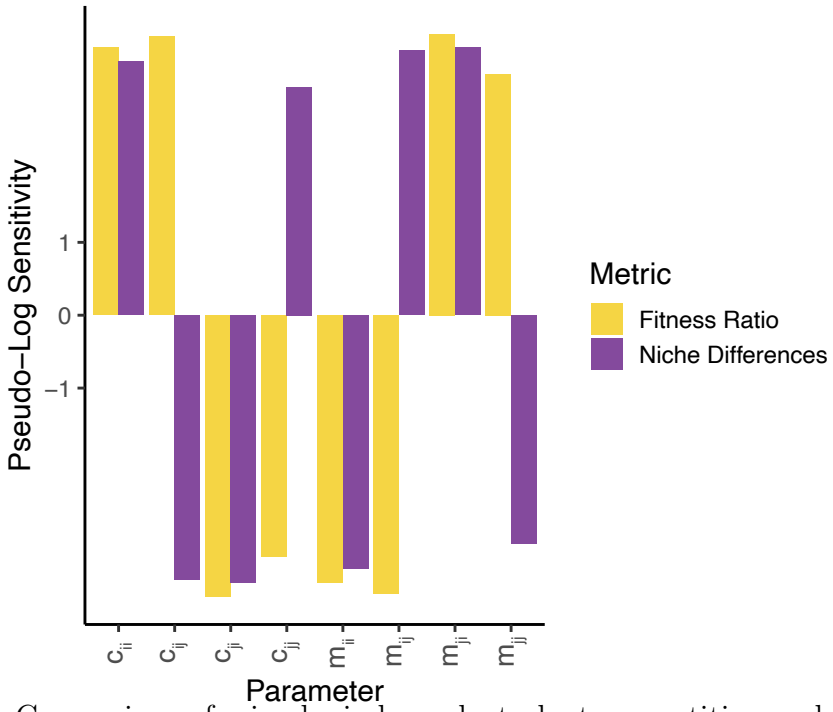

Figure S5. Comparison of microbe-independent plant competition and microbial feedback term partial derivatives for the fitness ratio and niche differences calculated at the baseline parameter values.

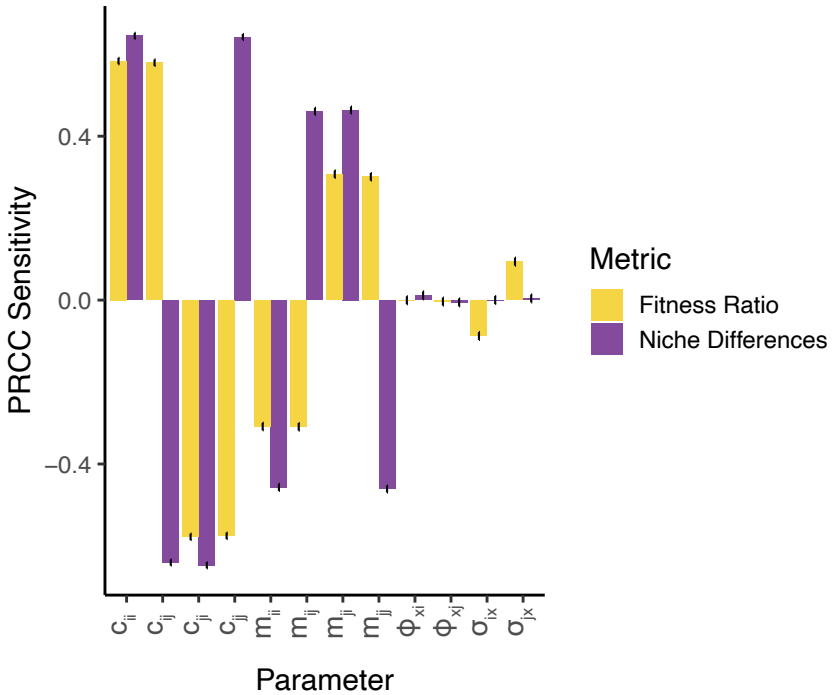

Figure S6. PRCC estimates for each parameter for the fitness ratio and niche differences. Error bars represent the 95% confidence intervals.

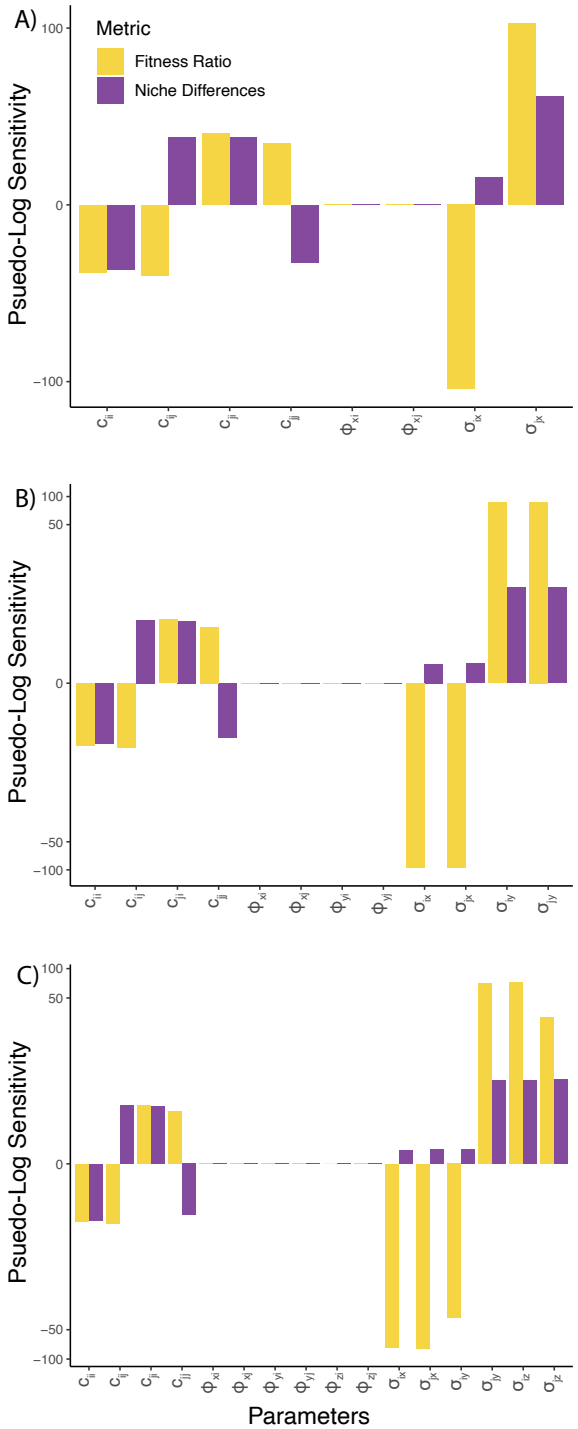

Figure S7. Comparison of microbe-independent plant competition and plant-microbe interaction term partial derivatives for the fitness ratio and niche differences calculated at the baseline parameter values across one (A), two (B), and three (C) microbe systems. These values are from the model run with unscaled cultivation rates.

APPENDIX C

SUPPLEMENTAL INFORMATION FOR CHAPTER 4

C.1 Model Comparison

To fit population models for our annual plants, we worked with the following simple model for annual plant population growth for some species i:

$$N_{i,t+1} = N_{i,t} g_{i,t} F_{i,t} \tag{C.1}$$

where $g_{i,t}$ is the germination rate for species i at time t, and the fecundity at time t is a function of the intrinsic growth rate, λ, intraspecific density-dependence, α_{ii}, interspecific density-dependence, α_{ij}, $N_{i,t}$, and $N_{j,t}$. While estimating germination rates is relatively straightforward (see Methods in the main text), estimating the phenomenological interaction coefficients (and thus the expected seed output in the absence of competition, λ, involves further consideration. An infinite amount of structural forms for density dependence could be used, and it is possible that structural uncertainty about the relationship between density and fitness may skew our results if we were to select a function that is innapropriate. Following the recommendations of Armitage 2024, we have fit a series of commonly used structural forms including a null model with no density dependence:

$$F_{i,t+1} = \lambda_i \tag{C.2}$$

a Lotka-Volterra style model with linear density-dependence:

$$F_{i,t+1} = \lambda_i + \sum_{j=1}^{J} (N_{j,t} \alpha_{i,j}) \tag{C.3}$$

a Beverton-Holt model:

$$F_{i,t+1} = \lambda_i/(1 + \sum_{j=1}^{J}(N_{j,t}\alpha_{i,j})) \tag{C.4}$$

and a Ricker model:

$$F_{i,t+1} = \lambda_i * e^{-\sum_{j=1}^{J}(N_{j,t}\alpha_{i,j})} \tag{C.5}$$

An additional decision point encountered when fitting these annual plant population models is whether to constrain species interactions to be competitive. While facilitation between plant species may in fact be an important process for structuring some communities, it has historically been neglected due to the potential for runaway population dynamics. Thus, the conditions by which facilitation can be accounted for in these relatively simple models are somewhat strict, and much of our theory about species coexistence is incompatible with intraspecific facilitation in such models. Thus, to acknowledge the potential importance for facilitation, we fit each of these models with constrained species interactions, and we fit the Lotka-Volterra and Ricker model with unconstrained species interactions. We did not fit the Beverton-Holt with unconstrained species interactions because this function quickly produces negative values with increasing facilitative strength.

For each of these six models, we used the log-likelihood estimates to calculate the estimated log pointwise predictive density (ELPD), a measure of predictive accuracy used in model comparison with Bayesian parameter estimates, using the loo package in R (Vehtari et al., 2023).

Because the Beverton-Holt had the highest ELPD value, we used the parameter estimates from this model for all results in the main text. However,

Model	SE ELPD	Δ ELPD
Beverton-Holt	-	-
Ricker (unconstrained)	23.7	-42.8
Lotka-Volterra	56.0	-300.7
Lotka-Volterra (Unconstrained)	56.0	-306.3
Null	56.8	-318.2
Ricker	70.4	-341.0

Table C.1. Model Comparison.

we also present the interaction estimates for the unconstrained Ricker model (the model with the second best ELPD value) in Appendix S2.

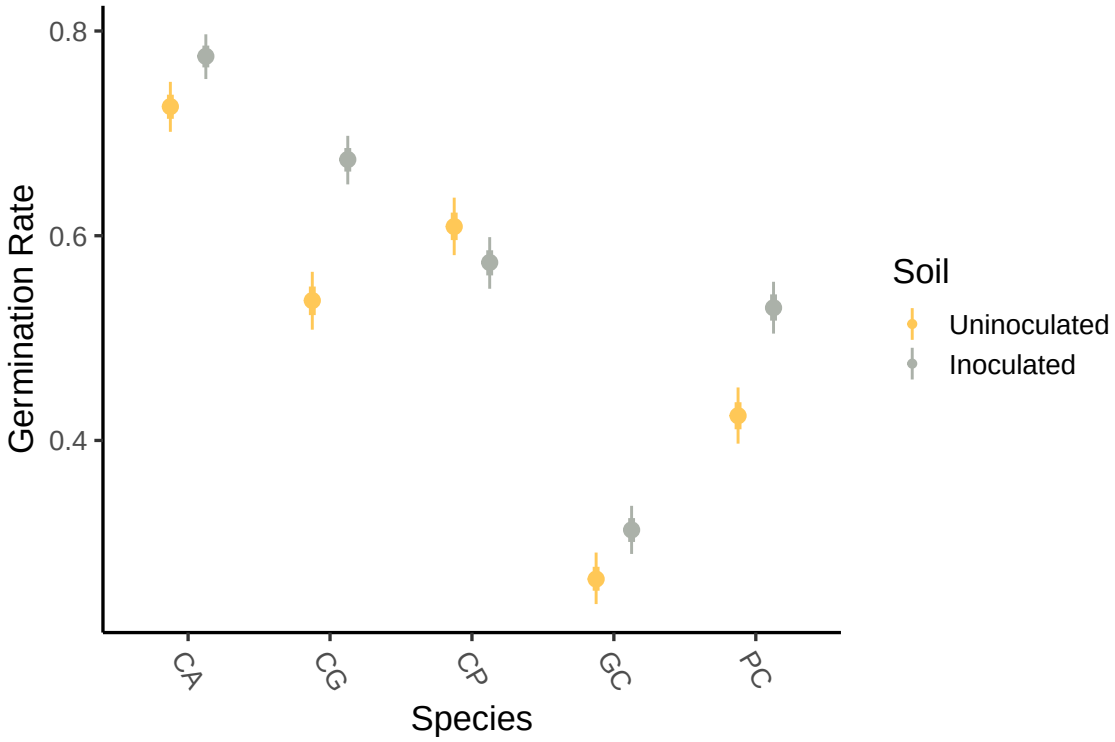

Figure S1. Estimated germination rates for each species in each soil treatment. Points represent median posterior estimates and error bars represent the 95% credible intervals.

C.2 Parameter Estimates

Below are some additional figures displaying the parameter estimates for the vital rates and species interactions as well as the downstream quantities of structural niche & fitness differences and the community pair differentials. Additionally, Figure S5 shows the estimated species interactions from the unconstrained Ricker model, which was the second best fitting model (Appendix S1) and suggests that facilitation was generally rare amongst the species in our study.

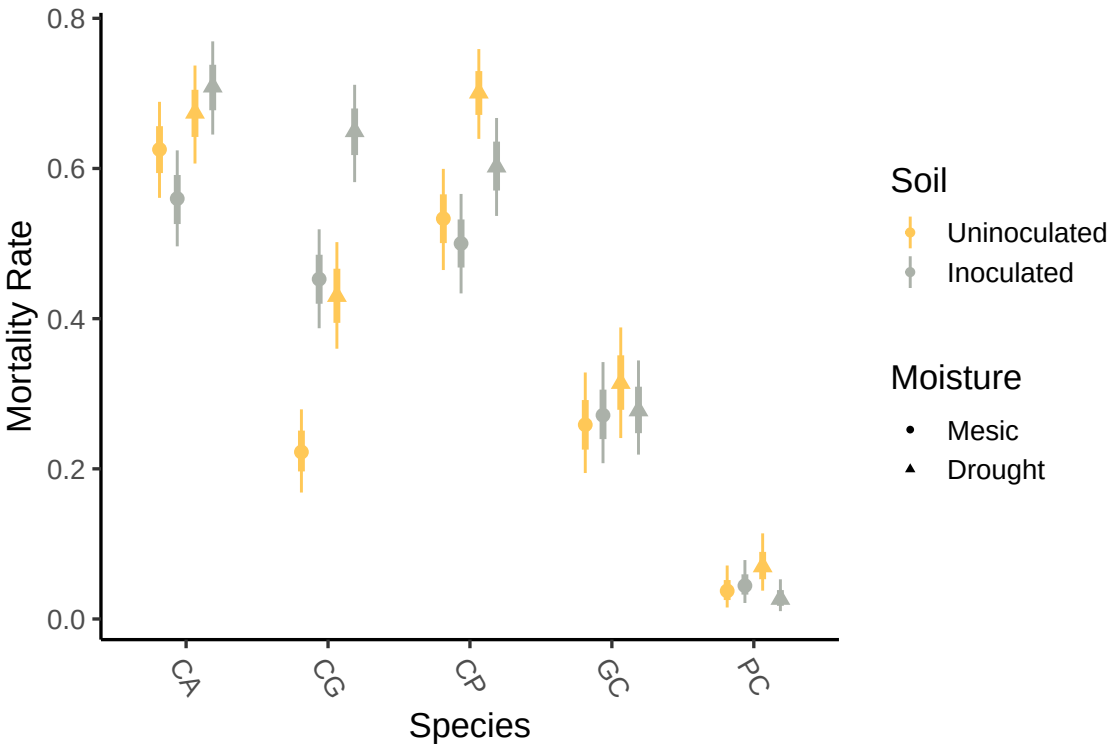

Figure S2. Estimated mortality rates for each species in each soil and moisture treatment. Points represent median posterior estimates and error bars represent the 95% credible intervals.

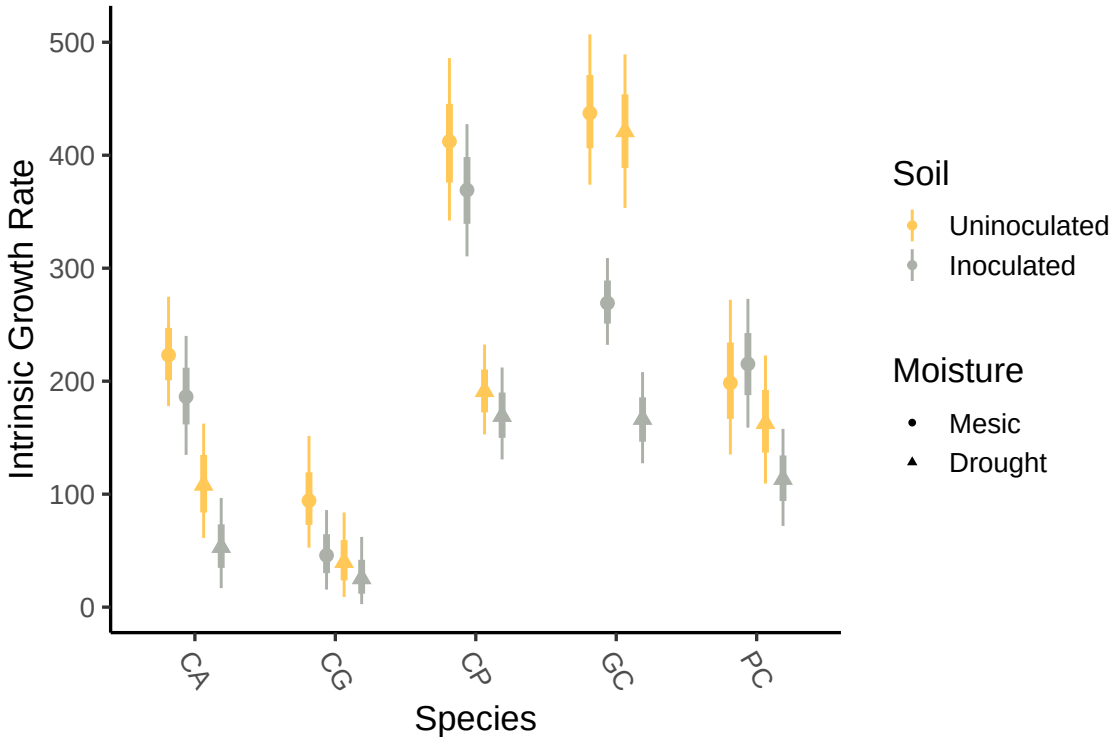

Figure S3. Estimated intrinsic growth rates for each species in each soil and moisture treatment. Points represent median posterior estimates and error bars represent the 95% credible intervals.

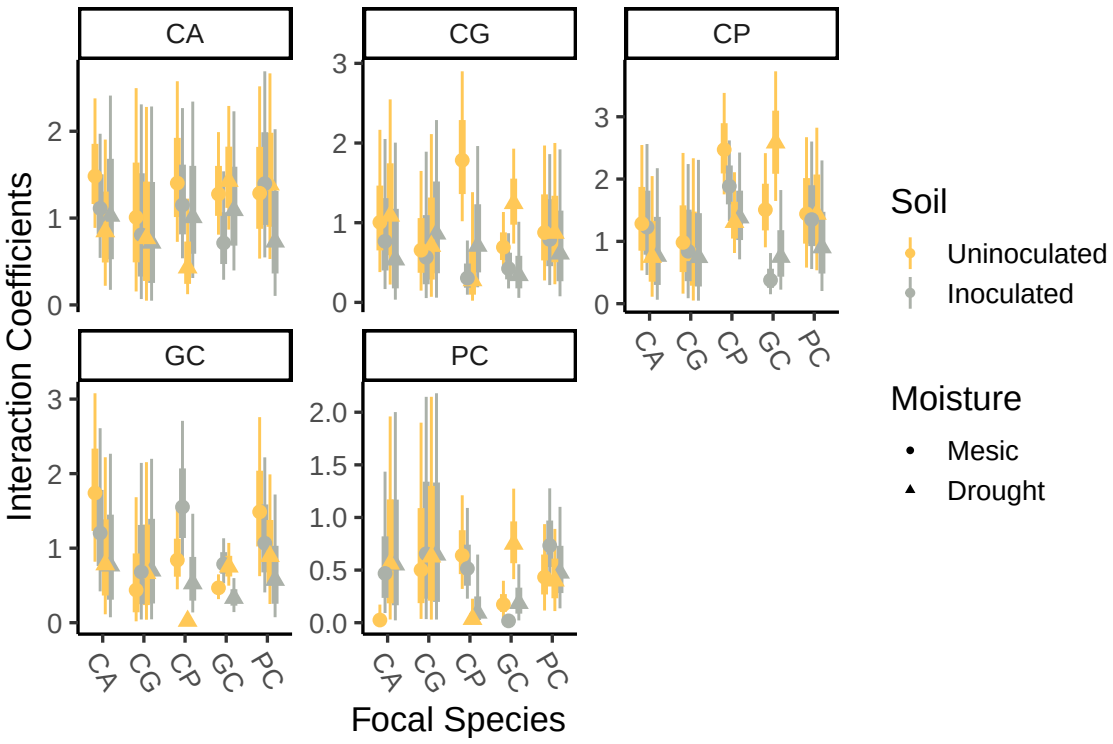

Figure S4. Estimated species interactions from the constrained Beverton-Holt model for each species in each soil and moisture treatment. Focal species (i) are plotted on the x-axis and the graph is faceted by the competitor species (j). Points represent median posterior estimates and error bars represent the 95% credible intervals.

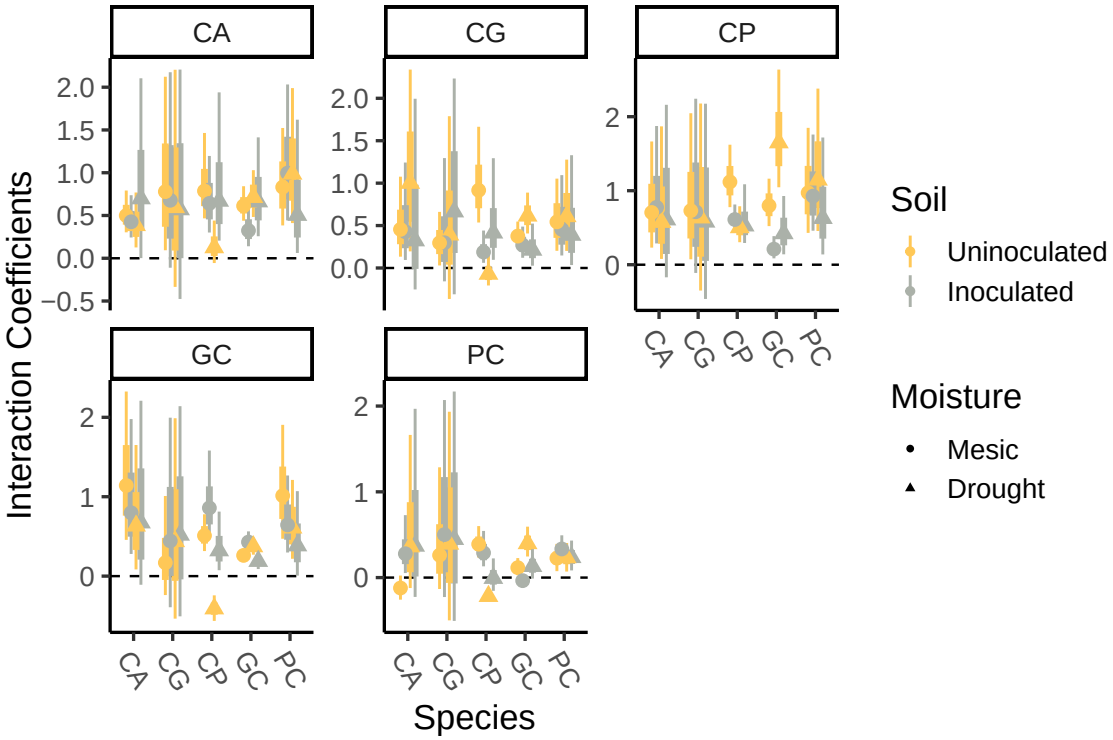

Figure S5. Estimated species interactions from the unconstrained Ricker model for each species in each soil and moisture treatment. Focal species (i) are plotted on the x-axis and the graph is faceted by the competitor species (j). Points represent median posterior estimates and error bars represent the 95% credible intervals.

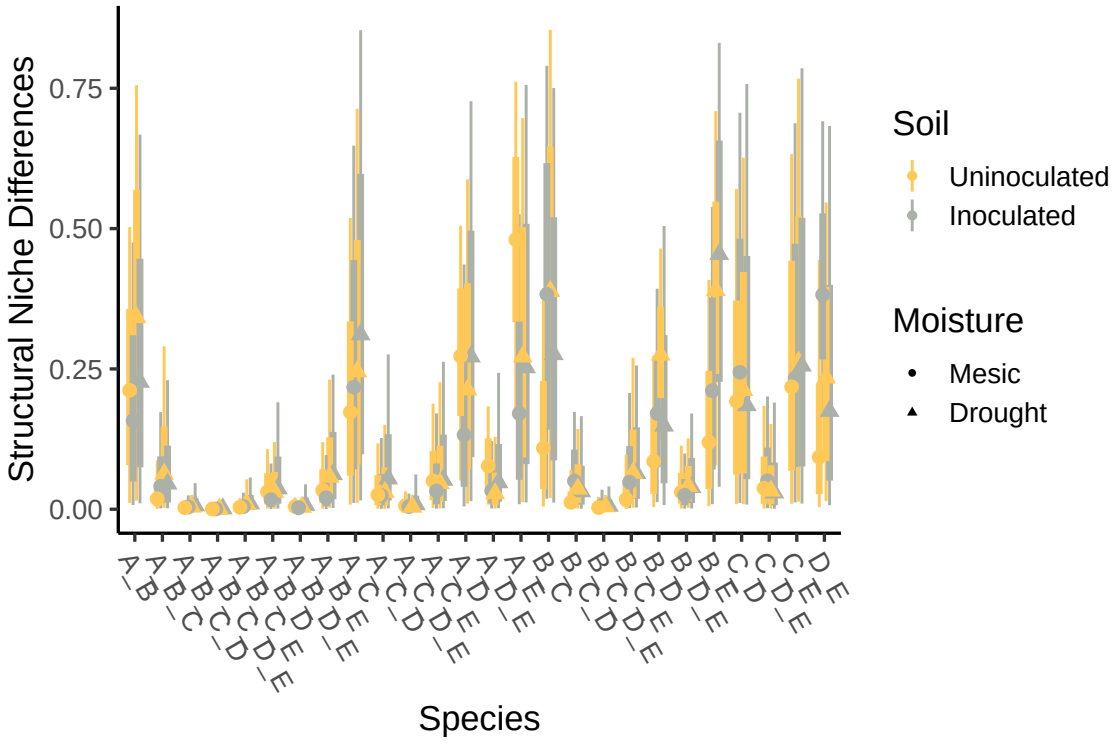

Figure S6. Calculated structural niche differences for each species combination in each soil and moisture treatment. Points represent median posterior estimates and error bars represent the 95% credible intervals.

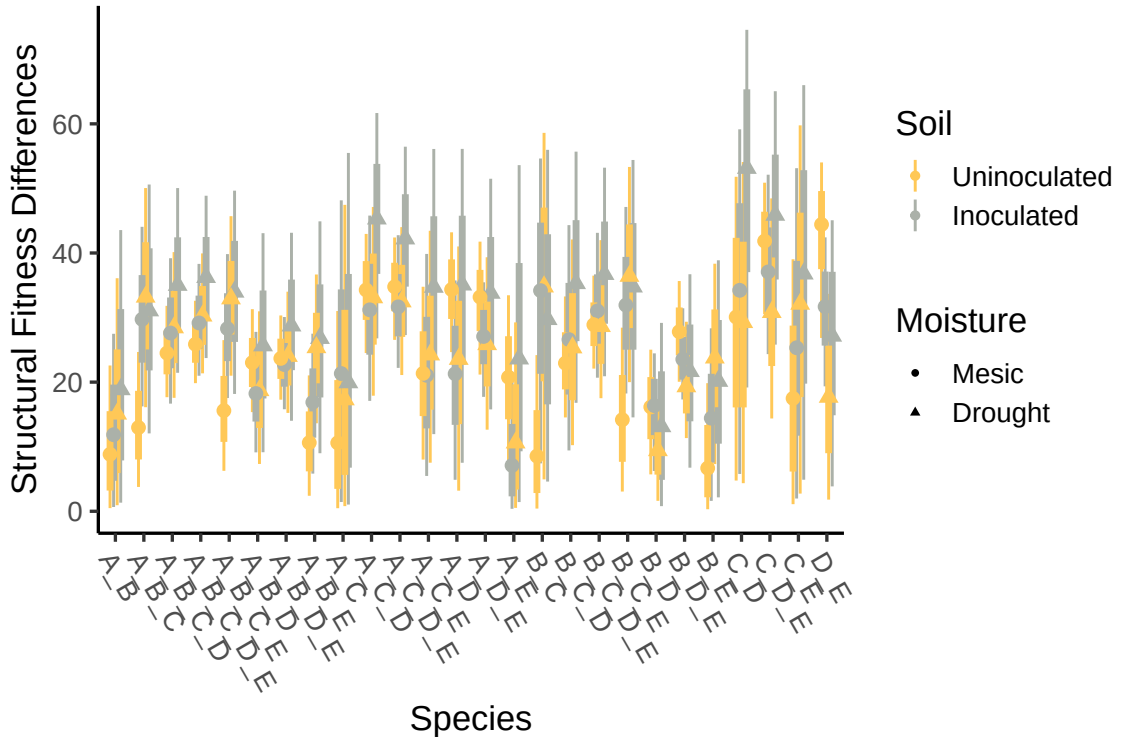

Figure S7. Calculated structural fitness differences for each species combination in each soil and moisture treatment. Points represent median posterior estimates and error bars represent the 95% credible intervals.

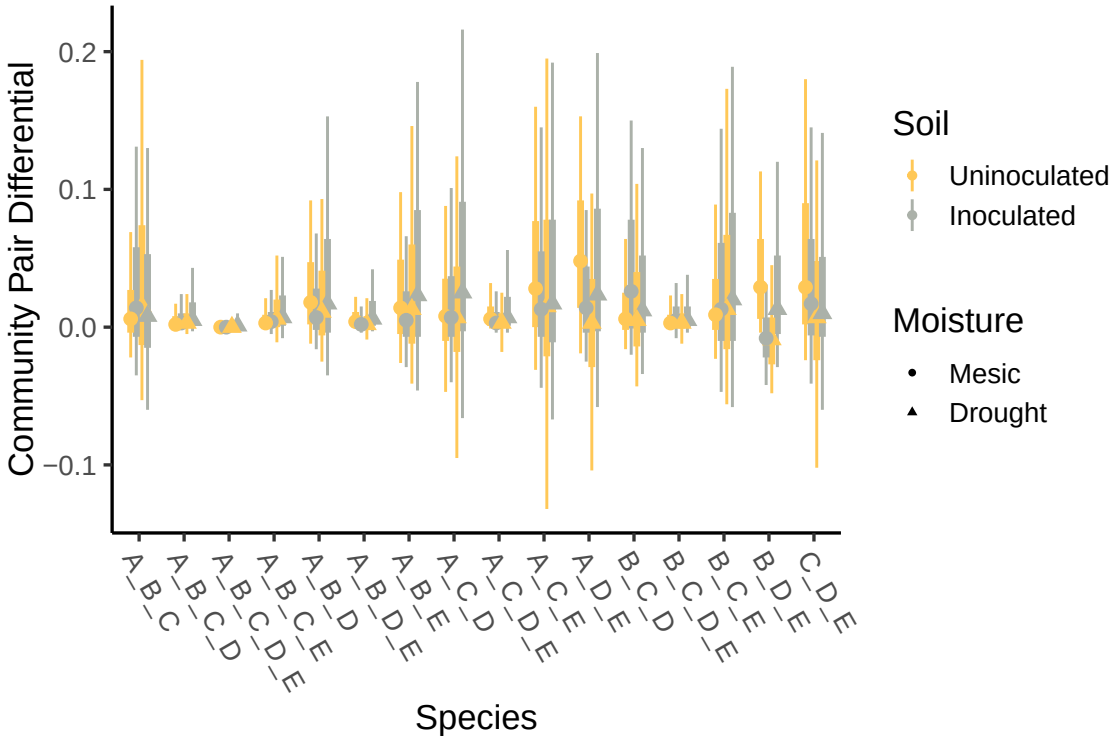

Figure S8. Calculated community pair differentials for each species combination in each soil and moisture treatment. Points represent median posterior estimates and error bars represent the 95% credible intervals. Only species combinations with three or more species are shown.

C.3 Simulations

To better understand how the results from our greenhouse experiment translate to multispecies communities, we performed a series of simulations described in the main text. Briefly, we simulated the population growth of each of our species, initializing each population at the same initial size, and let each population grow in response to its own and its competitors' densities. We first ran completely deterministic simulations for 100 years and recorded the species richness, evenness, and Shannon diversity at the end of the simulation. We then accounted for demographic stochasticity by pulling random values from the posterior distributions of each vital rate and interaction coefficient each year, assuming that year-to-year variation in these parameters is reflected in the variation of the posterior distributions. For such random simulations, we repeated the simulation 1000 times, recording the species richness, evenness, and Shannon diversity for each of the 1000 iterations. Finally, we accounted for environmental stochasticity by generating a random timeseries of binary drought data for each simulation. Depending on the value of the variable each year, parameters estimated from our mesic or drought treatments would be used. We ran 1000 of these simulations for eleven drought frequencies ranging from 0 to 1. We tested whether our initial values biased the results by repeating these simulations with initial population sizes of 1, 25, 50 and 100, but the results did not qualitatively change so we present the results from the $N_0 = 50$ simulations in the main text. Below are some additional figures from these simulations.

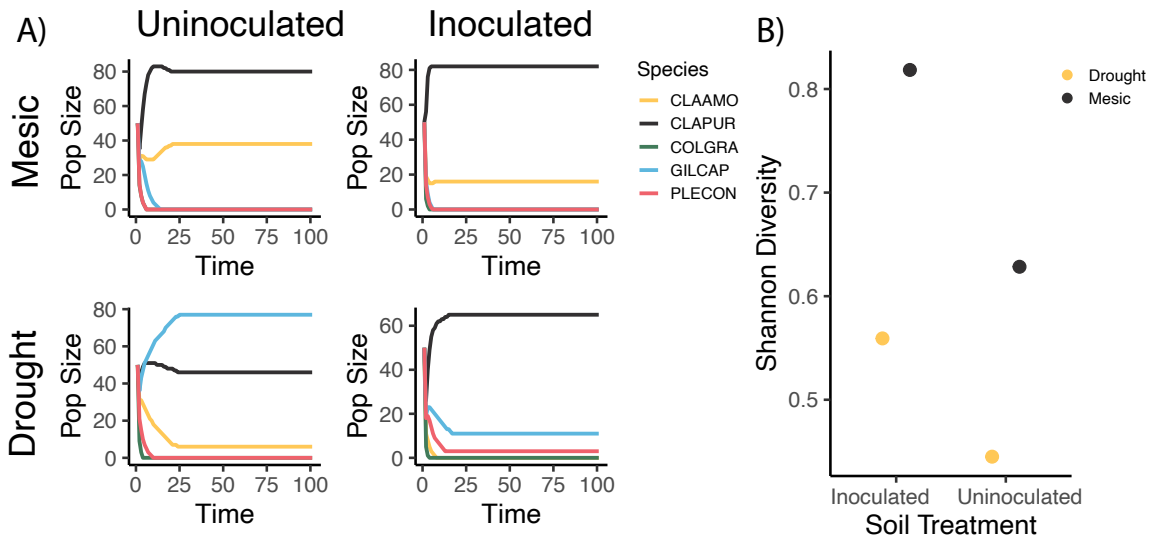

Figure S9. Results from deterministic simulations. A) Timeseries of population size for each species from deterministic simulations in each treatment combination. B) Final Shannon diversity of the communities in each treatment combination.

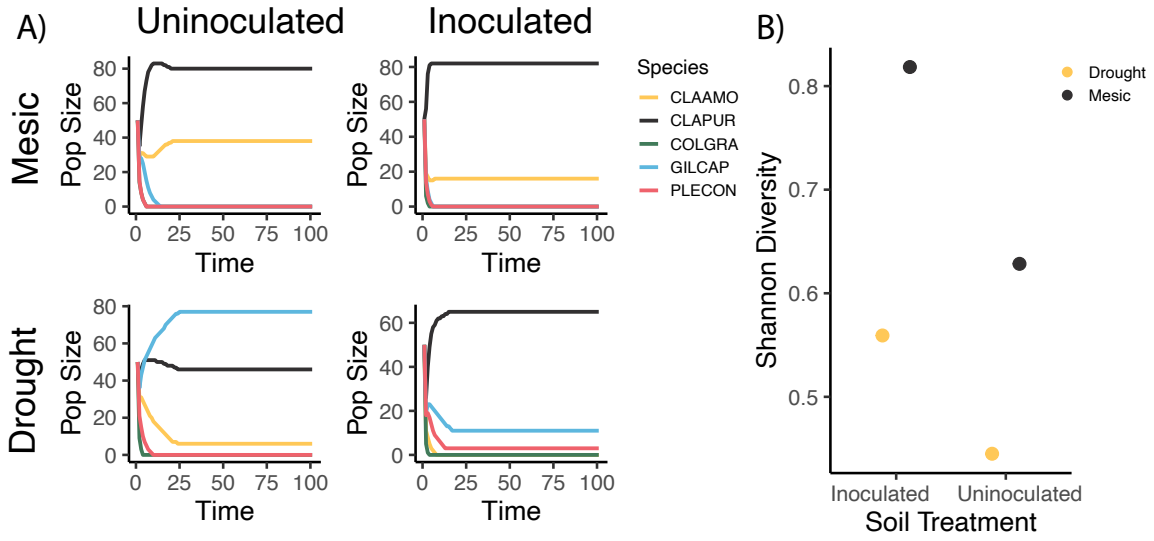

Figure S10. Results from simulations with just demographic stochasticity. A) Example timeseries of population size for each species from demographically stochastic simulations in each treatment combination. B) Final Shannon diversity of the communities in each treatment combination. Points represent mean diversity and error bars represent the 2.5^{th} and 97.5^{th} quantiles across all 1000 simulation runs.

REFERENCES CITED

Adler, P. B., HilleRisLambers, J., & Levine, J. M. (2007). A niche for neutrality. *Ecology letters*, *10*(2), 95–104.

Anthony, M., Stinson, K., Trautwig, A., Coates-Connor, E., & Frey, S. (2019). Fungal communities do not recover after removing invasive alliaria petiolata (garlic mustard). *Biological Invasions*, *21*(10), 3085–3099.

Armitage, D. W. (2022). To remain modern, the coexistence program requires modern statistical rigor. *bioRxiv*, 2022–12.

Armitage, D. W. (2024). To remain modern the coexistence program requires modern statistical rigour. *Nature*, *632*(8027), E15–E20.

Armitage, D. W., & Jones, S. E. (2019). Negative frequency-dependent growth underlies the stable coexistence of two cosmopolitan aquatic plants. *Ecology*, *100*(5), e02657.

Azizi, S., Tabari, M., Abad, A. R. F. N., Ammer, C., Guidi, L., & Bader, M. K.-F. (2022). Soil inoculation with beneficial microbes buffers negative drought effects on biomass, nutrients, and water relations of common myrtle. *Frontiers in Plant Science*, *13*, 892826.

Barrera, D., Luera, J., Lavallee, K., & Soti, P. (2021). Influence of microbial priming and seeding depth on germination and growth of native wildflowers. *Ecological Processes*, *10*, 1–8.

Barry, K. E., Mommer, L., van Ruijven, J., Wirth, C., Wright, A. J., Bai, Y., ... others (2019). The future of complementarity: disentangling causes from consequences. *Trends in ecology & evolution*, *34*(2), 167–180.

Bauer, J. T., Blumenthal, N., Miller, A. J., Ferguson, J. K., & Reynolds, H. L. (2017). Effects of between-site variation in soil microbial communities and plant-soil feedbacks on the productivity and composition of plant communities. *Journal of Applied Ecology*, *54*(4), 1028–1039.

Bennett, J. A., & Klironomos, J. (2019). Mechanisms of plant–soil feedback: interactions among biotic and abiotic drivers. *New Phytologist*, *222*(1), 91–96.

Bever, J. D. (1994). Feeback between plants and their soil communities in an old field community. *Ecology*, *75*(7), 1965–1977.

Bever, J. D. (2003). Soil community feedback and the coexistence of competitors: conceptual frameworks and empirical tests. *New phytologist*, *157*(3), 465–473.

Bever, J. D., Dickie, I. A., Facelli, E., Facelli, J. M., Klironomos, J., Moora, M., ... Zobel, M. (2010). Rooting theories of plant community ecology in microbial interactions. *Trends in ecology & evolution*, *25*(8), 468–478.

Bever, J. D., Westover, K. M., & Antonovics, J. (1997). Incorporating the soil community into plant population dynamics: the utility of the feedback approach. *Journal of Ecology*, 561–573.

Bimler, M. D., Mayfield, M. M., Martyn, T. E., & Stouffer, D. B. (2023). Estimating interaction strengths for diverse horizontal systems using performance data. *Methods in Ecology and Evolution*, *14*(3), 968–980.

Bimler, M. D., Stouffer, D. B., Lai, H. R., & Mayfield, M. M. (2018). Accurate predictions of coexistence in natural systems require the inclusion of facilitative interactions and environmental dependency. *Journal of Ecology*, *106*(5), 1839–1852.

Bimler, M. D., Stouffer, D. B., Martyn, T. E., & Mayfield, M. M. (2024). Plant interaction networks reveal the limits of our understanding of diversity maintenance. *Ecology Letters*, *27*(2), e14376.

Bittencourt, P. P., Alves, A. F., Ferreira, M. B., da Silva Irineu, L. E. S., Pinto, V. B., & Olivares, F. L. (2023). Mechanisms and applications of bacterial inoculants in plant drought stress tolerance. *Microorganisms*, *11*(2), 502.

Blackford, C., Germain, R. M., & Gilbert, B. (2020). Species differences in phenology shape coexistence. *The American Naturalist*, *195*(6), E168–E180.

Blossey, B., Nuzzo, V., Dávalos, A., Mayer, M., Dunbar, R., Landis, D. A., ... Minter, B. (2021). Residence time determines invasiveness and performance of garlic mustard (alliaria petiolata) in north america. *Ecology letters*, *24*(2), 327–336.

Bowler, C. H., Weiss-Lehman, C., Towers, I. R., Mayfield, M. M., & Shoemaker, L. G. (2022). Accounting for demographic uncertainty increases predictions for species coexistence: A case study with annual plants. *Ecology Letters*.

Burns, J. H., Anacker, B. L., Strauss, S. Y., & Burke, D. J. (2015). Soil microbial community variation correlates most strongly with plant species identity, followed by soil chemistry, spatial location and plant genus. *AoB plants*, *7*.

Cadotte, M. W., Davies, T. J., & Peres-Neto, P. R. (2017). Why phylogenies do not always predict ecological differences. *Ecological Monographs*, *87*(4), 535–551.

Callahan, B. J., McMurdie, P. J., Rosen, M. J., Han, A. W., Johnson, A. J. A., & Holmes, S. P. (2016). Dada2: High-resolution sample inference from illumina amplicon data. *Nature methods*, *13*(7), 581–583.

Cardarelli, M., Woo, S. L., Rouphael, Y., & Colla, G. (2022). Seed treatments with microorganisms can have a biostimulant effect by influencing germination and seedling growth of crops. *Plants*, *11*(3), 259.

Cariboni, J., Gatelli, D., Liska, R., & Saltelli, A. (2007). The role of sensitivity analysis in ecological modelling. *Ecological modelling*, *203*(1-2), 167–182.

Carlton, L., Duncritts, N. C., Chung, Y. A., & Rudgers, J. A. (2018). Plant-microbe interactions as a cause of ring formation in bouteloua gracilis. *Journal of Arid Environments*, *152*, 1–5.

Caruso, T., & Rillig, M. C. (2022). A general stochastic model shows that plant-soil feedbacks can buffer plant species from extinction risks in unpredictable environments. *Plant and Soil*, 1–12.

Chang, C.-W., Miki, T., Ushio, M., Ke, P.-J., Lu, H.-P., Shiah, F.-K., & Hsieh, C.-h. (2021). Reconstructing large interaction networks from empirical time series data. *Ecology Letters*, *24*(12), 2763–2774.

Chesson, P. (1994). Multispecies competition in variable environments. *Theoretical population biology*, *45*(3), 227–276.

Chesson, P. (2000). Mechanisms of maintenance of species diversity. *Annual review of Ecology and Systematics*, *31*(1), 343–366.

Chesson, P. (2013). Species competition and predation. In *Ecological systems* (pp. 223–256). Springer.

Chesson, P., & Kuang, J. J. (2008). The interaction between predation and competition. *Nature*, *456*(7219), 235–238.

Cipollini, D. (2016). A review of garlic mustard (alliaria petiolata, brassicaceae) as an allelopathic plant. *The Journal of the Torrey Botanical Society*, *143*(4), 339–348.

Clements, F. E. (1916). *Plant succession: an analysis of the development of vegetation* (No. 242). Carnegie institution of Washington.

Connell, J. H. (1978). Diversity in tropical rain forests and coral reefs: high diversity of trees and corals is maintained only in a nonequilibrium state. *Science*, *199*(4335), 1302–1310.

Connolly, B. M., Carris, L., & Mack, R. (2018). Soil-borne seed pathogens: contributors to the naturalization gauntlet in pacific northwest (usa) forest and steppe communities? *Plant ecology*, *219*, 359–368.

Crawford, K. M., Bauer, J. T., Comita, L. S., Eppinga, M. B., Johnson, D. J., Mangan, S. A., ... others (2019). When and where plant-soil feedback may promote plant coexistence: a meta-analysis. *Ecology Letters*, *22*(8), 1274–1284.

Dagher, D. J., de la Providencia, I. E., Pitre, F. E., St-Arnaud, M., & Hijri, M. (2019). Plant identity shaped rhizospheric microbial communities more strongly than bacterial bioaugmentation in petroleum hydrocarbon-polluted sediments. *Frontiers in microbiology*, *10*, 2144.

David, A. S., Quintana-Ascencio, P. F., Menges, E. S., Thapa-Magar, K. B., Afkhami, M. E., & Searcy, C. A. (2019). Soil microbiomes underlie population persistence of an endangered plant species. *The American Naturalist*, *194*(4), 488–494.

de la Fuente Cantó, C., Simonin, M., King, E., Moulin, L., Bennett, M. J., Castrillo, G., & Laplaze, L. (2020). An extended root phenotype: the rhizosphere, its formation and impacts on plant fitness. *The Plant Journal*, *103*(3), 951–964.

de Vries, F., Lau, J., Hawkes, C., & Semchenko, M. (2023). Plant–soil feedback under drought: does history shape the future? *Trends in Ecology & Evolution*.

Di Cecco, G. J., & Gouhier, T. C. (2018). Increased spatial and temporal autocorrelation of temperature under climate change. *Scientific reports*, *8*(1), 1–9.

Donald, M. L., Bohner, T. F., Kolis, K. M., Shadow, R. A., Rudgers, J. A., & Miller, T. E. (2021). Context-dependent variability in the population prevalence and individual fitness effects of plant–fungal symbiosis. *Journal of Ecology*, *109*(2), 847–859.

Dostál, P. (2023). Fitness and niche differences are both important in explaining responses of plant diversity to nutrient addition. *Ecology*, *104*(8), e4125.

Dostálek, T., Knappová, J., & Münzbergová, Z. (2022). The role of plant–soil feedback in long-term species coexistence cannot be predicted from its effects on plant performance. *Annals of Botany*, *130*(4), 535–546.

Duchesneau, K., Golemiec, A., Colautti, R. I., & Antunes, P. M. (2021). Functional shifts of soil microbial communities associated with alliaria petiolata invasion. *Pedobiologia*, *84*, 150700.

Dudenhöffer, J.-H., Luecke, N. C., & Crawford, K. M. (2022). Changes in precipitation patterns can destabilize plant species coexistence via changes in plant–soil feedback. *Nature Ecology & Evolution*, *6*(5), 546–554.

Dundore-Arias, J., Michalska-Smith, M., Millican, M., & Kinkel, L. (2023). More than the sum of its parts: unlocking the power of network structure for understanding organization and function in microbiomes. *Annual Review of Phytopathology*, *61*(1), 403–423.

Ellner, S. P., Snyder, R. E., Adler, P. B., & Hooker, G. (2019). An expanded modern coexistence theory for empirical applications. *Ecology letters*, *22*(1), 3–18.

Enders, M., Havemann, F., Ruland, F., Bernard-Verdier, M., Catford, J. A., Gómez-Aparicio, L., ... others (2020). A conceptual map of invasion biology: Integrating hypotheses into a consensus network. *Global Ecology and Biogeography*, *29*(6), 978–991.

Eppinga, M. B., Baudena, M., Johnson, D. J., Jiang, J., Mack, K. M., Strand, A. E., & Bever, J. D. (2018). Frequency-dependent feedback constrains plant community coexistence. *Nature Ecology & Evolution*, *2*(9), 1403–1407.

Eppinga, M. B., Van der Putten, W. H., & Bever, J. D. (2022). Plant-soil feedback as a driver of spatial structure in ecosystems. *Physics of Life Reviews*, *40*(C).

Fahey, C., Koyama, A., Antunes, P. M., Dunfield, K., & Flory, S. L. (2020). Plant communities mediate the interactive effects of invasion and drought on soil microbial communities. *The ISME Journal*, *14*(6), 1396–1409.

Faust, K., Lahti, L., Gonze, D., De Vos, W. M., & Raes, J. (2015). Metagenomics meets time series analysis: unraveling microbial community dynamics. *Current opinion in microbiology*, *25*, 56–66.

Fitzpatrick, C. R., Mustafa, Z., & Viliunas, J. (2019). Soil microbes alter plant fitness under competition and drought. *Journal of evolutionary biology*, *32*(5), 438–450.

Forero, L. E., Grenzer, J., Heinze, J., Schittko, C., & Kulmatiski, A. (2019). Greenhouse-and field-measured plant-soil feedbacks are not correlated. *Frontiers in Environmental Science*, *7*, 184.

Foster, B. S., Haile, B. B., Campnell, J. T., Canam, T., Gallagher, M. J., & Meiners, S. J. (2022). Plant performance responds to intraspecific variation in soil inocula from individual solidago clones. *Plant Ecology*, *223*(2), 201–212.

Fox, A., Lüscher, A., & Widmer, F. (2020). Plant species identity drives soil microbial community structures that persist under a following crop. *Ecology and Evolution*, *10*(16), 8652–8668.

Francioli, D., Schulz, E., Buscot, F., & Reitz, T. (2018). Dynamics of soil bacterial communities over a vegetation season relate to both soil nutrient status and plant growth phenology. *Microbial ecology*, *75*(1), 216–227.

Fry, E. L., Johnson, G. N., Hall, A. L., Pritchard, W. J., Bullock, J. M., & Bardgett, R. D. (2018). Drought neutralises plant–soil feedback of two mesic grassland forbs. *Oecologia*, *186*, 1113–1125.

Gallien, L., & Carboni, M. (2017). The community ecology of invasive species: where are we and what's next? *Ecography*, *40*(2), 335–352.

Gardes, M., & Bruns, T. D. (1993). Its primers with enhanced specificity for basidiomycetes-application to the identification of mycorrhizae and rusts. *Molecular ecology*, *2*(2), 113–118.

Germain, R. M., Mayfield, M. M., & Gilbert, B. (2018). The 'filtering'metaphor revisited: competition and environment jointly structure invasibility and coexistence. *Biology letters*, *14*(8), 20180460.

Godoy, O., Kraft, N. J., & Levine, J. M. (2014). Phylogenetic relatedness and the determinants of competitive outcomes. *Ecology letters*, *17*(7), 836–844.

Godoy, O., & Levine, J. M. (2014). Phenology effects on invasion success: insights from coupling field experiments to coexistence theory. *Ecology*, *95*(3), 726–736.

Grainger, T. N., Letten, A. D., Gilbert, B., & Fukami, T. (2019). Applying modern coexistence theory to priority effects. *Proceedings of the National Academy of Sciences*, *116*(13), 6205–6210.

Granjel, R. R., Allan, E., & Godoy, O. (2023). Nitrogen enrichment and foliar fungal pathogens affect the mechanisms of multispecies plant coexistence. *New Phytologist*, *237*(6), 2332–2346.

Griffin-Nolan, R. J., Mohanbabu, N., Araldi-Brondolo, S., Ebert, A. R., LeVonne, J., Lumbsden-Pinto, J. I., ... others (2021). Friend or foe? the role of biotic agents in drought-induced plant mortality. *Plant ecology*, *222*, 537–548.

Gudmundson, S., Eklöf, A., & Wennergren, U. (2015). Environmental variability uncovers disruptive effects of species' interactions on population dynamics. *Proceedings of the Royal Society B: Biological Sciences*, *282*(1812), 20151126.

Guerrero, R., Margulis, L., Berlanga, M., et al. (2013). Symbiogenesis: the holobiont as a unit of evolution. *Int Microbiol*, *16*(3), 133–143.

Hahn, P. G., Bullington, L., Larkin, B., LaFlamme, K., Maron, J. L., & Lekberg, Y. (2018). Effects of short-and long-term variation in resource conditions on soil fungal communities and plant responses to soil biota. *Frontiers in plant science*, 1605.

Hallett, L. M., Shoemaker, L. G., White, C. T., & Suding, K. N. (2019). Rainfall variability maintains grass-forb species coexistence. *Ecology Letters*, *22*(10), 1658–1667.

Harris, J. (2009). Soil microbial communities and restoration ecology: facilitators or followers? *Science*, *325*(5940), 573–574.

Hart, S. P., Freckleton, R. P., & Levine, J. M. (2018). How to quantify competitive ability. *Journal of Ecology*, *106*(5), 1902–1909.

Hart, S. P., & Marshall, D. J. (2013). Environmental stress, facilitation, competition, and coexistence. *Ecology*, *94*(12), 2719–2731.

Hassan, K., Carrillo, Y., & Nielsen, U. N. (2022). Prolonged drought causes negative plant-soil feedbacks in grassland species under field conditions. *Soil Biology and Biochemistry*, *172*, 108772.

Heinze, J., Sitte, M., Schindhelm, A., Wright, J., & Joshi, J. (2016). Plant-soil feedbacks: a comparative study on the relative importance of soil feedbacks in the greenhouse versus the field. *Oecologia*, *181*, 559–569.

Hoeksema, J. D., Chaudhary, V. B., Gehring, C. A., Johnson, N. C., Karst, J., Koide, R. T., ... others (2010). A meta-analysis of context-dependency in plant response to inoculation with mycorrhizal fungi. *Ecology letters*, *13*(3), 394–407.

Hubbard, M., Germida, J., & Vujanovic, V. (2012). Fungal endophytes improve wheat seed germination under heat and drought stress. *Botany*, *90*(2), 137–149.

Hutchinson, G. E. (1961). The paradox of the plankton. *The American Naturalist*, *95*(882), 137–145.

Janos, D. P. (1980). Mycorrhizae influence tropical succession. *Biotropica*, 56–64.

J Gundale, M., & Kardol, P. (2021). Multi-dimensionality as a path forward in plant-soil feedback research. *Journal of Ecology*, *109*(10), 3446–3465.

Jin, Y., & Qian, H. (2019). V. phylomaker: an r package that can generate very large phylogenies for vascular plants. *Ecography*, *42*(8), 1353–1359.

Johnson, C. A. (2021). *How mutualisms influence the coexistence of competing species*. Wiley Online Library.

Johnson, N. C., Graham, J. H., & Smith, F. A. (1997). Functioning of mycorrhizal associations along the mutualism–parasitism continuum. *The New Phytologist*, *135*(4), 575–585.

Johnson, N. C., & Pfleger, F. (1992). Vesicular-arbuscular mycorrhizae and cultural stresses. *Mycorrhizae in sustainable agriculture*, *54*, 71–99.

Kaisermann, A., de Vries, F. T., Griffiths, R. I., & Bardgett, R. D. (2017). Legacy effects of drought on plant–soil feedbacks and plant–plant interactions. *New Phytologist*, *215*(4), 1413–1424.

Kalamulla, R., Karunarathna, S. C., Tibpromma, S., Galappaththi, M. C., Suwannarach, N., Stephenson, S. L., ... Yapa, N. (2022). Arbuscular mycorrhizal fungi in sustainable agriculture. *Sustainability*, *14*(19), 12250.

Kandlikar, G. S. (2024). Quantifying soil microbial effects on plant species coexistence: A conceptual synthesis. *American Journal of Botany*, *111*(4), e16316.

Kandlikar, G. S., Johnson, C. A., Yan, X., Kraft, N. J., & Levine, J. M. (2019). Winning and losing with microbes: how microbially mediated fitness differences influence plant diversity. *Ecology letters*, *22*(8), 1178–1191.

Kandlikar, G. S., Yan, X., Levine, J. M., & Kraft, N. J. (2021). Soil microbes generate stronger fitness differences than stabilization among california annual plants. *The American Naturalist*, *197*(1), E30–E39.

Karakoç, C., Clark, A. T., & Chatzinotas, A. (2020). Diversity and coexistence are influenced by time-dependent species interactions in a predator–prey system. *Ecology Letters*, *23*(6), 983–993.

Kardol, P., Veen, G. C., Teste, F. P., & Perring, M. P. (2015). Peeking into the black box: a traitbased approach to predicting plant–soil feedback. *New Phytologist*, *206*(1), 1–4.

Ke, P.-J., & Levine, J. M. (2021). The temporal dimension of plant-soil microbe interactions: mechanisms promoting feedback between generations. *The American Naturalist*, *198*(3), E80–E94.

Ke, P.-J., & Wan, J. (2020). Effects of soil microbes on plant competition: a perspective from modern coexistence theory. *Ecological Monographs*, *90*(1), e01391.

Ke, P.-J., & Wan, J. (2022). A general approach for quantifying microbial effects on plant competition. *Plant and Soil*, 1–14.

Ke, P.-J., & Wan, J. (2023). A general approach for quantifying microbial effects on plant competition. *Plant and Soil*, *485*(1), 57–70.

Ke, P.-J., Zee, P. C., & Fukami, T. (2021). Dynamic plant–soil microbe interactions: the neglected effect of soil conditioning time. *New Phytologist*, *231*(4), 1546–1558.

Keane, R. M., & Crawley, M. J. (2002). Exotic plant invasions and the enemy release hypothesis. *Trends in ecology & evolution*, *17*(4), 164–170.

Kraft, N. J., Godoy, O., & Levine, J. M. (2015). Plant functional traits and the multidimensional nature of species coexistence. *Proceedings of the National Academy of Sciences*, *112*(3), 797–802.

Kulmatiski, A., Beard, K. H., Stevens, J. R., & Cobbold, S. M. (2008). Plant–soil feedbacks: a meta-analytical review. *Ecology letters*, *11*(9), 980–992.

Lankau, R. A. (2011). Intraspecific variation in allelochemistry determines an invasive species' impact on soil microbial communities. *Oecologia*, *165*(2), 453–463.

Lee, E.-H., Eo, J.-K., Ka, K.-H., & Eom, A.-H. (2013). Diversity of arbuscular mycorrhizal fungi and their roles in ecosystems. *Mycobiology*, *41*(3), 121–125.

Leff, J. W., Bardgett, R. D., Wilkinson, A., Jackson, B. G., Pritchard, W. J., De Long, J. R., ... others (2018). Predicting the structure of soil communities from plant community taxonomy, phylogeny, and traits. *The ISME journal*, *12*(7), 1794–1805.

Liu, S., Moon, C. D., Zheng, N., Huws, S., Zhao, S., & Wang, J. (2022). Opportunities and challenges of using metagenomic data to bring uncultured microbes into cultivation. *Microbiome*, *10*(1), 76.

Liu, Y., Yu, S., Xie, Z.-P., & Staehelin, C. (2012). Analysis of a negative plant–soil feedback in a subtropical monsoon forest. *Journal of Ecology*, *100*(4), 1019–1028.

Lozano, Y. M., Aguilar-Trigueros, C. A., Roy, J., & Rillig, M. C. (2021). Drought induces shifts in soil fungal communities that can be linked to root traits across 24 plant species. *New Phytologist*, *232*, 1917–1929.

Lumibao, C. Y., Bernik, B. M., Formel, S. K., Kandalepas, D., Mighell, K. L., Pardue, J., ... Blum, M. J. (2020). Rhizosphere microbial communities reflect genotypic and trait variation in a salt marsh ecosystem engineer. *American journal of botany*, *107*(6), 941–949.

Manning, P., Morrison, S., Bonkowski, M., & Bardgett, R. D. (2008). Nitrogen enrichment modifies plant community structure via changes to plant–soil feedback. *Oecologia*, *157*, 661–673.

Martin, M. (2011). Cutadapt removes adapter sequences from high-throughput sequencing reads. *EMBnet. journal*, *17*(1), 10–12.

Martorell, C., MartÍnez-Blancas, A., & García-Meza, D. (2021). Plant–soil feedbacks depend on drought stress, functional group, and evolutionary relatedness in a semiarid grassland. *Ecology*, *102*(11), e03499.

Mauro, A. A., Shah, A. A., Martin, P. R., & Ghalambor, C. K. (2022). An integrative perspective on the mechanistic basis of context-dependent species interactions. *Integrative and Comparative Biology*, *62*(2), 164–178.

McGinn, K. J., van der Putten, W. H., Hulme, P. E., Shelby, N., Weser, C., & Duncan, R. P. (2018). The influence of residence time and geographic extent on the strength of plant–soil feedbacks for naturalised trifolium. *Journal of Ecology*, *106*(1), 207–217.

Mehrabi, Z., & Tuck, S. L. (2015). Relatedness is a poor predictor of negative plant–soil feedbacks. *New Phytologist*, *205*(3), 1071–1075.

Mersmann, O., Trautmann, H., Steuer, D., & Bornkamp, B. (2023). truncnorm: Truncated normal distribution [Computer software manual]. Retrieved from `https://CRAN.R-project.org/package=truncnorm` (R package version 1.0-9)

Miller, Z. R., Lechón-Alonso, P., & Allesina, S. (2022). No robust multispecies coexistence in a canonical model of plant–soil feedbacks. *Ecology Letters*, *25*(7), 1690–1698.

Mordecai, E. A. (2013). Consequences of pathogen spillover for cheatgrass-invaded grasslands: coexistence, competitive exclusion, or priority effects. *The American Naturalist*, *181*(6), 737–747.

Munch, S. B., Rogers, T. L., & Sugihara, G. (2023). Recent developments in empirical dynamic modelling. *Methods in Ecology and Evolution*, *14*(3), 732–745.

Nguyen, N. H., Song, Z., Bates, S. T., Branco, S., Tedersoo, L., Menke, J., ... Kennedy, P. G. (2016). Funguild: an open annotation tool for parsing fungal community datasets by ecological guild. *Fungal Ecology*, *20*, 241–248.

Nilsson, R. H., Larsson, K.-H., Taylor, A. F. S., Bengtsson-Palme, J., Jeppesen, T. S., Schigel, D., ... others (2019). The unite database for molecular identification of fungi: handling dark taxa and parallel taxonomic classifications. *Nucleic acids research*, *47*(D1), D259–D264.

Nuske, S. J., Fajardo, A., Nuñez, M. A., Pauchard, A., Wardle, D. A., Nilsson, M.-C., ... others (2021). Soil biotic and abiotic effects on seedling growth exhibit context-dependent interactions: evidence from a multi-country experiment on pinus contorta invasion. *New Phytologist*, *232*(1), 303–317.

Oksanen, J., Simpson, G. L., Blanchet, F. G., Kindt, R., Legendre, P., Minchin, P. R., ... Weedon, J. (2022). vegan: Community ecology package [Computer software manual]. Retrieved from `https://CRAN.R-project.org/package=vegan` (R package version 2.6-4)

Opstal, E. J. v., & Bordenstein, S. R. (2015). Rethinking heritability of the microbiome. *Science*, *349*(6253), 1172–1173.

Pajares-Murgó, M., Garrido, J. L., Perea, A. J., López-García, Á., Bastida, J. M., Prieto-Rubio, J., ... Alcántara, J. M. (2024). Intransitivity in plant–soil feedbacks is rare but is associated with multispecies coexistence. *Ecology Letters*, *27*(3), e14408.

Pérez-Jaramillo, J. E., de Hollander, M., Ramírez, C. A., Mendes, R., Raaijmakers, J. M., & Carrión, V. J. (2019). Deciphering rhizosphere microbiome assembly of wild and modern common bean (phaseolus vulgaris) in native and agricultural soils from colombia. *Microbiome*, *7*(1), 1–16.

Pernilla Brinkman, E., Van der Putten, W. H., Bakker, E.-J., & Verhoeven, K. J. (2010). Plant–soil feedback: experimental approaches, statistical analyses and ecological interpretations. *Journal of Ecology*, *98*(5), 1063–1073.

Pugnaire, F. I., Morillo, J. A., Peñuelas, J., Reich, P. B., Bardgett, R. D., Gaxiola, A., ... Van Der Putten, W. H. (2019). Climate change effects on plant-soil feedbacks and consequences for biodiversity and functioning of terrestrial ecosystems. *Science advances*, *5*(11), eaaz1834.

Rallo, P., Hannula, S. E., ten Hooven, F. C., Verhoeven, K. J., Kammenga, J., & van der Putten, W. H. (2023). Inter-and intraspecific plant-soil feedbacks of grass species. *Plant and Soil*, 1–12.

Reed, P. B., & Hallett, L. M. (2023). Spatiotemporal patterns of rising annual plant abundance in grasslands of the willamette valley, oregon (usa). *Landscape Ecology*, *38*(11), 2885–2898.

Revilla, T. A., Veen, G., Eppinga, M. B., & Weissing, F. J. (2013). Plant–soil feedbacks and the coexistence of competing plants. *Theoretical Ecology*, *6*, 99–113.

Rinella, M. J., & Reinhart, K. O. (2018). Toward more robust plant-soil feedback research. *Ecology*, *99*(3), 550–556.

Rodgers, V. L., Scanga, S. E., Kolozsvary, M. B., Garneau, D. E., Kilgore, J. S., Anderson, L. J., ... Juneau, K. J. (2022). Where is garlic mustard? understanding the ecological context for invasions of alliaria petiolata. *BioScience*.

Rodgers, V. L., Stinson, K. A., & Finzi, A. C. (2008). Ready or not, garlic mustard is moving in: Alliaria petiolata as a member of eastern north american forests. *Bioscience*, *58*(5), 426–436.

Rogalski, M. A., Stewart Merrill, T., Gowler, C. D., Cáceres, C. E., & Duffy, M. A. (2021). Context-dependent host-symbiont interactions: Shifts along the parasitism-mutualism continuum. *The American Naturalist*, *198*(5), 563–575.

Roughgarden, J. (2023). Holobiont evolution: Population theory for the hologenome. *The American Naturalist*, *201*(6), 763–778.

Roughgarden, J., Gilbert, S. F., Rosenberg, E., Zilber-Rosenberg, I., & Lloyd, E. A. (2018). Holobionts as units of selection and a model of their population dynamics and evolution. *Biological Theory*, *13*, 44–65.

Rudgers, J. A., Afkhami, M. E., Bell-Dereske, L., Chung, Y. A., Crawford, K. M., Kivlin, S. N., ... Nuñez, M. A. (2020). Climate disruption of plant-microbe interactions. *Annual review of ecology, evolution, and systematics*, *51*, 561–586.

Saavedra, S., Rohr, R. P., Bascompte, J., Godoy, O., Kraft, N. J., & Levine, J. M. (2017). A structural approach for understanding multispecies coexistence. *Ecological Monographs*, *87*(3), 470–486.

Schenk, P. M., Carvalhais, L. C., & Kazan, K. (2012). Unraveling plant–microbe interactions: can multi-species transcriptomics help? *Trends in biotechnology*, *30*(3), 177–184.

Schroeder, J. W., Dobson, A., Mangan, S. A., Petticord, D. F., & Herre, E. A. (2020). Mutualist and pathogen traits interact to affect plant community structure in a spatially explicit model. *Nature communications*, *11*(1), 2204.

Sears, A. L., & Chesson, P. (2007). New methods for quantifying the spatial storage effect: an illustration with desert annuals. *Ecology*, *88*(9), 2240–2247.

Selosse, M.-A., & Le Tacon, F. (1998). The land flora: a phototroph-fungus partnership? *Trends in Ecology & Evolution*, *13*(1), 15–20.

Semchenko, M., Barry, K. E., de Vries, F. T., Mommer, L., Moora, M., & Maciá-Vicente, J. G. (2022). Deciphering the role of specialist and generalist plant–microbial interactions as drivers of plant–soil feedback. *New Phytologist*, *234*(6), 1929–1944.

Shang, Y., Sikorski, J., Bonkowski, M., Fiore-Donno, A.-M., Kandeler, E., Marhan, S., ... others (2017). Inferring interactions in complex microbial communities from nucleotide sequence data and environmental parameters. *PLoS One*, *12*(3), e0173765.

Shoemaker, L. G., Barner, A. K., Bittleston, L. S., & Teufel, A. I. (2020). Quantifying the relative importance of variation in predation and the environment for species coexistence. *Ecology letters*, *23*(6), 939–950.

Smith, L. M., & Reynolds, H. L. (2015). Plant–soil feedbacks shift from negative to positive with decreasing light in forest understory species. *Ecology*, *96*(9), 2523–2532.

Smith-Ramesh, L. M., & Reynolds, H. L. (2017). The next frontier of plant–soil feedback research: unraveling context dependence across biotic and abiotic gradients. *Journal of Vegetation Science*, *28*(3), 484–494.

Song, C., Barabás, G., & Saavedra, S. (2019). On the consequences of the interdependence of stabilizing and equalizing mechanisms. *The American Naturalist*, *194*(5), 627–639.

Song, C., Rohr, R. P., & Saavedra, S. (2017). Why are some plant–pollinator networks more nested than others? *Journal of Animal Ecology*, *86*(6), 1417–1424.

Song, C., & Spaak, J. W. (2024). Trophic tug-of-war: Coexistence mechanisms within and across trophic levels. *Ecology Letters*, *27*(4), e14409.

Song, C. W., & Spaak, J. W. (2023). Multitrophic assembly: a perspective from modern coexistence theory. *bioRxiv*, 2023–03.

Stan Development Team. (2023a). *RStan: the R interface to Stan.* Retrieved from `https://mc-stan.org/` (R package version 2.21.8)

Stan Development Team. (2023b). *RStan: the R interface to Stan.* Retrieved from `https://mc-stan.org/` (R package version 2.32.3)

Stevenson, M., Sergeant, E., & Firestone, S. (2024). epir: Tools for the analysis of epidemiological data [Computer software manual]. Retrieved from `https://CRAN.R-project.org/package=epiR` (R package version 2.0.70)

Sweet, D. D., & Burns, J. H. (2017). Plant performance was greater in the soils of more distantly related plants for an herbaceous understory species. *AoB Plants*, *9*(1), plx005.

Terborgh, J. (2020). At 50, janzen–connell has come of age. *BioScience*, *70*(12), 1082–1092.

Terry, J. C. D., Chen, J., & Lewis, O. T. (2021). Natural enemies have inconsistent impacts on the coexistence of competing species. *Journal of Animal Ecology*, *90*(10), 2277–2288.

Thakur, M. P., van der Putten, W. H., Wilschut, R. A., Veen, G. C., Kardol, P., van Ruijven, J., ... Bezemer, T. M. (2021). Plant–soil feedbacks and temporal dynamics of plant diversity–productivity relationships. *Trends in Ecology & Evolution*, *36*(7), 651–661.

Thurman, L. L., Barner, A. K., Garcia, T. S., & Chestnut, T. (2019). Testing the link between species interactions and species co-occurrence in a trophic network. *Ecography*, *42*(10), 1658–1670.

Usinowicz, J., & Levine, J. M. (2018). Species persistence under climate change: a geographical scale coexistence problem. *Ecology letters*, *21*(11), 1589–1603.

Valladares, F., Bastias, C. C., Godoy, O., Granda, E., & Escudero, A. (2015). Species coexistence in a changing world. *Frontiers in plant science*, *6*, 866.

Valliere, J. M., Wong, W. S., Nevill, P. G., Zhong, H., & Dixon, K. W. (2020). Preparing for the worst: Utilizing stress-tolerant soil microbial communities to aid ecological restoration in the anthropocene. *Ecological Solutions and Evidence*, *1*(2), e12027.

Van der Putten, W. H., Bardgett, R. D., Bever, J. D., Bezemer, T. M., Casper, B. B., Fukami, T., ... others (2013). Plant–soil feedbacks: the past, the present and future challenges. *Journal of ecology*, *101*(2), 265–276.

van der Putten, W. H., Bradford, M. A., Pernilla Brinkman, E., van de Voorde, T. F., & Veen, G. (2016). Where, when and how plant–soil feedback matters in a changing world. *Functional Ecology*, *30*(7), 1109–1121.

Van Dyke, M. N., Levine, J. M., & Kraft, N. J. (2022). Small rainfall changes drive substantial changes in plant coexistence. *Nature*, *611*(7936), 507–511.

Van Grunsven, R. H., Van Der Putten, W. H., Bzemer, T. M., Tamis, W. L., Berendse, F., & Veenendaal, E. M. (2007). Reduced plant-soil feedback of plant species expanding their range as sompared to natives. *Journal of Ecology*, 1050–1057.

Van Grunsven, R. H. A., Van der Putten, W. H., Bezemer, T. M., & Veenendaal, E. M. (2010). Plant–soil feedback of native and range-expanding plant species is insensitive to temperature. *Oecologia*, *162*(4), 1059–1069.

Van Nuland, M. E., Ke, P.-J., Wan, J., & Peay, K. G. (2023). Mycorrhizal nutrient acquisition strategies shape tree competition and coexistence dynamics. *Journal of Ecology*, *111*(3), 564–577.

Vehtari, A., Gabry, J., Magnusson, M., Yao, Y., Bürkner, P.-C., Paananen, T., & Gelman, A. (2023). *loo: Efficient leave-one-out cross-validation and waic for bayesian models.* Retrieved from `https://mc-stan.org/loo/` (R package version 2.6.0)

Vehtari, A., Gelman, A., & Gabry, J. (2017). Practical bayesian model evaluation using leave-one-out cross-validation and waic. *Statistics and Computing*, *27*, 1413–1432. doi: 10.1007/s11222-016-9696-4

Veresoglou, S. D., Li, G. C., Chen, J., & Johnson, D. (2022). Direction of plant–soil feedback determines plant responses to drought. *Global Change Biology*, *28*(13), 3995–3997.

Wagner, M. R. (2021). Prioritizing host phenotype to understand microbiome heritability in plants. *New Phytologist*, *232*(2), 502–509.

Wainwright, C. E., HilleRisLambers, J., Lai, H. R., Loy, X., & Mayfield, M. M. (2019). Distinct responses of niche and fitness differences to water availability underlie variable coexistence outcomes in semi-arid annual plant communities. *Journal of Ecology*, *107*(1), 293–306.

Wang, J., Bonser, S. P., Liu, K., Liu, Z., Gao, H., Cui, H., ... others (2023). Warming affects herbaceous germination, early survival, and growth by shifting plant-soil microbe interactions in an alpine ecosystem. *Plant and Soil*, *487*(1), 249–265.

Wang, Q., Garrity, G. M., Tiedje, J. M., & Cole, J. R. (2007). Naive bayesian classifier for rapid assignment of rrna sequences into the new bacterial taxonomy. *Applied and environmental microbiology*, *73*(16), 5261–5267.

Weiss-Lehman, C. P., Werner, C. M., Bowler, C. H., Hallett, L. M., Mayfield, M. M., Godoy, O., ... others (2022). Disentangling key species interactions in diverse and heterogeneous communities: A bayesian sparse modelling approach. *Ecology Letters*, *25*(5), 1263–1276.

White, T. J., Bruns, T., Lee, S., Taylor, J., et al. (1990). Amplification and direct sequencing of fungal ribosomal rna genes for phylogenetics. *PCR protocols: a guide to methods and applications*, *18*(1), 315–322.

Williams, A., Langridge, H., Straathof, A. L., Muhamadali, H., Hollywood, K. A., Goodacre, R., & de Vries, F. T. (2022). Root functional traits explain root exudation rate and composition across a range of grassland species. *Journal of Ecology*, *110*(1), 21–33.

Wilschut, R. A., van der Putten, W. H., Garbeva, P., Harkes, P., Konings, W., Kulkarni, P., ... Geisen, S. (2019). Root traits and belowground herbivores relate to plant–soil feedback variation among congeners. *Nature Communications*, *10*(1), 1564.

Wolfe, B. E., Rodgers, V. L., Stinson, K. A., & Pringle, A. (2008). The invasive plant alliaria petiolata (garlic mustard) inhibits ectomycorrhizal fungi in its introduced range. *Journal of Ecology*, *96*(4), 777–783.

Wu, J., Dhingra, R., Gambhir, M., & Remais, J. V. (2013). Sensitivity analysis of infectious disease models: methods, advances and their application. *Journal of The Royal Society Interface*, *10*(86), 20121018.

Wubs, E. J., & Bezemer, T. M. (2016). Effects of spatial plant–soil feedback heterogeneity on plant performance in monocultures. *Journal of Ecology*, *104*(2), 364–376.

Xia, Y., Dong, M., Yu, L., Kong, L., Seviour, R., & Kong, Y. (2021). Compositional and functional profiling of the rhizosphere microbiomes of the invasive weed ageratina adenophora and native plants. *PeerJ*, *9*, e10844.

Yan, X., Levine, J. M., & Kandlikar, G. S. (2022). A quantitative synthesis of soil microbial effects on plant species coexistence. *Proceedings of the National Academy of Sciences*, *119*(22), e2122088119.

Yergeau, E., Tremblay, J., Joly, S., Labrecque, M., Maynard, C., Pitre, F. E., ... Greer, C. W. (2014). Soil contamination alters the willow root and rhizosphere metatranscriptome and the root–rhizosphere interactome. *The ISME journal*, *12*(3), 869–884.

Zanne, A. E., Abarenkov, K., Afkhami, M. E., Aguilar-Trigueros, C. A., Bates, S., Bhatnagar, J. M., ... others (2020). Fungal functional ecology: bringing a trait-based approach to plant-associated fungi. *Biological Reviews*, *95*(2), 409–433.

Zepeda, V., & Martorell, C. (2019). Fluctuation-independent niche differentiation and relative non-linearity drive coexistence in a species-rich grassland. *Ecology*, *100*(8), e02726.

Zhang, Q., Yang, R., Tang, J., Yang, H., Hu, S., & Chen, X. (2010). Positive feedback between mycorrhizal fungi and plants influences plant invasion success and resistance to invasion. *PLoS one*, *5*(8), e12380.